Paleoceanography and Paleoclimatology

FEATURE ARTICLE
10.1029/2018PA003433

GRAND CHALLENGES CENTENNIAL COLLECTION

The Late Mesozoic-Cenozoic Arctic Ocean Climate and Sea Ice History: A Challenge for Past and Future Scientific Ocean Drilling

Ruediger Stein[1,2]

[1]Alfred Wegener Institute Helmholtz Centre for Polar and Marine Research, Bremerhaven, Germany, [2]MARUM and Faculty of Geosciences, University of Bremen, Bremen, Germany

Key Points:
- Arctic climate records from Cretaceous-Paleogene Greenhouse to Neogene-Quaternary Icehouse help to understand modern climate change
- Ice-free summers occurred during a late Miocene warm climate with pCO2 concentrations of 450 ppm, a value we might reach in the near future
- An IODP drilling on Lomonosov Ridge with a focus on the complete Cenozoic Arctic Ocean climate history is scheduled for 2021

Correspondence to:
R. Stein,
ruediger.stein@awi.de

Citation:
Stein, R. (2019). The late Mesozoic-Cenozoic Arctic Ocean climate and sea ice history: A challenge for past and future scientific ocean drilling. *Paleoceanography and Paleoclimatology*, *34*. https://doi.org/10.1029/2018PA003433

Received 20 JUN 2019
Accepted 27 AUG 2019
Accepted article online 6 NOV 2019

Abstract Over the past 3–4 decades, coincident with global warming and atmospheric CO_2 increase, Arctic sea ice has significantly decreased in its extent as well as in thickness. When extrapolating this alarming trend, the central Arctic Ocean might become ice-free during summers within about the next 2–5 decades. Paleoclimate records allow us to better understand the processes controlling modern climate change and distinguish between natural and anthropogenic forcing. In this context, detailed studies of the earlier Earth history characterized by a much warmer global climate with elevated atmospheric CO_2 concentrations are important. The main focus of this review paper is the long-term late Mesozoic-Cenozoic Arctic Ocean climate history from Greenhouse to Icehouse conditions, with special emphasis on Arctic sea ice history. Starting with some information on the Cretaceous Arctic Ocean climate, this paper will concentrate on selected results from Integrated Ocean Drilling Program (IODP) Expedition 302 (Arctic Ocean Coring Expedition (ACEX)), the first scientific drilling in the permanently ice-covered Arctic Ocean, dealing with the Cenozoic climate history. While these results from ACEX were unprecedented, key questions related to the Cenozoic Arctic climate history remain unanswered, largely due to the major mid-Cenozoic hiatus (if existing) and partly to the poor recovery of the ACEX record. Following-up ACEX and its cutting-edge science, a second scientific drilling on Lomonosov Ridge with a focus on the reconstruction of the continuous and complete Cenozoic Arctic Ocean climate history has currently been proposed and scheduled as IODP Expedition 377 for 2021.

1. Introduction

During the last few decades, the remote Arctic Ocean, characterized by strong seasonal forcing and variability in runoff, sea ice formation, and sunlight, became a major focus within the ongoing debate of climate change as the high latitudes mirror the global warming trend strongly amplified (AMAP, 2017; Park et al., 2018; Serreze & Barry, 2011; Stocker et al., 2013). Due to complex feedback processes (collectively known as "polar amplification"), the Arctic is both a contributor of climate change and a region that will be most affected by global warming (ACIA, 2004, 2005; Serreze & Barry, 2011; Stocker et al., 2013). That means, the Arctic Ocean and surrounding areas are (in real time) and were (over historic and geologic timescales) subject to rapid and dramatic change. Although the Arctic Ocean was and is a key player in the past, present, and future global climate/Earth system (AMAP, 2017; Stocker et al., 2013), the marine geoscience research in the Arctic lags behind other world oceans, especially from a paleoclimatic perspective (e.g., Jakobsson et al., 2014; Stein, 2008). That means, detailed records of the short- and long-term geological and paleoclimate history of the Arctic Ocean are still sparse. This lack in knowledge is mainly due to the major technological/logistical problems in operating within the permanently ice-covered Arctic region.

During the last ~20 years, several international expeditions have greatly advanced our knowledge on central Arctic Ocean paleoenvironment and its variability through Quaternary times (Stein et al., 2015). Prior to 2004, however, central Arctic Ocean piston and gravity coring was mainly restricted to obtaining near-surface sediments; that is, only the upper 15 m could be sampled. Thus, almost all studies were restricted to the late Pliocene/Quaternary time interval, with only a few exceptions based on short sediment cores representing some isolated sections of late Mesozoic/early Cenozoic climate history. A breakthrough in Arctic Ocean paleoclimate research was the first scientific drilling in the permanently ice-covered central Arctic Ocean that was carried out within the Integrated Ocean Drilling Program (IODP) in 2004, that is,

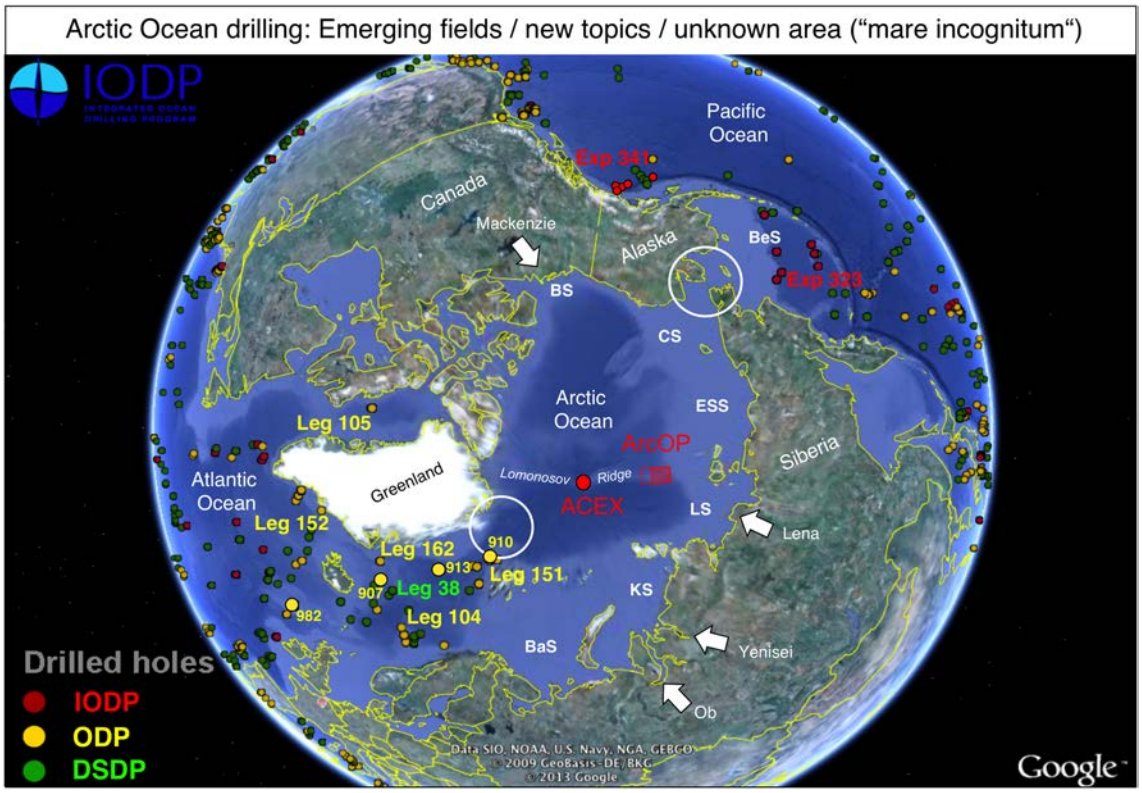

Figure 1. Arctic Ocean drilling: Emerging fields and new topics in an unknown area "mare incognitum." Google map showing the Northern Hemisphere with locations of Deep-Sea Drilling Project, ODP, and IODP sites; selected high northern latitude expeditions are highlighted. Locations of ODP sites 907, 910, 913, and 982 for which SST records are included in Figure 15 are shown as well. Large white circles indicate the connection via Fram Strait between Greenland and Svalbard, and Bering Strait between Alaska and Siberia to the Atlantic Ocean and Pacific Ocean, respectively. White arrows indicate discharge into the Arctic Ocean by major rivers. BS = Beaufort Sea, BeS = Bering Sea, CS = Chukchi Sea, ESS = East Siberian Sea, LS = Laptev Sea, KS = Kara Sea, BaS = Barents Sea. The location of the ACEX drill site and the working area of the IODP Expedition 377 (ArcOP) are shown in red.

IODP Expedition 302—the Arctic Ocean Coring Expedition (ACEX), penetrating 428 m of Upper Cretaceous to Quaternary sediments on the crest of Lomonosov Ridge between 87° and 88°N (Backman et al., 2006; Moran et al., 2006). The main objectives of the ACEX drilling campaign focused on the reconstruction of Cenozoic Arctic ice, temperatures, and climates from early (Paleogene) Greenhouse to modern-type (Neogene) Icehouse conditions. Some of the key questions to be answered from ACEX were framed around the evolution of sea ice and ice sheets, the past physical oceanographic structure, Arctic gateways, links between Arctic land and ocean climate, and major changes in depositional environments (Backman et al., 2006, Backman et al., 2008; Backman & Moran, 2009; for reviews, see O'Regan et al., 2011; Stein, Blackman, et al., 2014; Stein, 2017). By studying the unique ACEX sedimentary sequence, >100 papers are now published in highly ranked international peer-reviewed scientific journals (see Stein, Weller, et al., 2014, Stein et al., 2015, for references). Some of the ACEX paleoceanographic themes and highlights with reference to the original literature are summarized in some more detail (see section 5.2). To date, the ACEX site remains the one and only scientific drilling location in the central Arctic Ocean (Figure 1). Thus, thinking about scientific ocean drilling campaigns that have been carried out under the umbrella of the Deep-Sea Drilling Project (DSDP), the Ocean Drilling Program (ODP), and/or the Integrated Ocean Drilling Program/International Ocean Discovery Program (IODP) in the other world oceans during the last five decades (Stein, Blackman, et al., 2014; Koppers et al., 2019), the Arctic Ocean is still a "mare incognitum" (Figure 1).

This review paper is structured as follows: After an overview about the main characteristics, significance, and recent climate change of the Arctic Ocean (sections 2 and 3) and some basic information about proxies used for the paleoenvironmental reconstructions (section 4), the main focus is on the long-term late

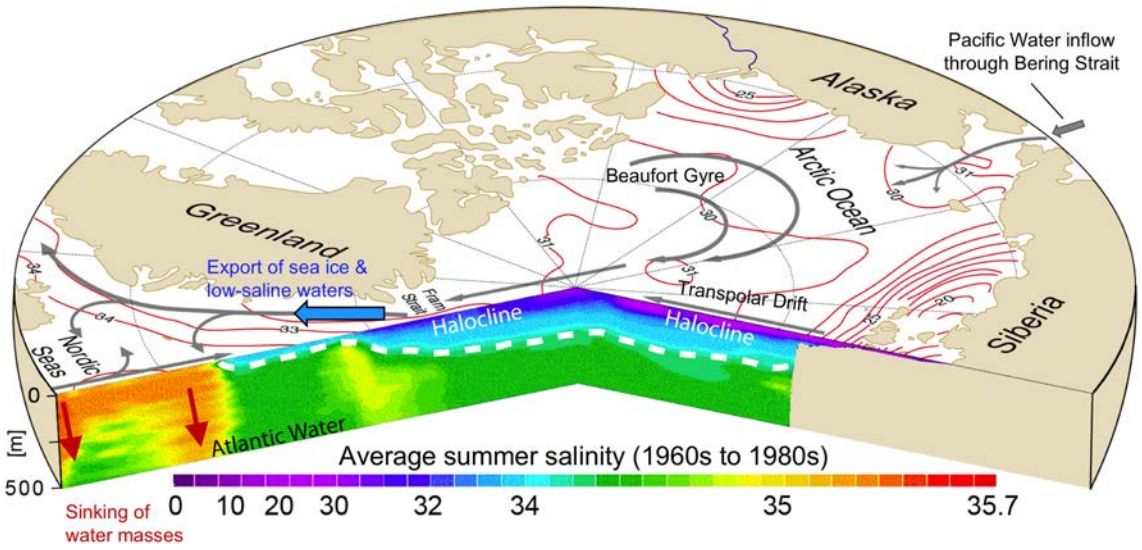

Figure 2. Map and vertical structure (500 m) of salinity in the Arctic Ocean. Inflow of Pacific Waters through Bering Strait and export of ice and low-saline waters through Fram Strait are indicated. Gray arrows mark the average surface water circulation within the Beaufort Gyre and the Transpolar Drift and red arrows the places of sinking water masses (Spielhagen & Bauch, 2015, supplemented; based on data from EWG, 1998).

Mesozoic-Cenozoic climate history from Greenhouse to Icehouse conditions, with special emphasis on the Arctic sea ice history during its course from ice-free to seasonal to permanent ice conditions (section 5). Starting with some information on the Cretaceous climate based on short gravity cores, this paper will concentrate on selected results from IODP Expedition 302 (ACEX) dealing with the Cenozoic climate history. Finally, an outlook on the key goals of the coming IODP Expedition 377 scheduled for 2021 will be presented (section 6).

2. The Arctic Ocean: Characteristics and Significance for the Climate System

What are the main characteristics that make the Arctic Ocean so unique in comparison to the other world oceans? Why is the Arctic Ocean so important in the global climate/Earth system? Several aspects can be listed:

2.1. Physiography and Water Mass Exchange

The Arctic Ocean is surrounded by continents and the world's largest shelf seas, with limited connections to the Pacific and Atlantic Oceans, making the Arctic Ocean a "Mediterranean Sea" (Figure 1). With an area of about 9.5×10^6 km^2, the entire Arctic Ocean comprises 2.6% of the total area of the world's oceans, but less than 1% of the volume (about 13×10^6 km^3; Jakobsson, 2002; Jakobsson et al., 2012). The relatively small total volume is due to the large shelf areas, which make up as much as 52.7% of the total area of the Arctic Ocean, resulting in a shallow mean depth of the entire Arctic ocean of about 1,360 m.

Fram Strait between northeastern Greenland and Svalbard is the only deep-water connection with the world ocean via the Atlantic Ocean (Figures.1 and 2). Furthermore, two major currents, with southward flowing waters on the west and northward flowing waters on the east, exchange surface-water water between the Arctic and the North Atlantic through Fram Strait (Figure 3; Aagaard et al., 1985; Rudels et al., 1994; Schauer et al., 2002): The cold, ice-transporting East Greenland Current is the main current out of the Arctic Ocean. In contrast, the eastern West Spitsbergen Current, an extension of the North Atlantic-Norwegian Current, carries warm, relatively saline Atlantic Water into the Arctic Ocean. This Atlantic Water branch cools down and, together with Atlantic water that is flowing across the Barents Sea and through the St. Anna Trough, follows the continental slope and ridges of the deep basins at intermediate water depths. Toward the Pacific Ocean, only a shallow-water connection exists. From there, relative low-saline, nutrient-rich Pacific Water enters the Arctic Ocean through the Bering Strait (Figure 2), primarily driven by a pressure-head difference between the Pacific and the Arctic Oceans (e.g., Coachman et al., 1975; Hunt et al., 2012; Woodgate et al., 2005).

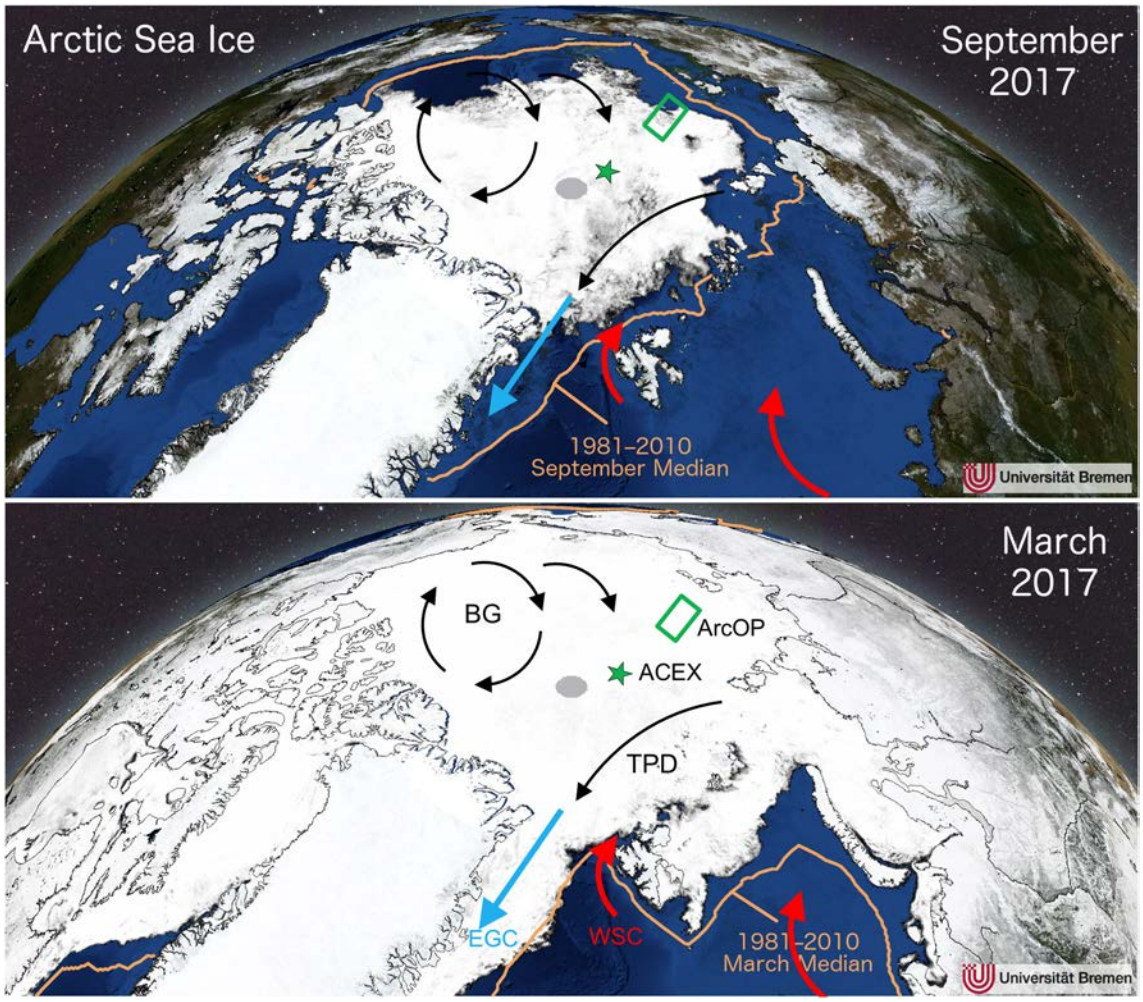

Figure 3. The extent of Arctic sea ice in 2017, showing the seasonal variability with maximum in March and minimum in September. During recent years, the sea ice extent has reduced significantly compared to the long-term median of the years 1981 to 2010 shown as yellow line (Spreen et al., 2008; https://seaice.uni-bremen.de/arctic-sea-ice-minima/). Beaufort Gyre (BG) and the Transpolar Drift (TPD) systems are shown as black arrows. Red arrows mark inflow of warm Atlantic waters, and blue arrow marks outflow of cold Arctic waters. WSC = West Spitsbergen Current, EGC = East Greenland Current. The location of the ACEX drill site and the working area of the IODP Expedition 377 (ArcOP) are shown in green.

2.2. Surface-Water Characteristics: Temperature and Salinity

Whereas the central Arctic Ocean mean sea-surface temperatures (SST) are <−1 °C throughout the year (resulting in a permanent sea-ice cover), a distinct seasonal variability is obvious in the marginal seas (Environmental Working Group, 1998; Singh et al., 2013). In the latter, mean SST reaches values of 0 to 5 °C during summer at times of increased river discharge and Atlantic Water inflow. During winter times, low mean SST of <−1 °C similar to those of the central Arctic Ocean were also measured in the marginal seas. An exception from this general picture is the Barents Sea, strongly influenced by Atlantic Water inflow. Here mean summer SST may increase to 8 °C and even during winter time; values of up to 4 °C were determined in the southwestern part.

The distribution of the sea-surface salinity (SSS) is strongly controlled by the river discharge and the Atlantic Water inflow (Figure 2; Environmental Working Group, 1998). The high river discharge results in a very low salinity in the Arctic Ocean proper as well as the marginal seas, except for the Barents Sea, influenced by more saline Atlantic Water inflow. The Beaufort, East Siberian, Laptev, and Kara seas are characterized by mean SSS of <29 during the summer, strongly decreasing toward the river mouths; in most part of the central Arctic, mean SSS is below 32. In the Barents Sea and adjacent continental slope, mean SSS

increases to >34. Due to seasonal variability in river discharge, the SSS also displays a strong variability, especially in the marginal seas.

2.3. Sea-Ice Cover

A key phenomenon of the Arctic Ocean is the perennial sea-ice cover in its central part and a strong seasonal variation of sea ice in the surrounding marginal (shelf) areas (Figure 3; Johannessen et al., 2004; Thomas & Diekmann, 2010; https://nsidc.org/data/seaice_index/). In winter these areas are usually completely covered with ice, whereas in summer they are mostly ice-free. An exception is the Barents Sea and the area around Svalbard, strongly influenced by the warm Norwegian/West Spitsbergen Current system. There, large parts are ice-free throughout the year.

In general, there are two primary forms of sea ice: seasonal (or first-year) ice and perennial (or multi-year) ice. The thickness of first-year ice ranges from a few tenths of a meter near the southern margin of the marine cryosphere to 2.5 m in the high Arctic at the end of winter. Some first-year ice survives the summer and becomes multiyear ice. In the present climate, old multiyear ice floes without ridges are about 3 m thick at the end of winter. In addition, land-fast ice (or fast ice) occurs in the coastal circum-Arctic area, which is immobilized for up to 10 months each year by coastal geometry or by grounded ice ridges (ACIA, 2004, 2005).

Sea-ice concentration (percent ice area per unit area) and derived parameters such as ice extent (the area within the ice-ocean margin defined as 15% ice concentration) can be reliably retrieved through satellite-borne passive microwave sensors, which are available continuously since 1978 and operating independently of cloud cover and light conditions (Gloersen et al., 1992; Johannessen et al., 2004). Satellite data have shown that the area of sea ice decreases from roughly 14–15 $\times 10^6$ km^2 in March to <5–7 $\times 10^6$ km^2 in September, as much of the first-year ice melts during the summer (Figure 3; Gloersen et al., 1992; Cavalieri et al., 1997; Johannessen et al., 2004; Stroeve et al., 2012; https://nsidc.org/). The area of multiyear sea ice, mostly over the Arctic Ocean basins, the East Siberian Sea, and the Canadian polar shelf, is about 4–5 $\times 10^6$ km^2 having decreased significantly during the last decades (e.g., AMAP, 2017; Johannessen et al., 1999; Nghiem et al., 2007).

The mean sea-ice drift pattern, a direct response to surface atmospheric pressure gradients and resulting wind patterns, is quite well known from drift buoy and geostrophic wind field data (Colony & Thorndike, 1985; Hibler, 1989; Pfirman et al., 1997; Thorndike & Colony, 1982). North of the Alaskan coast, the ice circulates in a big anticyclonic structure, the Beaufort Gyre (Figure 3), corresponding to the high-pressure system over the Beaufort Sea. Speed varies from almost 0 in the center to 3 cm/s in the marginal zones. Toward the Siberian Arctic, this gyre opens up to a linear structure, the Transpolar Drift (Figure 3). Its origin is in the area of the Chukchi-East Siberian Sea, and it leads to the West. Ice drifts with mean velocities of about 2 cm/s past the North Pole and Franz Josef Land, accelerating to mean values of up to 10 cm/s through Fram Strait between Svalbard and Greenland.

Sea ice is a very critical component of the Arctic system that responds sensitively to changes in atmospheric circulation, incoming radiation, atmospheric and oceanic heat fluxes, and the hydrological cycle (Figure 4). Ice significantly reduces the heat flux between ocean and atmosphere; through its high albedo, it has a strong influence on the radiation budget of the entire Arctic. The albedo of open water is as low as 0.10, whereas the ice albedo ranges between 0.6 and 0.8 (Figure 4; Barry, 1996; Serreze & Barry, 2011). Thus, over ice surfaces as compared with open water, up to 8 times as much of the incoming shortwave radiation is reflected, resulting in lower surface temperatures. Furthermore, the sea-ice cover strongly affects the biological productivity (e.g., Sakshaug, 2004), as a more closed sea-ice cover restricts primary production due to low light influx into the surface waters (Figure 4). Sea ice is also an important agent for sediment transport from the shelves into, across, and out of the Arctic Ocean. Increased export of sea ice via the East Greenland Current will reduce the surface salinity in the Greenland Sea, which subsequently diminishes the global thermohaline circulation by slowing the production of North Atlantic Deep Water (Aagaard & Carmack, 1989; Broecker, 1997; Raymo et al., 1990).

2.4. River Discharge

One of the main characteristics of the Arctic Ocean is its huge river discharge (e.g., Aagaard & Carmack, 1989; Holmes et al., 2002, 2018). Today, the annual direct freshwater inflow by major rivers into the Arctic Ocean reaches a total of about 3,300 km^3 (Holmes et al., 2002, 2018; Rachold et al., 2004). For

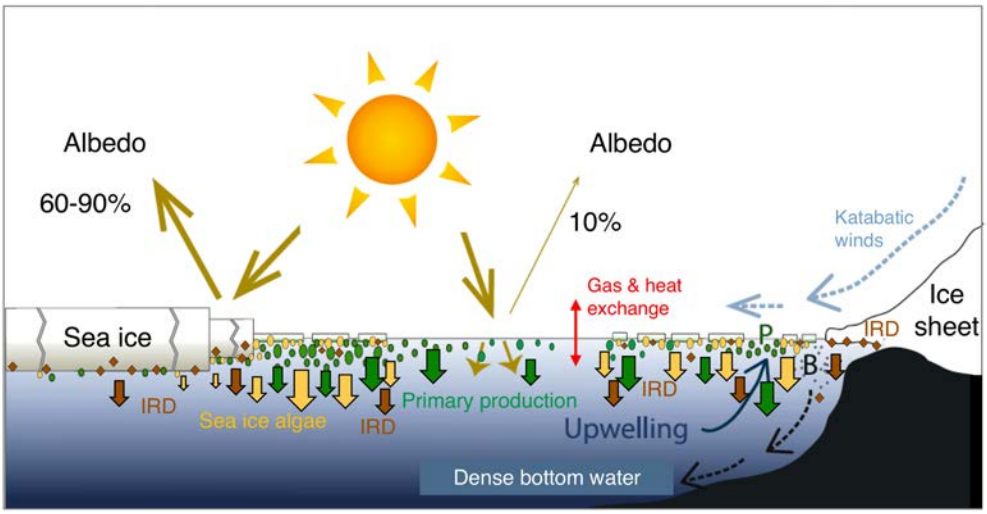

Figure 4. Simplified scheme of the role of sea ice in the climate and ocean system, indicating the modern central and ice-edge Arctic area (left) and the glacial Arctic situation with ice sheets reaching the shelf break, a situation similar to the modern circum-Antarctic situation (right). Furthermore, solar energy (yellow-olive arrows), katabatic winds (light blue arrow), albedo effect, and ocean processes such as upwelling and brine (B) formation, polynyas (P), phytoplankton production (little green circles), and sea-ice algae (and IP_{25}) production (little yellow circles) with related fluxes (green and yellow arrows, respectively) are shown. Figure adapted from De Vernal, Gersonde, et al. (2013), supplemented.

comparison, the amount of water discharged by the world rivers to the present-day ocean is estimated to be between 32 and 37 × 10^3 km^3/year (Milliman & Meade, 1983; Chakrapani, 2005). That means, the Arctic Ocean discharge is equivalent to >10% of the global runoff. Major contributors are the Yenisei (620 km^3/year), the Ob (429 km^3/year), the Lena (525 km^3/year), and the MacKenzie (249 km^3/year; Figure 1; Holmes et al., 2002, 2018; Rachold et al., 2004; McClelland et al., 2012).

The overall importance of Arctic river discharge for the Arctic Ocean and its significance for the global ocean system can be summarized as follows:

- The fluvial fresh-water supply is essential for the maintenance of the approx. 200-m-thick low-salinity layer of the central Arctic Ocean and, thus, contributes significantly to the strong stratification of the near-surface water masses (Figure 2), encouraging sea-ice formation. Thus, changes in the fresh-water balance would influence the extent of sea-ice cover.
- The fresh-water exported from the Arctic Ocean through Fram Strait influences global thermohaline circulation (Figure 2). Today, the annual liquid fresh-water export of the East Greenland Current is about 1,160 km^3. Estimates based on sea-ice export even reach values of 1,680 (Aagaard & Carmack, 1989) to 2,850 km^3/year (Eicken, 2004). Because factors such as the global thermohaline circulation as well as sea-ice cover and earth albedo have a strong influence on the Earth's climate system, the fresh-water input to the Arctic and its change through time may have triggered global climate changes in the past (e.g., the initiation of the Northern Hemisphere Glaciation during mid-Pliocene times; Driscoll & Haug, 1998; for further discussion, see section 6).
- The Arctic rivers transport large amounts of nutrients, dissolved and particulate material (i.e., chemical elements, siliciclastic suspension, terrestrial organic matter, etc.; Martin et al., 1993; Gordeev et al., 1996; Stein & Macdonald, 2004; Bring et al., 2016), and anthropogenic pollutants (i.e., radioactive elements, heavy metals, etc.; Nies et al., 1998; Crane et al., 2001) onto the shelves (see above) where it is accumulated or further transported by different mechanisms (sea ice, icebergs, turbidity currents, etc.) toward the open ocean (e.g., Stein, 2008 for review). Thus, river-derived materials contribute in major proportions to the entire Arctic Ocean sedimentary and chemical budgets.

2.5. Permafrost

Large areas around the Arctic Ocean reaching about one quarter of the landmass of the Northern Hemisphere (Brown et al., 1997) are occupied by permafrost, that is, perennially frozen ground (Romanovskii et al., 2004; Vonk et al., 2015). The thickness of permafrost ranges from very thin layers of only a few centimeters thick to several hundreds of meters; in unglaciated areas of Siberia, even thicknesses of about 1,500 m may be reached (Washburn, 1980; Nelson et al., 1999). Furthermore, thermal modelling and geophysical data (e.g., Rekant et al., 2005; Romanovskii et al., 2005) indicate that large areas of the Arctic shelves, as a result of their exposure during the Last Glacial Maximum, are thought to be almost entirely underlain by subsea permafrost from the coastline down to a water depth of about 100 m (Rachold et al., 2007).

Many of the potential environmental and socioeconomic impacts of global warming in the Arctic are associated with permafrost. The effects of climatic warming on permafrost and the overlying "active layer"can severely disrupt ecosystems and human infrastructure and may intensify global warming (e.g., Frey et al., 2007; Jorgenson et al., 2001; Nelson et al., 1999). Huge amounts of soil organic carbon are currently stored frozen in permafrost soils (e.g., Tarnocai et al., 2009; Zimov et al., 2009), and vast amounts of methane, in a solid form as gas hydrates, are trapped in permafrost and at shallow depths in cold ocean sediments (e.g., Romanovskii et al., 2005). With increasing temperature of the permafrost (Romanovsky et al., 2010) and the water at the seafloor, as a result of increased surface warming in Arctic regions (Stocker et al., 2013), a widespread increase in the thickness of the thawed layer and the decomposition of hydrates could lead to the release of large quantities of CH_4 (and CO_2) to the atmosphere (ACIA, 2004, 2005; Anisimov et al., 1997; Goulden et al., 1998; Michaelson et al., 1996) as well as an enhanced mobilization and export of old, previously frozen soil-derived organic carbon (e.g., Bröder et al., 2018; Bröder et al., 2019; Schuur et al., 2008; Tesi et al., 2016; Vonk et al., 2012; Winterfeld et al., 2015, 2018). The release of these greenhouse gases in turn would create a positive feedback mechanism that can amplify regional and global warming.

3. Recent Arctic Climate Change, Future Predictions, and Paleorecords

During the 1990s, it became widely recognized that the Arctic was undergoing a dramatic change (Dickson et al., 2000; Macdonald, 1996; Morison et al., 2000; Moritz et al., 2002; Serreze et al., 2000). Over the past decades, a significant increase in Siberian river discharge, associated with a warmer climate and enhanced precipitation in the river basins, has been observed (Semiletov et al., 2000; Serreze et al., 2000; Peterson et al., 2002). At the same time, an increase in the amount and temperature of Atlantic Water inflow into the Arctic, a reduced sea-ice cover, a thawing of permafrost, and a retreat of small Arctic glaciers are observed (Dickson et al., 2000; Serreze et al., 2000).

The most obvious indicator for the ongoing rapid changes in the climate state of our planet, however, is certainly the observed loss in Arctic sea ice (Serreze et al., 2007; Notz & Stroeve, 2018; Stroeve & Notz, 2018). Over the past three to four decades, coincident with global warming and atmospheric CO_2 increase, Arctic sea ice has significantly decreased in its extent (Figure 5) as well as in thickness (Cavalieri & Parkinson, 2012; Kwok & Cunningham, 2015; Stocker et al., 2013; Stroeve et al., 2007, 2012). The loss of sea ice results in a distinct decrease in albedo, causing further warming of ocean surface waters. When extrapolating this trend, the central Arctic Ocean might become ice-free during summers within about the next three to five decades or even sooner, depending on the different IPCC scenarios used for prediction (Figure 5; Wang & Overland, 2012; Stocker et al., 2013; Niederdrenk & Notz, 2018; Notz & Stroeve, 2018; Stroeve & Notz, 2018; Screen & Deser, 2019). Furthermore, the recent decrease in sea ice seems to be more rapid than predicted by climate models (Figure 5; Stroeve et al., 2007, 2012), suggesting that the processes causing these recent rapid climate changes are still not fully understood and subject of intense scientific and societal debate. Based on the relationship between the September sea-ice extent and cumulative atmospheric CO_2 emissions, however, Notz and Stroeve (2016) have demonstrated quite clearly that the observed decrease in sea-ice cover is mainly driven by anthropogenic warming. Based on their records, these authors emphasized the importance of limiting future CO_2 emissions to values compatible with a global warming well below 2 °C in order to keep the ice cover during summer (cf.Sigmond et al., 2018 ; Stroeve & Notz, 2018). In any case, a key aspect within the debate about present climate change is to distinguish and quantify

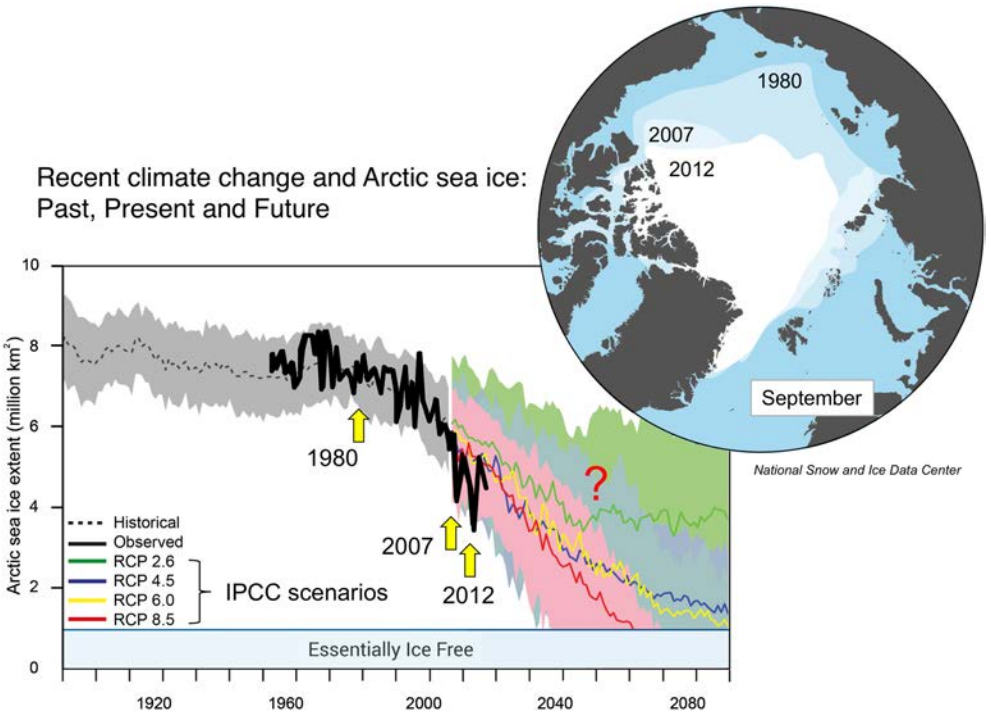

Figure 5. September sea ice extent in the Arctic Ocean (1890–2090) based on historical data, direct observations/measurements, and projected by different climate models and different IPCC scenarios toward 2090. RCP = Representative Concentration Pathways of greenhouse gases in relation to the probable radiative forcing in 2100. The shaded area represents the standard deviation (Stocker et al., 2013; Stroeve et al., 2007; Stroeve et al., 2012). Map shows September sea-ice extent in 1980, 2007, and 2012 (Source: National Snow and Ice Data Center; https://nsidc.org/).

more precisely natural and anthropogenic forcing of global climate change and related sea ice decrease (AMAP, 2017; Stocker et al., 2013).

In order to better understand the processes controlling modern climate change and distinguish between natural and anthropogenic forcing, it is certainly very useful and important to study paleoclimate records. In general, such paleoclimate records document the natural climate, rates of change, and variability prior to anthropogenic influence. The instrumental records of temperature, salinity, precipitation, and other environmental observations span only a very short interval (<150 years) of the Earth's climate history and provide an inadequate perspective of natural climate variability, as they are biased by an unknown amplitude of anthropogenic forcing. Paleoclimate reconstructions, however, can be used to assess the sensitivity of the Earth's climate system to changes of different forcing parameters (e.g., CO_2) and to test the reliability of climate models by evaluating their simulations for conditions very different from the modern climate. In this context, not only high-resolution studies of the most recent (Holocene) climate history are of importance but also detailed studies of the earlier Earth history characterized by a much warmer (Greenhouse-type) global climate with elevated atmospheric CO_2 concentrations, such as the Late Cretaceous and the Paleogene (Hong & Lee, 2012; Kent & Muttoni, 2013; O'Brien et al., 2017; Zachos et al., 2008). A precise knowledge of rates and scales of past climate change are the only mode to separate natural and anthropogenic forcings and will enable us to further increase the reliability of climate change predictions. Thus, understanding the mechanisms of natural climate change is one of the major challenges for mankind in the coming years. In this context, the polar regions certainly play a key role, and detailed climate records from the Arctic Ocean spanning time intervals from the Cretaceous-Paleogene Greenhouse world to the Neogene-Quaternary Icehouse world will give new insight into the functioning of the Arctic Ocean within the global climate system.

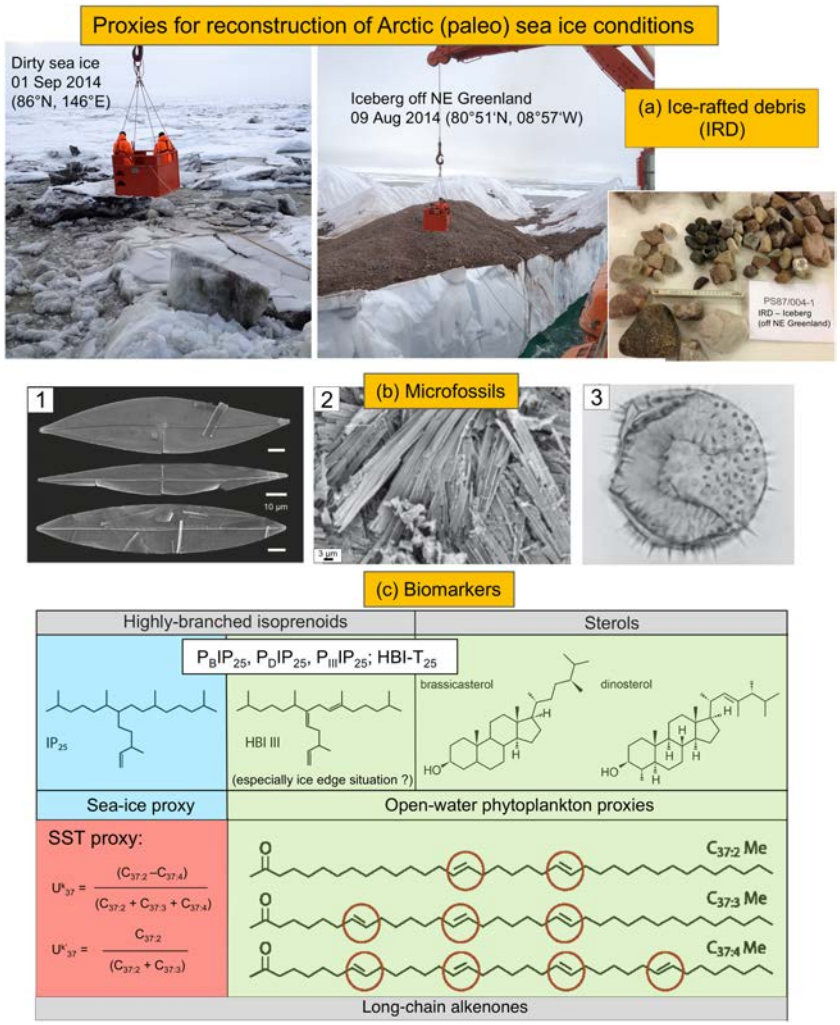

Figure 6. Proxies for reconstruction of Arctic (paleo) sea ice conditions and sea-surface temperature (SST). (a) Ice-rafted debris, (b) examples of microfossils (from left to right: modern sea-ice algae/Brown et al., 2014; Eocene sea-ice algae/Stickley et al., 2009; dinocyst *Islandinium minutum*/de Vernal & Rochon, 2011), and (c) specific biomarkers indicative for sea ice cover ("IP_{25}"), phytoplankton open-water productivity (specific sterols, highly brached isoprenoids (HBIs), and long-chain alkenones) and SST. By combining IP_{25} and open-water phytoplankton biomarkers ("PIP_{25}"; cf. Müller et al., 2011) or specific HBIs ("HBI-T_{25}"; cf. Belt et al., 2019), even information about temporal and spatial changes in sea-ice coverage can be obtained (for further details, see text).

4. Proxies for Reconstructing Past Arctic Ocean Paleoenvironmental Conditions

What type of proxies are available for reconstruction of Arctic paleoclimate and, especially, paleo-sea ice conditions? A large number of studies are based on sedimentological, mineralogical, geochemical, and geophysical data (e.g., Darby, 2003, 2008, 2014; Jakobsson et al., 2014; Knies et al., 2000; Nørgaard-Pedersen et al., 2003; Polyak et al., 2010; Spielhagen et al., 2004), as well as microfossils such as diatoms, dinoflagellates, ostracods, coccoliths, and foraminifers (e.g., Koç et al., 1993; Matthiessen et al., 2001, Matthiessen, Brinkhuis, et al., 2009; Sarnthein et al., 2003; Polyak et al., 2010; de Vernal & Rochon, 2011; Cronin et al., 2013; De Vernal, Gersonde, et al., 2013; De Vernal, Rochon, et al., 2013; Seidenkrantz, 2013; Limoges et al., 2018; Figure 6). These proxies may give information about water-mass characteristics (e.g., temperature, salinity, oxygenation, and ocean currents), primary productivity, sea-ice cover, iceberg-related processes and discharge, sources and pathways of terrigenous sediment fractions, etc. (for overviews, see Hillaire-Marcel & de Vernal, 2007; Stein, 2008). As the reconstruction of Arctic sea ice history is a major focus of this review, sea-ice indicative proxies are discussed in some more detail in the following paragraphs.

Sea ice often contains large amount of terrigenous material that has been entrained into the ice in the marginal seas (sediment-laden or "dirty" sea ice; Figure 6a; e.g., Pfirman et al., 1989; Nürnberg et al., 1994; Eicken et al., 1997, Eicken et al., 2005; Dethleff et al., 2000). In areas of sea-ice melting, sediment particles are released and deposited at the sea floor, contributing significantly to the present and past Arctic Ocean sedimentary budget. This sea-ice sediment—or "ice-rafted debris (IRD)"—mainly consists of terrigenous material with clay minerals, quartz, feldspars, heavy minerals, and specific Fe oxide grains as the main components. The mineralogy of sea-ice sediments may be very variable in time and space, depending on the geology of the source areas in the hinterland. Thus, studies of the mineralogical composition may allow the identification of source areas of the IRD particles and, based on these data, the reconstruction of past and present transport pathways (e.g., Nürnberg et al., 1994; Wahsner et al., 1999; Darby, 2003, 2014; see Stein, 2008 for review). IRD, however, can also be transported by icebergs (Figure 6a). If IRD is related to iceberg transport and not sea ice, the IRD proxy records the existence of extended continental ice sheets reaching the shelf-break. Here a first-order proxy to discriminate between sea-ice and iceberg-rafted sediments is the grain-size distribution. It is generally accepted that very coarse-grained material >250 μm up to pebble size (Figure 6a) are mainly restricted to iceberg transport, whereas the dominance of finer-grained (silt and clay) sediments are more typical for sea-ice transport (e.g., Clark & Hanson, 1983; Nørgaard-Pedersen et al., 1998; Spielhagen et al., 2004; Dethleff, 2005).

Sea-ice associated organisms like pennate ice diatoms are frequently used for reconstructing present and past sea-ice conditions (e.g., Koç et al., 1993; Stickley et al., 2009). However, it has also been shown that the preservation of fragile siliceous diatom frustules can be relatively poor in surface sediments from the Arctic realm, and the same is also true (if not worse) for calcareous-walled microfossils, thus limiting their applicability (Matthiessen et al., 2001; Schlüter et al., 2000; Steinsund & Hald, 1994). De Vernal, Rochon, et al. (2013) present a status report about reconstructing past sea-ice cover of the Northern Hemisphere using dinoflagellate cysts. Based on a study of Arctic Greenland shelf sediments, Limoges et al. (2018) provide new insights into the distribution of a sea ice-associated dinoflagellate species, species *Polarella glacialis* and its cysts, and propose that this species might have the potential to become a useful proxy for reconstructing past seasonal sea ice.

A multiproxy approach considering sediment texture in combination with lithology and sediment provenance as well as micropaleontological and geochemical data indicative for surface-water characteristics certainly provides a much sounder interpretation of sea-ice versus iceberg-rafted sediments and reconstruction of past sea-ice conditions.

The ability to (semi-)quantitatively reconstruct paleo-sea-ice distributions has been significantly improved by a biomarker approach based on determination of a highly branched isoprenoid (HBI) with 25 carbons (C_{25} HBI monoene—"IP_{25}"; Figure 6c; Belt et al., 2007). This biomarker is only biosynthesized by specific diatoms living in Arctic sea ice (Figure 6b; Brown et al., 2014); that is, its presence in the sediment is a direct proof of the presence of past Arctic sea ice. Furthermore, IP_{25} appears to be a specific, sensitive, and stable proxy for Arctic sea ice in sedimentary sections representing late Miocene to Holocene times (Belt, 2018; Belt & Müller, 2013; Knies et al., 2014; Stein et al., 2012, 2016, and references therein). When using this proxy, however, one has to consider that IP_{25} is more or less absent under a permanent sea-ice cover that limits light penetration and, in consequence, sea-ice algal growth. The same consequence applies to totally ice-free conditions where no ice algae live, that is, $IP_{25} = 0$. This difficulty in interpreting IP_{25} data can be overcome by the additional use of phytoplankton-derived, open-water biomarkers such as brassicasterol and dinosterol (Müller et al., 2009, 2011) or specific tri-unsaturated HBIs (Belt et al., 2015, 2019; Limoges et al., 2018; Ribeiro et al., 2017; Smik et al., 2016). By combining the environmental information carried by IP_{25} and the different phytoplankton biomarkers (Figure 6c), even more semiquantitative estimates of present and past sea-ice coverage, seasonal variability, and marginal ice zone situations are possible (Müller et al., 2011; Belt et al., 2015, 2019; Stein et al., 2017; for recent and critical review of this biomarker approach, see Belt, 2018).

Another useful option to distinguish between the two "$IP_{25} = 0$" extremes, that is, ice-free versus thick closed ice coverage, is the determination of SST. SST values significantly above 0 °C give important information about surface water characteristics per se, but also clearly point to ice-free conditions if $IP_{25} = 0$. For reconstructions of past SST conditions in the central Arctic Ocean during the Cretaceous, Paleocene-Eocene and Miocene, very promising biomarker SST tools such as the alkenone-based U^{K}_{37} index (Brassell et al., 1986;

Prahl & Wakeham, 1987) and the TEX_{86} index (Schouten et al., 2002, 2004) have been used successfully (Jenkyns et al., 2004; Sluijs et al., 2006, Sluijs et al., 2009; Weller & Stein, 2008; Stein, Weller, et al., 2014; for further discussion, see below).

The alkenone-based U^{K}_{37} approach evolved from the observation that certain microalgae of the class *Prymnesiophyceae*, notably the marine coccolithophorids *Emiliania huxleyi* and *Gephyrocapsa oceanica* (e.g., Conte et al., 1992; Marlowe et al., 1984; Volkman et al., 1980), and presumably other living and extinct members of the family *Gephyrocapsae* (Marlowe et al., 1990; Müller et al., 1998), have or had the capability to synthesize alkenones whose extent of unsaturation changes with growth temperature (Brassell et al., 1986; Marlowe et al., 1984; Prahl & Wakeham, 1987). Based on this correlation, paleo-SST can be calculated from the so-called ketone unsaturation index U^{K}_{37} or the simplified version of the index U^{K}_{37}' (Figure 6c; Brassell et al., 1986; Prahl & Wakeham, 1987; Müller et al., 1998). The TEX_{86} approach is based on specific membrane lipids, that is, tetraether lipids (glycerol dialkyl glycerol tetraethers) with 0–4 cyclopentane rings and, in one case, a cyclohexane ring, synthesized by marine *Crenarchaeota* (Schouten et al., 2002). As shown in a study of marine surface sediments from the world oceans, these organisms adjust the composition of these tetraether lipids in response to SST (Ho et al., 2014; Kim et al., 2008; Schouten et al., 2002, 2004; Weijers et al., 2006; Wuchter et al., 2004). This response is quantified as the so-called TEX_{86} (tetraether index of 86 carbon atoms).

5. Long-Term Climate Change From Greenhouse to Icehouse Conditions

The Mesozoic to Cenozoic time interval is a period when the climate on Earth changed from one extreme (Cretaceous-Paleogene Greenhouse lacking major ice sheets) to another (Neogene Icehouse with bipolar glaciation; Figure 7; Pearson & Palmer, 2000; Norris et al., 2002; Zachos et al., 2008; Friedrich et al., 2012; Kent & Muttoni, 2013; O'Brien et al., 2017; O'Connor et al., 2019). This long-term climatic evolution, including prominent warm and cold phases, is best reflected in marine deep-water and surface-water temperatures determined from benthic and planktic oxygen isotope, Mg/Ca thermometry, and biomarker (TEX_{86} and U^{K}_{37}) records, respectively, from low to middle latitudes (e.g., Alsenz et al., 2013; Bijl et al., 2009; Friedrich et al., 2012; Lear et al., 2000; Littler et al., 2011; Liu et al., 2009; Miller et al., 1987; Mutterlose et al., 2010; O'Brien et al., 2017; Zachos et al., 2001; Zachos et al., 2008). Peak warm intervals occurred around the Cenomanian/Turonian boundary, during the Paleocene-Eocene Thermal Maximum (PETM), the Early Eocene Climate Optimum (EECO), and the Middle Eocene Climate Optimum (Figure 7), most probably related to higher atmospheric CO_2 concentrations. The long-term, post-EECO high-latitude cooling started near 50 Ma and is punctuated by four major steps in the early mid-Eocene (about 48–45 Ma), at the Eocene/Oligocene boundary (near 34 Ma), in the mid-Miocene (at about 14 Ma), and in the mid-Pliocene (at about 3.5–2.6 Ma; Figure 7; Miller et al., 1987; Lear et al., 2000; Pearson & Palmer, 2000; Zachos et al., 2001, Zachos et al., 2008; Westerhold & Röhl, 2009). Furthermore, long-term climatic changes on global and regional (e.g., Arctic) scales are also controlled by plate tectonic processes such as opening and closure of oceanic gateways, isolating single ocean basins from the World Ocean, configuration of continents, and uplift of mountain ranges and plateaus (Hay et al., 1999; Scotese, 2001; Müller et al., 2008; references with focus on the Arctic Ocean: Kristoffersen, 1990; Grantz et al., 2011; Shephard et al., 2013; Kanao et al., 2015; Petrov et al., 2016).

The long-term paleoclimatic and paleoceanographic history of the Arctic Ocean through this time interval, however, is still poorly known in comparison to other world ocean areas. Major information on the paleoenvironment of the early Arctic is derived from circum-Arctic terrestrial data sets (for references, see next sections) and—concerning the marine records—from petroleum exploration drill holes from the Arctic marginal seas (e.g., Leith et al., 1992; Spencer et al., 2011) and Deep-Sea Drilling Project and ODP drill cores from subarctic regions (Leg 38: Talwani et al., 1976; Leg 104: Eldholm et al., 1989; Leg 105: Srivastava et al., 1989; Leg 151: Thiede et al., 1996; Leg 152: Larsen et al., 1994; Leg 162: Raymo et al., 1999; see Figure 1 for locations). Direct information from sediment cores derived from the central Arctic Ocean is restricted to a very few short sections—at least prior to the IODP-ACEX drilling campaign in 2004 (Figure 7; Thiede et al., 1990; Backman et al., 2008; see below). From Figure 7 it is obvious that for almost the entire Miocene, the Oligocene, Eocene, and Paleocene, no sediment-core data are available at all. For the Cretaceous, data from

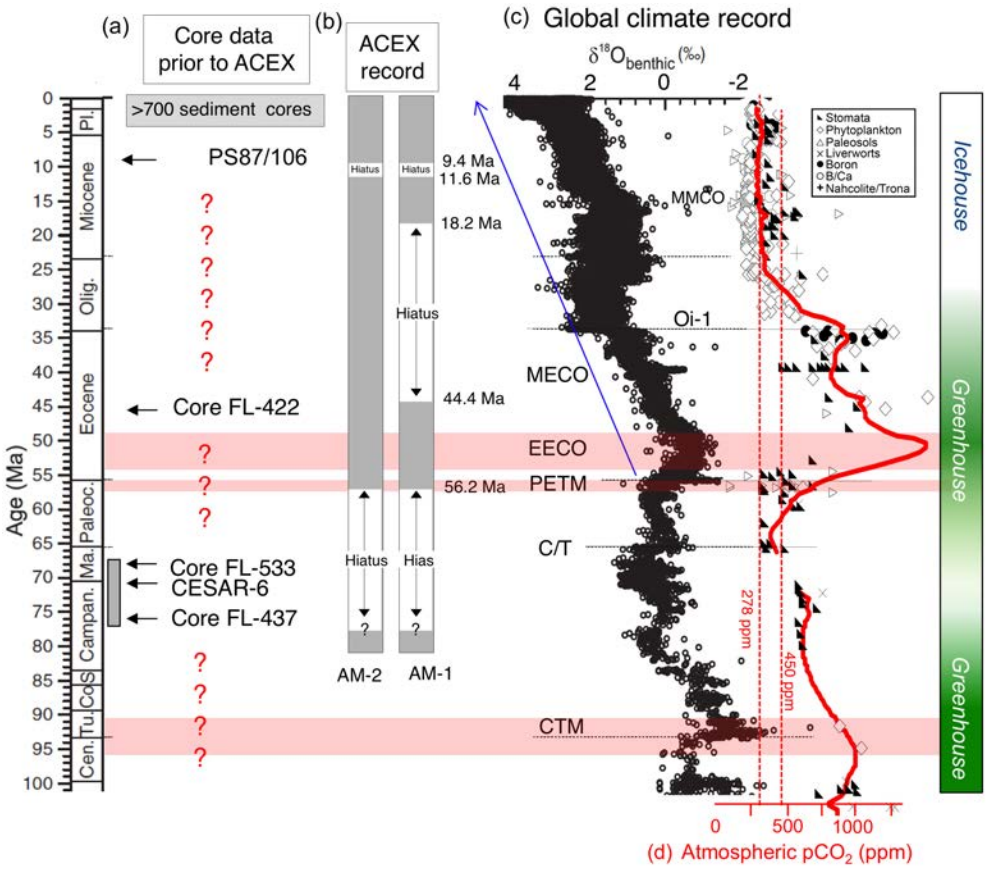

Figure 7. (a) Stratigraphic coverage of existing sediment cores in the central Arctic Ocean prior to IODP-ACEX (2004) over the last 100 Ma, including the four short cores representing short sections of Eocene and/or Maastrichtian/Campanian sediments (Backman et al., 2008; Stein et al., 2015; Thiede et al., 1990) and one core representing late Miocene sediments (Stein, 2015; Stein et al., 2016). Red question marks indicate time interval with no information. (b) The stratigraphic range of the sedimentary section recovered during the ACEX drilling expedition used on the two age models by Backman et al. (2008; AM-1) and Poirier and Hillaire-Marcel (2011; AM-2). (c) Global $\delta^{18}O$ stack of benthic foraminifera for the past 100 million years representing the Greenhouse-Icehouse transition (Friedrich et al., 2012; Zachos et al., 2008). CTM = Cretaceous Thermal Maximum (Cenomanian/Turonian boundary); C/T = Cretaceous/Tertiary Boundary; PETM = Paleocene-Eocene Thermal Maximum; EECO = Early Eocene Climate Optimum; MECO = Middle Eocene Climate Optimum; Oi-1 = Major Oligocene Glaciation Event; MMCO = Middle Miocene Climate Optimum. (d) Single data points and smoothed record (red line) of atmospheric CO_2 estimates from various proxies (see different symbols), based on compilations by Royer (2010) for the pre-70-Ma interval and by Beerling and Royer (2011) for the post-70-Ma interval (Kent & Muttoni, 2013, supplemented). Red stippled lines indicate atmospheric CO_2 levels of 278 (preindustrial value) and 450 ppm, respectively.

central Arctic Ocean cores are limited to three short sections representing isolated, discontinuous fragments of the late Campanian and Maastrichtian climate history (see next section).

5.1. The Cretaceous Arctic Ocean: Warm, Euxinic, and Productive, but Occasionally Ice

Up to the 1980s, the general global climate of the Cretaceous was viewed as a period of great warmth over the entire globe (Frakes, 1979; Hallam, 1985). According to these authors, tropical-subtropical conditions prevailed to at least 45°N and possibly to 70°S, and warm to cool-temperate climates extended to the ice-free polar regions. Such a greenhouse world was characterized by significantly higher temperatures and reduced latitudinal temperature gradients (O'Brien et al., 2017; Robinson et al., 2019; Sinninghe Damsté et al., 2010). The overall warm climatic conditions most likely resulted from an enhanced greenhouse effect due to higher atmospheric CO_2 concentrations as inferred from various proxies (Figure 7; Crowley & Berner, 2001; Royer, 2010; Kent & Muttoni, 2013; Foster et al., 2017) and conventionally attributed to the balance between the input of CO_2 from ocean crust production, volcanism, metamorphism, and organic carbon weathering and the output of CO_2 from silicate weathering and organic carbon burial (Foster et al., 2017; Kent & Muttoni, 2013; Walker et al., 1981; Weissert & Erba, 2004). During the 1990s, however, the view of constant equable warmth and sluggish oceanic circulation during the Cretaceous was questioned, and much more

variable climatic conditions were suggested for this time period (e.g., Kemper, 1987; Miller et al., 2005; Mutterlose et al., 2003; Price et al., 2000; Weissert & Lini, 1991). Even if warm climates in the high latitudes dominated much of the Cretaceous (to early Eocene) and warmth may have been caused by high CO_2, short intervals of more restricted glaciations probably occurred (at least) on Antarctica (Miller et al., 2005). These authors propose a vision of Earth's cryospheric evolution that reconciles warm, generally ice-free poles with cold snaps that resulted in glacio-eustatic lowerings of 20–40 m, probably driven by orbital forcing (Matthews & Frohlich, 2002; DeConto & Pollard, 2003; for general review and references, see Haq, 2014).

The availability of nutrients and elevated atmospheric CO_2 may have stimulated primary production, which is thought to be one of the main factors (besides bottom-water stagnation) causing anoxic conditions in large parts of the oceans (e.g., Arthur et al., 1984, 1987; de Graciansky et al., 1984; Demaison & Moore, 1980; Erbacher et al., 2001; Ohkouchi et al., 2015; Schlanger & Jenkyns, 1976). These major episodes are known as "oceanic anoxic events" (Schlanger & Jenkyns, 1976) and represent major perturbations in the global climate and ocean system defined by massive organic carbon (OC) burial and black shale formation in marine environments. Oceanic anoxic events occurred on a regional to worldwide scale with the most prominent and widespread ones in the Toarcian, the Valanginian, the Aptian-Albian, the Cenomanian-Turonian, and the Coniacian-Santonian (Arthur et al., 1984, 1987; Brumsack, 1980; de Graciansky et al., 1984; Erba et al., 2004, 2015; Erba et al., 2019; Gambacorta et al., 2016; Méhay et al., 2009; Ohkouchi et al., 2015; Rais et al., 2007; Schlanger & Jenkyns, 1976; Stein et al., 1986). Upper Jurassic to Cretaceous black shales were also deposited in all the large circum-Arctic sedimentary basins (e.g., North Alaskan Basin, Mackenzie Delta Basin, Sverdrup Basin, Barents Shelf, and western Siberia) that are highly productive in terms of gas and oil (e.g., Bakke et al., 1998; Dixon et al., 1992; Leith et al., 1992; Lenniger et al., 2014; Spencer et al., 2011).

A dominantly warm climate probably existed in the Northern High Latitudes during Middle to Late Cretaceous times as indicated by the presence of deciduous trees and leaves with characteristic morphologies, at 80–85°N (Herman & Spicer, 1996; Parrish & Spicer, 1988; Spicer & Herman, 2010), the presence of crocodiles beyond 60°N (Markwick, 1998), and most specifically, the discovery of champosaurs (cold-blooded reptiles; closest living relatives are crocodiles) in the Turonian of the Sverdrup Basin (Axel Heiberg Island) at 72°N paleolatitude (Tarduno et al., 1998; Huber, 1998; for summary, see O'Regan et al., 2011). Besides indication for a relatively warm (sub-) Arctic climate during Cretaceous times, there are also signals pointing to cold climatic conditions. In particular for parts of the Early Cretaceous, hints of Icehouse conditions or at least cool climates in the higher latitudes were found. Glendonites (pseudomorphs of the low-temperature hydrated form of calcium carbonate, ikaiite) found in lower Valanginian and upper Aptian sediments from the Sverdrup Basin in Arctic Canada (70–80°N paleolatitude) imply that Early Cretaceous seawater temperatures were at times close to freezing (Kemper, 1987). Almost certainly these cooler temperatures record global changes because, at least in the case of the late Aptian, coeval glendonites are also known from the Southern Hemisphere, found in the Eromanga Basin in Australia at a paleolatitude of 65°S (De Lurio & Frakes, 1999; Frakes & Francis, 1988). Furthermore, Frakes and Francis (1988) postulate at least seasonally cold ocean temperatures and limited polar ice caps for the Early Cretaceous from the occurrence of ice-rafted deposits in Siberia, Australia, and Spitsbergen. Nannofossil assemblages from offshore mid-Norway and the Barents Sea also suggest cold conditions (Mutterlose et al., 2003; Mutterlose & Kessels, 2000). Based on oxygen stable isotope paleothermometry of well-preserved Middle Jurassic to Lower Cretaceous belemnites from Kong Karls Land, Svalbard, cool high-latitude marine paleotemperatures of <8 °C were estimated for the early to middle Valanginian, which may be compatible with the formation of high-latitude ice (Ditchfield, 1997).

What about marine sedimentary records from the Arctic Ocean representing information about climatic conditions during (late Jurassic to) Cretaceous times, that is, at times when the Arctic Ocean was probably much more isolated from the world ocean in terms of deep-water connection (Figure 8)? The isolation of the Arctic Ocean at those times was an important prerequisite for the development of widespread anoxic/euxinic conditions during the Late Jurassic/Early Cretaceous (e.g., Spencer et al., 2011). As already mentioned above, most of the sedimentological, micropaleontological, and geochemical data available for paleoenvironmental reconstructions of the Arctic realm during this time interval are from petroleum exploration drill holes from the marginal seas such as the Barents Sea and along the Norwegian continental

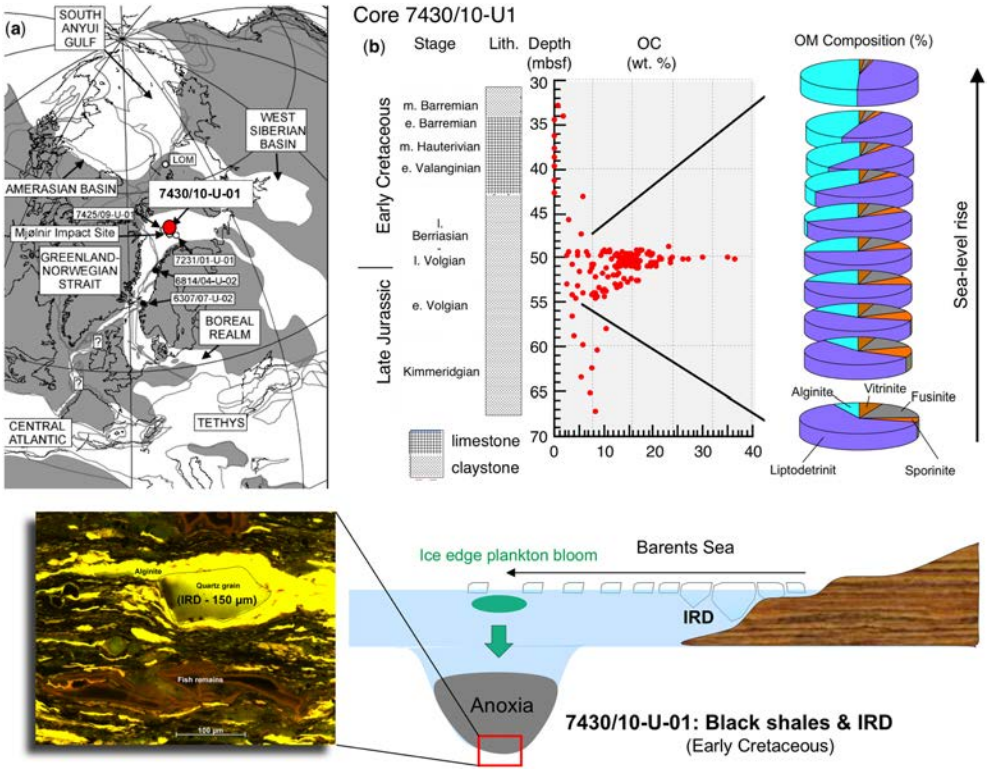

Figure 8. (a) Paleogeographic map for the Valanginian (lowermost Cretaceous) from Africa to the Arctic, showing transcontinental seaways, major marine embayments and basins, and selected cores west and north of Norway (Mutterlose et al., 2003). Core 7430/10-U-01 is marked as a red circle. (b) Core depth, stratigraphic correlation, lithology, regional formational limits, and total organic carbon (TOC) record of the interval between 67 and 32 mbsf of Core 7430/10-U-01. For the TOC-rich interval between 49 and 55 mbsf, organic matter composition has been determined in detail by means of maceral analysis. For maceral analysis, small blocks of rock (3–4 cm^3) were collected perpendicular to the bedding and fixed by a cold-setting epoxy resin, polished, and analyzed by point-counting with a 25-point ocular grid using a Zeiss Axiophot microscope under incident and fluorescence light (cf. Langrock et al., 2003a). The records were correlated and interpreted in relationship to the global sea-level curve of Haq et al. (1988). Photograph of a finely laminated section showing layers of algae-type organic matter (yellow color due to fluorescence light) and fish remains, alternating with nonorganic siliciclastic layers (black). The cartoon illustrates the interpretation of organic-carbon data in terms of paleoenvironmental situation (Langrock et al., 2003a, supplemented).

margin (Figure 8), whereas data from the central Arctic Ocean are restricted to a few short sediment cores (Figure 9; see below).

In the southern Barents Sea, for example, OC-rich sediments of Late Jurassic/Early Cretaceous age were recovered, characterized by OC contents of up to about 35% (Figure 8; Langrock et al., 2003a). High hydrogen-index values of 400–600 mg HC/g C obtained by Rock-Eval pyrolysis (Langrock et al., 2003a) and maceral compositions of the sediments dominated by lipid-rich organic matter derived from mainly marine but also brackish and freshwater algae ("alginites") as well as fine-grained "liptodetrinites" (Figure 8) support a type II kerogen characterization. The excellent preservation of the labile, easily degradable organic matter particles and the significant amounts of freshwater algae argue for deposition in a restricted shallow basin very close to land rather than an upwelling regime (Arthur et al., 1987; Taylor et al., 1998). The increasing OC content in the late Volgian section was most likely caused by a combination of increasing preservation by bottom-water anoxia, coupled with periods of increasing primary production as well as a low and decreasing dilution of clastic material, related to a marked rise in sea level (Figure 8; Langrock et al., 2003a). During the Late Jurassic and Early Cretaceous, such anoxic conditions proposed for large parts of the proto-Arctic Ocean, probably extended toward the south into the Norwegian-Greenland Sea as shown in geochemistry and microscopy data sets from black shale sequences recovered in drill cores along the Norwegian shelf (Figure 8; Langrock et al., 2003b; Langrock & Stein, 2004). The high abundance of autochthonous small-sized pyrite framboids indicative for an anoxic water column (i.e., under euxinic conditions), such as typical for the modern Black Sea (cf. Wilkin et al., 1997), the carbon-sulfur-iron

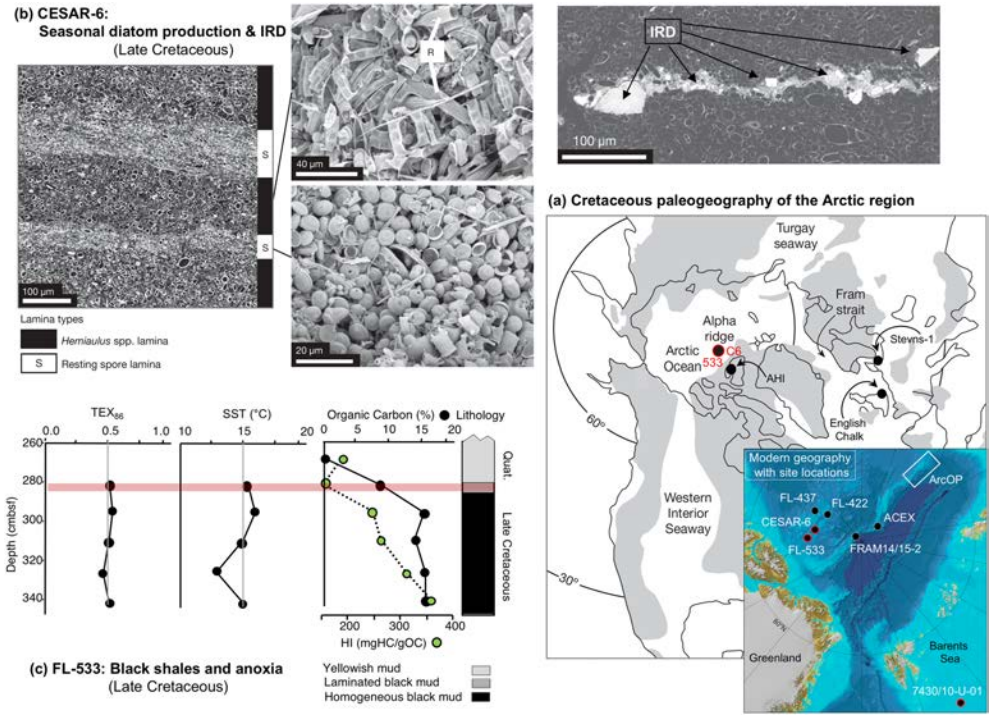

Figure 9. (a) Map showing the late Cretaceous paleogeography of the Arctic region with the Alpha Ridge and the locations of sites CESAR-6 (C6) and FL-533, and the locations of the English Chalk and Boreal Chalk Sea (Stevns-1 Core) sections; inset shows modern geography and locations of cores CESAR-6, FL-437 and Fl-533 (Alpha Ridge), the ACEX site (Lomonosov Ridge), Core FRAM14/15-2 (Lomonosov Ridge), and Core 7430/10-U-01 (Barents Sea). (b) Core CESAR-6: Backscattered Electron Image of resin-embedded sediment showing darker diatom vegetative cell laminae, interbedded with paler layers composed primarily of diatom resting spores, and enlargements of representative topographic SEM images of the diatom vegetative cells and the diatom resting spores, and thin laminae of poorly sorted terrigenous sediment occurring dominantly within the spring diatom bloom layer, interpreted as evidence for ice-rafted debris (IRD; Davies et al., 2009). (c) TEX_{86} values and related SST values (Jenkyns et al., 2004), and organic carbon, hydrogen index values, and lithologies of the lowermost upper Cretaceous section of Core FL-533 (data from Clark et al., 1986; Firth & Clark, 1998).

relationships (cf.Hofmann et al., 2000 ; Lückge et al., 1996), the high concentrations of Mo, and the Re/Mo ratios also support widespread euxinic conditions (Langrock et al., 2003a, 2003b; Lipinski et al., 2003).

In addition, patchily distributed, coarse-grained minerals (apparently quartz) are found, which are 60 to 200 µm in diameter (Figure 8). These minerals could not have been transported along with the claystone facies. Here a possible mechanism for the input of these large sand grains was ice rafting. Episodes of a relatively cool climate were already suggested for the earliest Cretaceous Boreal realm as described above. Hence, episodic (or even seasonal) IRD input might have occurred in the late Volgian Barents Sea (Figure 8) at a paleolatitude of almost 55°N (Langrock et al., 2003a).

In the central Arctic Ocean, Cretaceous sediments were only cored at three locations on the Alpha Ridge: cores Fl-437 and Fl-533 taken during the drift of the ice-island T-3 from 1963 to 1974 and Core CESAR-6 of the Canadian Expedition to Study the Alpha Ridge (CESAR) in 1983 (Figure 9a; Thiede et al., 1990). In 2004, an about 3-m-thick interval of Campanian very dark gray clayey mud and silty sands with OC values of about 1–2% was recovered in the lowermost part of the ACEX record from Lomonosov Ridge (Backman et al., 2006; Stein, 2007). During the FRAM-2014/2015 Ice Drift Expedition (Kristoffersen et al., 2016; Kristoffersen & Tholfsen, 2016), a 300-m-thick sequence of flat-lying Cenozoic sediments overlying dipping (probably) Mesozoic sediments, separated by an unconformity, were recognized in a seismic reflection profile across Lomonosov Ridge close to the North Pole (the age classification proposed by the authors is based on comparison with the ACEX drilling results). A gravity corer was dropped down where the potential for exposure of sedimentary rocks below the unconformity was high, and, as result, a short core (FRAM14/15-2) containing a "20 cm thick section of very cohesive, light cream colored sediments – something we have not seen so far from the Arctic Ocean" was recovered (Kristoffersen & Tholfsen, 2016; see Figure 9a for core

location). These sediments are almost pure siliceous oozes composed of well-preserved diatoms, radiolarians, silicoflagellates, etc. (first observations by R. Stein, unpubl. data, 2019). More detailed work by micropaleontologists on the species identification and age determination (Campanian/Maastrichtian? or younger?) are in process now; thus, no further discussion is presented at this stage.

At Core CESAR-6, siliceous, well-laminated Campanian-Maastrichtian sediments with excellently preserved microfossils were retrieved (Jackson et al., 1985). Very similar sediments of Campanian age were also recovered at Core Fl-437: a yellowish laminated siliceous ooze rich in diatoms, ebrideans, silicoflagellates, and archaeomonads with sparse fish remains (Clark et al., 1986; Dell'Agnese & Clark, 1994). More recently, Davies et al. (2009), Davies et al., 2011) analyzed in detail the laminated section of Core CESAR-6 using "backscattered electron imagery" and identified a seasonal succession of two distinct lamina types that represent an annual lamina couplet (Figure 9b). Type A of laminae consists of diatom resting spores representing flux from the spring bloom, and type B of laminae consists of diatom vegetative cells representing flux from production during the stratified months of the Arctic summer (Davies et al., 2011). In some of these lamina couplets, coarse-grained terrigenous particles (mainly quartz) indicative of ice-rafting (IRD) were found (Figure 9b). The diatom laminae point to a strong seasonality, that is, to ice-free summers, whereas the presence of IRD is interpreted as a signal for sea ice that occasionally may have occurred during severe winters (Davies et al., 2009; Davies et al., 2011).

In Core Fl-533, the lowermost 67 cm of the 348-cm-long sequence comprise OC-rich black mud (black shales) of early Maastrichtian age (Clark et al., 1986; Firth & Clark, 1998). These black shales are characterized by very high OC contents of up to almost 16% and hydrogen index values of about 250 to 350 mg HC/g OC (Figure 9c), indicating an immature, mixed marine-terrigenous type of organic matter with major contributions from marine/aquatic algae. That means, both OC content and composition were totally different in comparison to those within the Quaternary deposits (Stein et al., 2001; Stein & Macdonald, 2004). Whereas the OC buried and preserved in Quaternary sediments is mainly refractory terrigenous matter, the OC found in the Cretaceous sediments mainly consists of labile algae-type organic matter. These data suggest that the Cretaceous Arctic Ocean basin may have been an important sink for algae-type OC (and CO_2) and, thus, of importance for the global climate system of that time.

In order to get some information about the Cretaceous SST of the central Arctic Ocean, Jenkyns et al. (2004) used the TEX_{86} approach (Schouten et al., 2002; see section 4) and analyzed black shale samples from Core Fl-533 for membrane lipids of marine Crenarchaeota (Figure 9c). The TEX_{86} results indicate an average Arctic Ocean SST of 15 ± 1 °C at a paleolatitude of about 80°N for that part of the early Maastrichtian represented by the black muds (Figure 9c). Considering the diatom and IRD data from the CESAR-6 Core (see above), this SST of about 15 °C should certainly represent summer conditions. A summer SST of about 15 °C and the presence of sea ice during winter may represent conditions similar to those described for the Eocene central Arctic Ocean (see section 5.2).

5.2. The Early Cenozoic Transition: Euxinic Conditions and Onset of Arctic Sea Ice

For the Arctic Ocean, information about the early Cenozoic climate history is quite limited (cf. Figure 7). A large amount of information is based on paleobotanic studies of circum-Arctic terrestrial outcrops. As reported from several localities around the Arctic Ocean such as Axel Heiberg Island, Ellesmere Island, Mackenzie Delta, Alaska, and the New Siberian Islands, floral and faunal assemblages indicate exceptionally warm and humid conditions during the late Paleocene-early Eocene (Basinger et al., 1994; Dolezych et al., 2018; Eberle et al., 2010; Eldrett et al., 2009; Greenwood et al., 2010; Salpin et al., 2018; Suan et al., 2017; West et al., 2015). Multiproxy data from early Eocene deltaic plain sediments of the Mackenzie Delta (Arctic Canada near 75°N), for example, indicate annual air temperatures averaging 21–22 and 10–14 °C in winter (Salpin et al., 2018). Late Paleocene mean annual shallow-marine temperatures between 11 and 22 °C were recorded from mollusk stable isotopes determined in sediments from the Prince Creek Formation (Alaska, 80°N; Brice et al., 1996). Direct information about paleoenvironmental conditions in the central Arctic Basin prior to the ACEX drilling in 2004 was coming from a single short sediment core obtained from the drifting ice island T3 in 1969 (Core FL-422; see Figure 9a for location). The sediments of this core representing part of the middle Eocene time interval are laminated, rich in siliceous microfossils, especially diatoms and silicoflagellates, and characterized by alternating layers of vegetative cells and resting spores, interpreted as evidence for strong seasonality, upwelling of nutrient-rich waters, and warm surface-

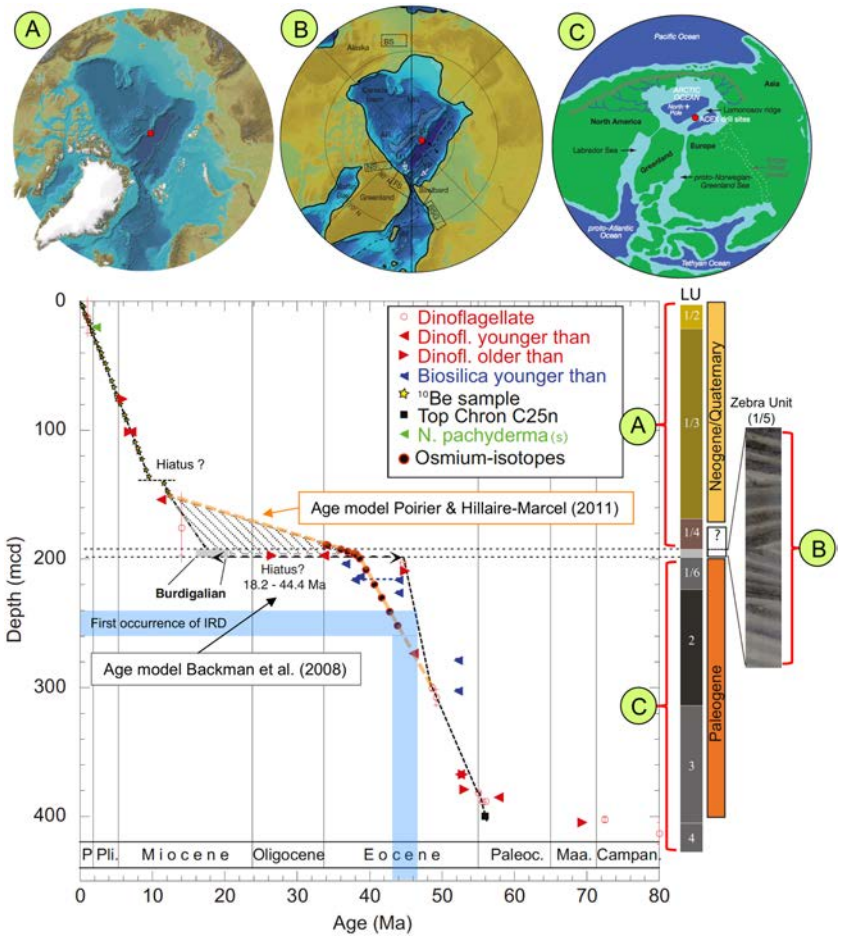

Figure 10. Age-depth diagram and main lithological units of the ACEX section (O'Regan, 2011, supplemented), based on the biostratigraphically derived age model by Backman et al. (2008) and the alternate chronology based on osmium isotopes (Poirier & Hillaire-Marcel, 2011). Depth of first occurrence of IRD between 240 and 260 mcd are marked as light blue horizontal bar. On top (a) International Bathymetric Chart of the Arctic Ocean (Jakobsson et al., 2012) representing modern boundary conditions with connections to the world ocean; (b) paleogeographic/paleobathymetric reconstruction for the late early Miocene. BSG = Barents Sea Gateway; JM = Jan Mayen Microcontinent; KR = Knipovich Ridge; MJ = Morris Jessup Rise; NS = Nares Strait; YP = Yermak Plateau (Jakobsson et al., 2007), and (c) Paleogeography of the Arctic region for the early middle Eocene during the phase of high biosilica production and preservation and euxinic conditions (50–45 Ma; Stickley et al., 2009). The location of the ACEX site is marked as a red circle.

water temperatures (Bukry, 1984; Clark, 1974; Dell'Agnese & Clark, 1994). As mentioned in the previous section, similar sediments with excellently preserved siliceous microfossils were also found in Core FRAM14/15-2 recovered from Lomonosov Ridge during the FRAM-2014/2015 Ice Drift Expedition (Kristoffersen & Tholfsen, 2016; Kristoffersen et al., 2016; for core location, see Figure 9a). However, the age of this sedimentary section (i.e., Campanian/Maastrichtian vs. Eocene) has not been determined yet.

With the ACEX drilling in 2004, a thick sequence of upper Cretaceous to Quaternary sediments became available for paleoclimatic reconstructions (Figure 10; Backman et al., 2006; Moran et al., 2006). These sediments are characterized by prominent changes in sediment composition and texture, suggesting drastic paleoenvironmental changes through time (Backman et al., 2006; Stein, 2007). Whereas the lower half of the ACEX sequence (Units 2 to 4) mainly consists of dark gray silty clay and biosiliceous ooze characterized by high TOC values of 1% to >5%, the upper half of the ACEX sequence (subunits 1/1 to 1/4) is composed of silty clay with very low TOC contents of <0.5% (Figure 11a), that is, values very similar to those known from upper Quaternary records determined in gravity cores from the Lomonosov Ridge and representing modern-type oxic deep-water conditions (Stein et al., 2001). In subunit 1/5 (about 193 to 199 m of composite depth (mcd)) characterized by distinct gray/black color bandings ("Zebra Unit"), TOC maxima of 7% to 14.5%

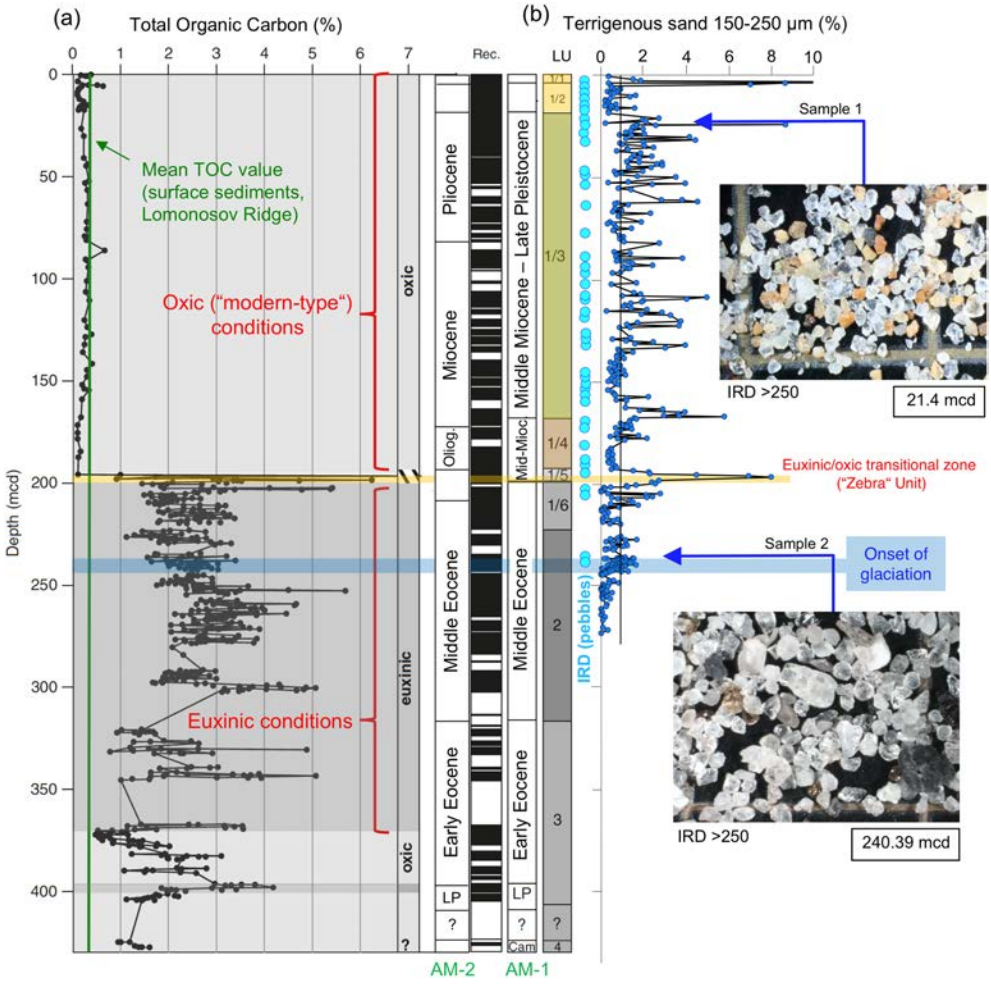

Figure 11. (a) Record of total organic carbon (TOC) contents as determined in the composite ACEX sedimentary sequence (Stein, 2007). Data on lithological units (LU) and core recovery (Rec.) from Backman et al. (2006). Age models AM-1 (Backman et al., 2008) and AM-2 (Poirier & Hillaire-Marcel, 2011) are shown. The "Zebra" Unit (Unit 1/5) marks the transition from an euxinic ocean to an oxygenated ocean that occurred when the formerly isolated Arctic Ocean became connected to the world ocean via Fram Strait (cf. Figure 10). Depending on the age model, this transition is in the mid-Miocene (17.5 Ma) or Oligocene (32 Ma). Cam = Campanian; LP = late Paleocene; Mid Mioc. = middle Miocene; L.Pl. = late Pleistocene. (b) Record of terrigenous sand (150–250 µm) interpreted as ice-rafted debris (IRD); blue circles mark occurrence of pebble-sized IRD (based on St. John, 2008). The onset of glaciation is marked as light blue bar. Photographs show coarse fraction >250 µm (IRD) in two samples from 240.39 and 21.4 m composite depth (mcd), respectively.

were measured (Stein, 2007). The Eocene section (about 200 to 385 mcd) characterized by high (algae-type) organic carbon content is mainly related to euxinic conditions predominant at that time when the Arctic Ocean was quite isolated from the world ocean (Figures 10 and 11; Backman et al., 2006; Stein et al., 2006, Stein, Weller, et al., 2014). The transition from euxinic conditions to the modern-type oxic conditions occurred during Oligocene-Miocene times and is related to the opening of Fram Strait, allowing the inflow of oxygen-rich deep water from the Atlantic into the Arctic Ocean (Jakobsson et al., 2007).

The exact timing of this prominent environmental change, that is, 17.5 versus 32 Ma, however, is still under debate and depends on the age model that is used, that is, Backman et al. (2008) versus Poirier and Hillaire-Marcel (2011); Figure 10). Backman et al. (2008) stratigraphic framework of the Cenozoic ACEX sequence is based on biostratigraphic, cosmogenic isotope, magneto- and cyclostratigraphic data, and they proposed a major hiatus spanning the time interval from 44.4 to 18.2 Ma. When following this age model, a large part of the climate history covering the transition from Greenhouse to Icehouse is missing in the ACEX

sequence (Figure 7b). That means, the late Eocene-Oligocene time interval characterized by major ice growth on Antarctica, global sea level drop, and possible growth of Northern Hemisphere ice sheets (Lear et al., 2000; Miller et al., 1987, 2005; Zachos et al., 2008) is not represented in the ACEX records. Poirier and Hillaire-Marcel (2011) report Rhenium-Osmium (Re-Os) isochron ages and complementary Os-isotope measurements, together with carbon and nitrogen data, that give information on the redox state of the sediment during deposition. Based on their new data, these authors challenged the existence of a major hiatus between subunits 1/6 and 1/5 (Figure 10). That means, they proposed an alternate age model sequence that closes the gap in the ACEX record, resulting in a more condensed sedimentary section with three to five times lower mean sedimentation rates (0.2–0.8 cm/kyr) between about 49 and 12 Ma (Figure 10). The alternate age model, of course, would significantly modify the reconstructions of the tectonic evolution of Lomonosov Ridge and the paleoclimatic Arctic Ocean history including the reconstruction of the early onset of sea ice in the Arctic Ocean during the Eocene. It questions the timing (i.e., early Miocene), duration, and mechanism (i.e., the opening of Fram Strait) for the sedimentological and geochemical transition recorded in the ACEX sequence (cf. Jakobsson et al., 2007).

Whereas it is widely accepted that near the Eocene/Oligocene boundary, large ice sheets first appeared on Antarctica, coincident with decreasing atmospheric carbon dioxide concentrations (Figure 7, "Oi-1 glaciation"; e.g., Shackleton & Kennett, 1975; Kennett & Shackleton, 1976; Miller et al., 1987; Lear et al., 2000; Zachos et al., 2001, Zachos et al., 2008; Escutia et al., 2011, 2014), the database for the onset of glacial conditions in the Northern High Latitudes is much more limited. Prior to the ACEX record, it was indirectly inferred from sub-Arctic IRD records in the Norwegian-Greenland Sea, Iceland Sea, and Irminger Sea and Fram Strait area that Northern Hemisphere Glaciation began at about 14 Ma (e.g., Thiede et al., 1998), that is, about 20 Ma later than the first appearance of large ice sheets on Antarctica. With the ACEX drilling results, however, the date of Northern Hemisphere cooling and the early onset of sea ice was pushed back into the Middle Eocene when for the first time significant amounts of IRD occur in ACEX sedimentary sequence at about 250-m core depth (Figure 11b; Backman et al., 2006, Backman et al., 2008; Moran et al., 2006; St. John, 2008; Stickley et al., 2009; Darby, 2014; Tripati & Darby, 2019). This early onset of Arctic sea-ice formation and the contemporaneous decrease in SST are clearly reflected in the ACEX micropaleontological (Stickley et al., 2009) and biomarker records (Stein et al., 2014).

The first occurrence of sea-ice related diatoms, contemporaneously with IRD, was at about 47–46 (when using the ACEX age model of Backman et al., 2008) or 44–41 Ma (when using the alternate chronology of Poirier & Hillaire-Marcel, 2011; "Age Model 2"; Figures 10 and 12b). Iceberg transport was probably also present in the middle Eocene, as indicated by mechanical surface-texture features on quartz grains from this interval (St. John, 2008; Stickley et al., 2009). An early onset/intensification of NHG during Eocene times is also supported by IRD records from the Greenland Basin ODP Site 913, indicating high input of ice-rafted grains from Greenland sources related to an extended Greenland Ice Sheet (Eldrett et al., 2007; Tripati et al., 2008; Tripati & Darby, 2019). These findings suggest that Earth's transition from the Greenhouse to the Icehouse world was probably bipolar, which points to greater control of global cooling linked to changes in greenhouse gases in contrast to tectonic forcing (Backman et al., 2006; Backman et al., 2008; DeConto et al., 2008; Moran et al., 2006; Stickley et al., 2009; Tripati & Darby, 2019).

The cooling trend and onset of sea-ice formation recorded in the ACEX IRD and diatom records, coinciding with the global post-EECO cooling trend (Zachos et al., 2008), are also reflected in the ACEX SST record (Figure 12a; Stein, Weller, et al., 2014). Prior to about 47.1 Ma (44.2 Ma according to Age Model 2), warm SSTs between 18 and 26 °C prevailed, interrupted by a prominent, short-lived cooling to 5–10 °C near 47.5 Ma (45.6 Ma according to Age Model 2). At about 46.3 Ma (41.7 Ma according to Age Model 2), summer SST dropped to <17 °C (range 8–17 °C), more or less coinciding with a significant increase in IRD (St. John, 2008; Stickley et al., 2009; Figure 12). An absolute SST minimum of 6–8 °C was reached at about 44.8 Ma (37.5 Ma according to Age Model 2), followed by a short but prominent warm phase with a SST around 17 °C near 44.5 Ma (36.8 Ma according to Age Model 2). This warming event is characterized by the absence of IRD (Figure 12), interpreted to reflect lack of sea ice. Apart from this warm event, however, widespread sea ice seems to be the more typical phenomenon of the Arctic Ocean after about 45.0 Ma (38.1 Ma according to Age Model 2; Figures 11 and 12).

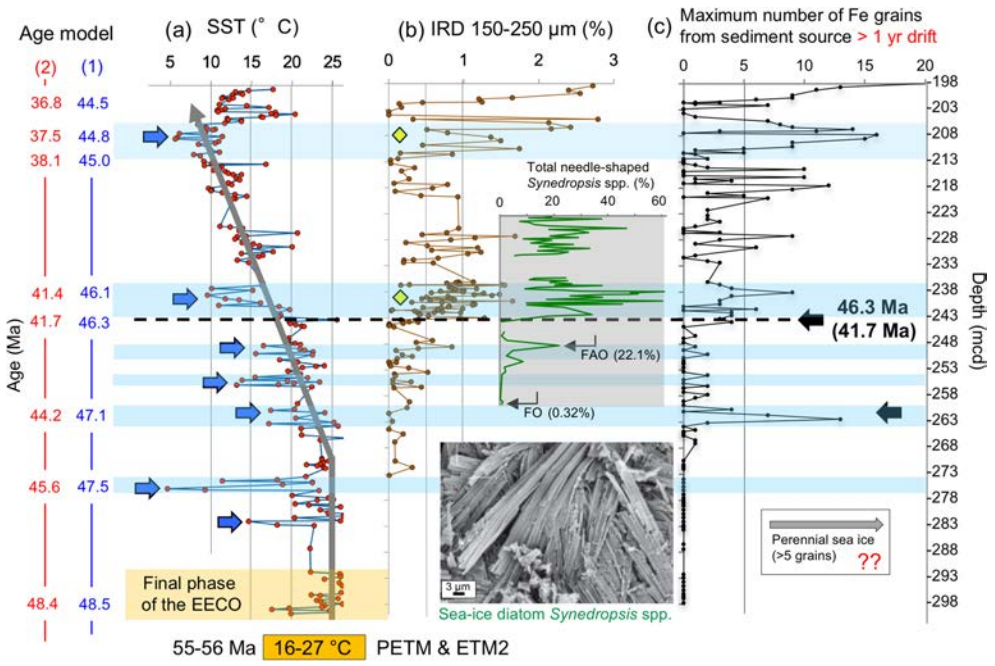

Figure 12. Proxy records for sea-surface temperature (SST) and sea-ice cover, determined in the ACEX sequence from 298 to 198 mcd. (a) Alkenone-based SST (red circles; Stein, Weller, et al., 2014). Lowermost part of the SST coincides with the Early Eocene Climate Optimum (EECO). For comparison, the range of ACEX TEX_{86}-based SSTs of the Paleocene-Eocene Thermal Maximum (PETM) interval (19–23 °C; Sluijs et al., 2006) and the Eocene Thermal Maximum 2 (ETM2) intervals (16–27 °C; Sluijs et al., 2009) are shown. Large blue arrows indicate major cooling events. (b) Abundance of ice-rafted debris (IRD; brown circles) and pebble-sized IRD (yellow rhombs; St. John, 2008), and abundance of sea-ice diatom species *Synedropsis* spp. (Stickley et al., 2009). In the diatom record, the first occurrence (FO) and first abundant occurrence (FAO) of the sea-ice species are also shown. (c) Maximum number of Fe grains from sediment sources with >1 year drift time (assuming modern sea-ice drift rates; Darby, 2014). Grain numbers >5 are interpreted by Darby as indicative for perennial sea ice (see text for further discussion and alternate interpretations). Large black arrows indicate major steps/increases in IRD related to sea-ice and/or iceberg input. On the left-hand side, the two different age scales discussed in the text are shown (cf. Figures 7 and 10).

Overall, the reconstructed central Arctic Ocean SST values remain surprisingly high, even in the upper part of the ACEX record. The apparent paradox of having such a warm SST and sea ice, however, can be explained. As the alkenone-producing coccolithophorids need sunlight for photosynthesis, the alkenone SST represents the summer SST. Then, considering the strong seasonal temperature variability of >10 °C during the early-middle Eocene (Basinger et al., 1994; Wolfe, 1994; Greenwood & Wing, 1995; Suan et al., 2017; see Weller & Stein, 2008, for more detailed discussion of ACEX alkenone data and references), favorable conditions for sea-ice formation may have occurred during winter time. That means, after about 46.3 Ma (or 41.7 Ma according to Age Model 2), the environmental conditions in part of the Arctic Ocean might have been similar to that observed in the modern Baltic Sea where summer SSTs >15 °C and winter SSTs <1 °C with sea-ice formation are typical (Krause, 1969; Schmelzer & Holfort, 2015; Wüst & Brögmus, 1955).

In contrast to the biomarker-based reconstructions clearly indicating a middle Eocene seasonal Arctic sea-ice cover (see above), Darby (2014) postulated ephemeral formation of even perennial sea ice in the Arctic Ocean during the middle Eocene. Darby's argument is based on the occurrence of specific coarse Fe grains (IRD) indicative of a distal source area (such as North America or Siberia). Taking the IRD with a North American or East Siberian origin found in the ACEX sediments and using modern sea-ice drift trajectories and velocities, Darby concluded that more than 1 year was needed to transport the sediments entrained in sea ice to the ACEX location. Hence, sea ice must have survived the summer melting season to reach the ACEX Site, indicating a perennial sea-ice cover. The onset of deposition of such Fe grains at the ACEX site (Figure 12c) is almost contemporaneous with the drop in SST (Figure 12a) as well as the appearance of IRD and sea-ice diatoms (Figure 12b). Thus, if present, phases of perennial sea ice should have been more the exception in the middle Eocene, whereas seasonal sea ice should have been the rule.

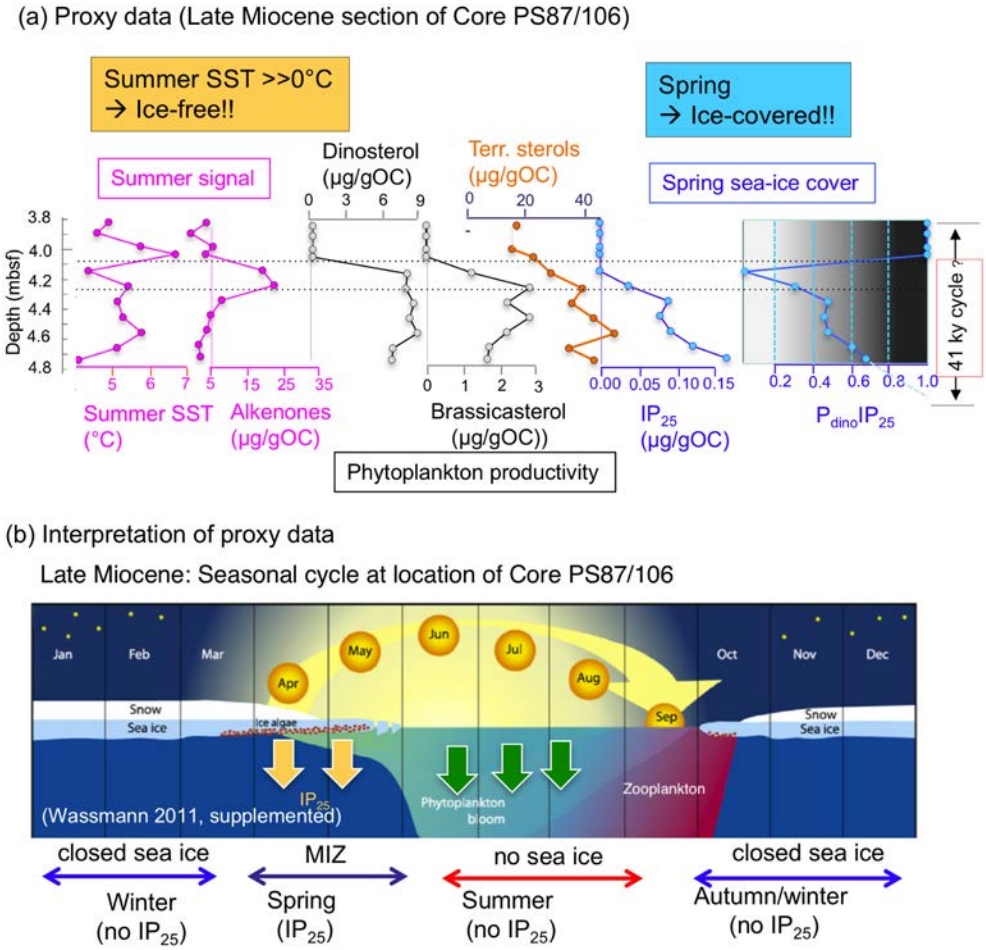

Figure 13. (a) Proxy evidence from Core PS87/106 (for location, see Figure 14) for late Miocene Arctic Ocean climate conditions (from Stein et al., 2016): alkenone-based summer sea-surface temperature (SST), concentrations of alkenones, dinosterol and brassicasterol as proxy for primary productivity, concentrations of terrigenous sterols (sum of campesterol and β-sitosterol), concentrations of sea-ice proxy IP_{25}, and sea-ice index $P_{dino}IP_{25}$ (cf. section 4; for further background and calculation, see Stein et al., 2016). (b) The seasonal sea-ice cycle and related principal processes controlling productivity and carbon flux in the central Arctic Ocean during the late Miocene (Stein et al., 2016, after Wassmann, 2011, supplemented). MIZ = Marginal Ice Zone. The dark period, height of the Sun, and changing thickness of snow and ice over the year as well as phytoplankton, zooplankton, and sea-ice productivity are shown. IP_{25} values for the different seasons are indicated.

Based on a simulation of ice-drift pattern and velocities under permanent and seasonal ice conditions, Tremblay et al. (2015) have demonstrated that sea-ice drift was probably significantly faster under warmer climatic conditions with less or much thinner sea ice than today and that IRD from the North American or East Siberian shelves may reach the North Pole and even beyond within first-year ice. Thus, they conclude that the presence of ice-rafted sediment of North American and East Siberian origin at the North Pole (and at the ACEX site) is not a definite indication of a perennial sea-ice cover in the Arctic Ocean. This may imply that one main assumption of Darby (2014) should be regarded critically.

5.3. Ice-Free Summers in the Central Arctic Ocean During the Late Miocene: An Analogue for the Near Future?

Late Miocene climatic conditions significantly warmer than today have been reconstructed from marine and terrestrial proxy records from around the globe (Pound et al., 2011; Zachos et al., 2008; Zhang et al., 2014). Quantitative SST proxy data from the High Arctic were restricted to a few terrestrial records (Utescher et al., 2015; Wolfe, 1994). Stein et al. (2016) complemented these studies with the first late Miocene SST and sea-ice records for the central Arctic Ocean that were obtained from a sediment core recovered at the steep lower slope of Lomonosov Ridge close to the Siberian continental margin where older sediments are

outcropping near the seafloor (Stein, 2015; Core PS87/106: 81°12.76′N, 141°10.47′E, water depth 1,472 m; see Figure 14a for location). In this core, a hiatus was identified at 3.7-m core depth that separates overconsolidated upper Miocene sediments from the overlying upper Quaternary sediments (Stein et al., 2016). The late Miocene age for the lower part of the sedimentary sequence was identified by the common occurrence of the acritarch *Decahedrella martinheadii* (cf. Matthiessen, Brinkhuis, et al., 2009; Schreck et al., 2012). Reworking of these late Miocene palynomorphs is excluded based on the excellent preservation of the delicate palynomorph specimens.

For the reconstruction of the late Miocene Arctic Ocean sea-ice and SST conditions, Stein et al. (2016) carried out biomarker analyses of the lower 1.3-m-thick section of Core PS87/106 using the IP_{25} sea-ice biomarker approach together with alkenone-based U^{K}_{37} index determinations (cf. Figure 6c). The results demonstrated for the first time that the late Miocene central Arctic Ocean was relatively warm with SSTs of about 5 °C and ice-free conditions during summer, whereas sea ice occurred during spring and autumn/winter (Figure 13). That means, in contrast to the modern situation characterized by a perennial sea-ice cover (cf. Figure 3) and SST values <0 °C, a seasonal sea-ice coverage was predominant in the late Miocene.

Although at a first sight the sedimentary section of Core PS87/106 only represents a short snapshot of late Miocene Arctic climate, more detailed information about the late Miocene climate on a regional to even global scale can be obtained from this record (Stein et al., 2016). Based on the biomarker data, this late Miocene section of Core PS87/106 probably represents one almost complete (glacial/interglacial) cycle with extended and reduced spring sea-ice conditions (Figure 13a). Using mean sedimentation rates of about 3.2 cm/kyr as calculated independently from close-by gravity cores (Stein et al., 2001), the duration of this cycle is about 40 kyr, that is, very similar to the 41-kyr obliquity cycle. Hence, the record may represent just one obliquity cycle with ice-free conditions during summers in both the cold ("glacial") as well as the warm ("interglacial") phase (Figure 13). As Core PS87/106 is of late Miocene age, ice-free summer conditions should have occurred in the central Arctic Ocean during the warmer middle Miocene to early late Miocene time interval a fortiori (Stein et al., 2016).

A seasonal sea-ice cover typical for this time interval is also supported by the occurrence of dinoflagellates and agglutinated benthic foraminifers (Cronin et al., 2008; Matthiessen, Brinkhuis, et al., 2009). In contrast to the biomarker-based reconstructions as well as the micropaleontological data, an Arctic Ocean perennial sea-ice cover from middle Miocene onward has been proposed by Darby (2008) and Krylov et al. (2008), based on provenance studies of IRD in ACEX sediments described for the middle Eocene situation (see above) and the use of modern sea-ice drift trajectories and velocities. Under warmer climatic conditions with less sea ice, however, this should be interpreted cautiously.

Further support for late/middle Miocene ice-free conditions during the summer months comes from climate simulations with CO_2 concentrations of 450 ppm, using a coupled atmosphere-ocean general circulation model (Stein et al., 2016; for details and background of the atmosphere-ocean general circulation model, see Knorr et al., 2011; Knorr & Lohmann, 2014). The simulated mean August SST as well as mean sea-ice concentrations for March, June, and September/August for a high (450 ppm) CO_2 level indicate (1) a winter season with a closed sea-ice cover in the central Arctic Ocean decreasing toward the marginal seas, (2) spring season with sea-ice concentrations of 20–60%, and (3) a summer season with ice-free conditions and SSTs >0 °C (Figure 14a), an almost perfect match with the proxy records (Figure 13a; Stein et al., 2016). When doing the model simulation with a relatively low CO_2 level of 278 ppm, however, summer SSTs are below 0 °C, and sea ice still occurs in the central Arctic Ocean during the summer season; that is, there is a mismatch between proxy and model results (Stein et al., 2016). Such lower CO_2 concentrations of 200–300 ppm have been reconstructed in earlier studies (e.g., Pagani et al., 2005), whereas more recent studies have resulted in higher CO_2 proxy estimates of 300–450 ppm for the late-middle Miocene (Tripati et al., 2009; Zhang et al., 2013; cf. also Ruddiman, 2010).

Extrapolating the Mauna Loa atmospheric CO_2 concentration record (https://www.co2.earth/) and the related temperature increase, CO_2 concentrations of 450 ppm and global warming to about 2 °C above the preindustrial level, respectively, will be reached in about 25 years, and the central Arctic Ocean will become ice-free during summer (Figure 14b; Niederdrenk & Notz, 2018; Notz & Stroeve, 2018; Stroeve & Notz, 2018). That means, sea-ice conditions similar to those reconstructed for the late Miocene may occur in about 2–3

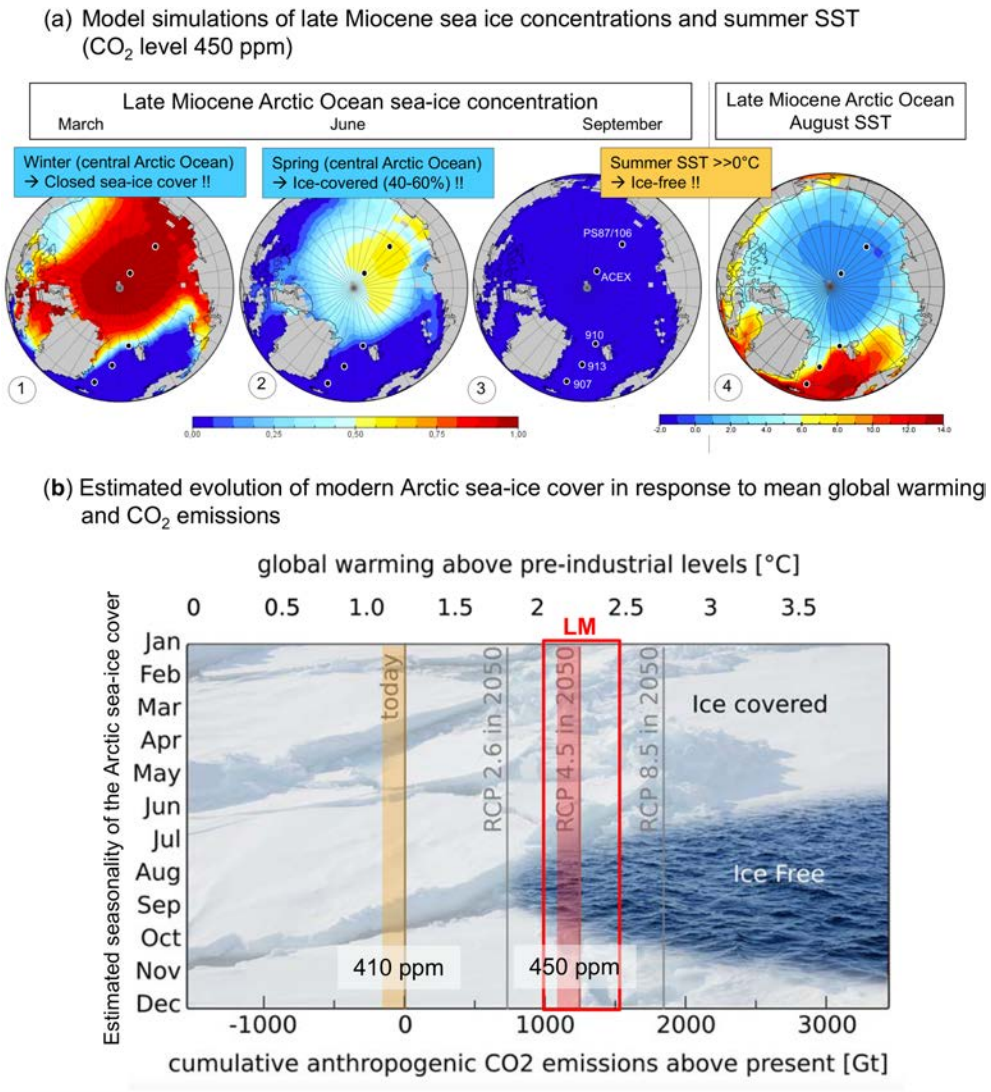

Figure 14. (a) Late Miocene Arctic Ocean climate simulations for high atmospheric CO_2 level of 450 ppm, using a coupled atmosphere-ocean general circulation model (Knorr et al., 2011; Knorr & Lohmann, 2014). (1–3) Sea-ice concentrations for March, June, and September, (4) Late Miocene August SST. Locations of Core PS87/106 as well as the ACEX Site and ODP sites 907, 910, and 913 are shown as black circles (figure from Stein et al., 2016, supplemented). (b) Estimated evolution of modern Arctic sea-ice cover in response to mean global warming and CO_2 emissions (Stroeve & Notz, 2018, supplemented; Niederdrenk & Notz, 2018; Notz & Stroeve, 2018). Cumulative CO_2 emissions and temperature increase until 2050 for different RCP scenarios (cf. Figure 5). Red rectangle indicates Late Miocene (LM) sea ice conditions based on proxy reconstruction (see Figures 13 and 14a).

decades. Although the sea-ice conditions might be similar, however, the rate of change was quite different between both situations. Whereas the recent change from a permanent to a seasonal central Arctic Ocean sea-ice cover (strongly driven by anthropogenic forcing; cf. Notz & Stroeve, 2016) proceeds over a few decades, the corresponding past (natural) change probably occurred over thousands of years.

5.4. A 100-Ma Summary Record of Arctic Ocean SST and Sea-Ice Evolution

In the following, the existing central Arctic Ocean SST data are summarized and related to multiproxy records of the global and middle to low latitude climate evolution throughout the last 100 Ma, including the global benthic isotope stack, CO_2 concentrations and SST records, and the Arctic sea ice history (Figure 15; Table 1). Most of the middle to low latitude records used in this study are from ODP sites. The locations of these sites are shown in a distribution map of modern annual SST (Figure 16). A similar

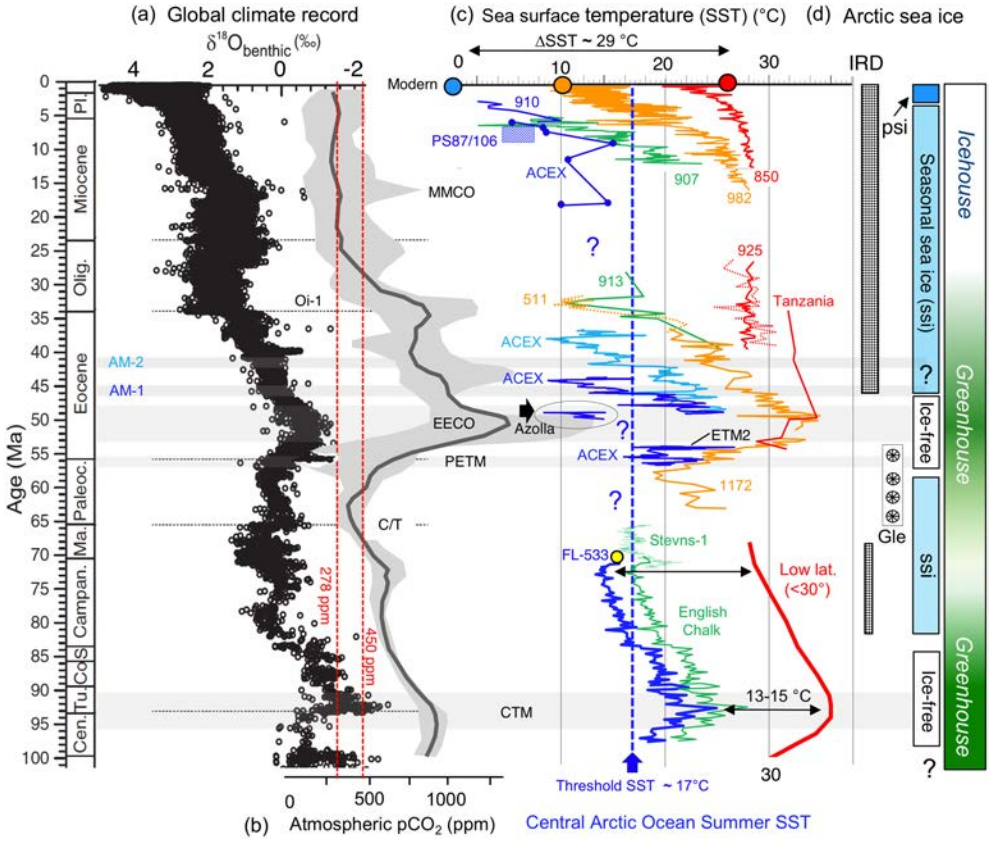

Figure 15. (a) Global $\delta^{18}O$ stack of benthic foraminifera for the past 100 million years representing the Greenhouse-Icehouse transition (Friedrich et al., 2012; Zachos et al., 2008). (b) Smoothed record of atmospheric CO_2 estimates (dark line) from various proxies; light gray envelope includes all single data points (Kent & Muttoni, 2013; see Figure 7 for further explanations). Red stippled lines indicate atmospheric CO_2 levels of 278 (preindustrial value) and 450 ppm, respectively. (c) Compilation of sea-surface temperature (SST) records from various sites (see Figure 16 for site locations), based on TEX_{86}, U^{K}_{37}, and/or $\delta^{18}O$ SST proxies (see Table 1 for further details including paleolatitudes of site locations and references of all records). In blue (summer) SST records from the central Arctic Ocean and Yermak Plateau: Cretaceous TEX_{86} data from Core FL-533 (yellow circle) extrapolated down to the Cenomanian/Turonian (see text for details); Early Eocene TEX_{86} data from ACEX (including the PETM, ETM2, and Azolla events); Middle and late Eocene U^{K}_{37}-based SST from ACEX using age model 1 (AM-1; blue record) and age model 2 (AM-2; light blue record; cf. Figures 10 and 12); middle and late Miocene U^{K}_{37}-based SST data from ACEX and Core PS87/106; Pliocene TEX_{86} data from Site 910. For comparison, SST records from middle (green and orange curves) and low latitudes (red curves) are shown. Late Cretaceous Boreal English Chalk and Stevns-1/Denmark based on $\delta^{18}O$ proxy data (for paleolocations, see Figure 9a); Late Cretaceous composite and smoothed low latitude SST record based on TEX_{86} and $\delta^{18}O_{pl}$ proxy data (sites included in the record are shown in Figure 16); Paleogene U^{K}_{37}-based SST records from ODP Sites 511, 925, and 913, TEX_{86} data from Site 925 (stippled line); (iii) Eocene TEX_{86} record from Tanzania (20°S; Pearson et al., 2007); Paleogene TEX_{86} record from ODP Site 1172; late Miocene-Quaternary U^{K}_{37}-based SST records from ODP Sites 907, 982, and 850. Large blue, orange, and red circles indicate modern SST at high (central Arctic Ocean), middle (Site 982), and low (Site 850) latitudes, respectively (cf. Figure 16). (d) Occurrence of IRD in the ACEX section (St. John, 2008) and interpretation of sedimentological, micropaleontological, and geochemical ACEX data in terms of Arctic sea ice coverage; psi = perennial sea ice, ssi = seasonal sea ice (Stein, Weller, et al., 2014; Stein, 2015; this paper). The stratigraphic occurrence of glendonites (Gle) in a Paleocene sedimentary sequence on Svalbard is indicated (Spielhagen & Tripati, 2009). CTM = Cretaceous Thermal Maximum (Cenomanian/Turonian boundary); C/T = Cretaceous/Tertiary Boundary; PETM = Paleocene-Eocene Thermal Maximum; ETM2 = Eocene Thermal Maximum 2; EECO = Early Eocene Climate Optimum; Oi-1 = Major Oligocene Glaciation Event; MMCO = Middle Miocene Climate Optimum.

compilation summarizing paleoclimate data from the Arctic that in addition also considers terrestrial climate information was published by O'Regan et al. (2011). The summary presented in Figure 15 highlights where data are available, where the gaps are, and—based on this—where the perspectives and needs for future activities are.

Late Cretaceous SST records based on $\delta^{18}O$ and TEX_{86}-SST proxy data from several localities show, independently of their environmental and diagenetic setting, a remarkable similarity, demonstrating that the climatic trends are probably global in nature (e.g., Huber et al., 1995; Jenkyns et al., 1994; O'Brien et al., 2017). There is a general warming trend during the Cenomanian reaching peak values at the Cenomanian/Turonian boundary, followed by a decline through the Coniacian to

Paleoceanography and Paleoclimatology

10.1029/2018PA003433

Table 1
Compilation of sea surface temperatures of Late Cretaceous and Cenozoic time intervals from high (Arctic Ocean), middle, and low latitudes, shown in Figure 15.

Location/area	Expedition, core	Epoch	Age (Ma)	(Paleo-) lat.	SST (°C)	Proxy	Reference
Arctic Ocean							
Alpha Ridge	FL533	Cenomanian/Turonian	93	80°N	24	Extrapolated	Jenkyns et al. (2004)
Alpha Ridge	FL533	Santonian	85	80°N	19	Extrapolated	Jenkyns et al. (2004)
Alpha Ridge	FL533	Campanian	82	80°N	16	Extrapolated	Jenkyns et al. (2004)
Alpha Ridge	FL533	Campanian	73	80°N	14	Extrapolated	Jenkyns et al. (2004)
Alpha Ridge	FL533	Maastrichtian	70	80°N	15	TEX86	Jenkyns et al. (2004)
Lomonosov Ridge	IODP Exp 302, ACEX	PETM	56	87.9°N	23	TEX86	Sluijs et al. (2006), Sluijs et al., 2008
Lomonosov Ridge	IODP Exp 302, ACEX	Lowermost Eocene	55	87.9°N	17	TEX86	Sluijs et al. (2006), Sluijs et al., 2008)
Lomonosov Ridge	IODP Exp 302, ACEX	EarlyEocene (ETM2)	53.5	87.9°N	27	TEX86	Sluijs et al. (2009)
Lomonosov Ridge	IODP Exp 302, ACEX	Early Eocene	50	87.9°N	13	TEX86	Sluijs et al. (2008)
Lomonosov Ridge	IODP Exp 302, ACEX	Early Eocene (Azolla)	48.6	87.9°N	9	TEX86	Brinkhuis et al. (2006)
Lomonosov Ridge	IODP Exp 302, ACEX	Early Eocene	48.5 (48.4)	87.9°N	25	Uk37	Stein, Weller, et al. (2014)
Lomonosov Ridge	IODP Exp 302, ACEX	Early Eocene	48.5 (48.4)	87.9°N	13	TEX86	Brinkhuis et al. (2006)
Lomonosov Ridge	IODP Exp 302, ACEX	Early Eocene	47.1 (44.2)	87.9°N	23	Uk37	Stein, Weller, et al. (2014)
Lomonosov Ridge	IODP Exp 302, ACEX	Middle Eocene	46.3 (41.7)	87.9°N	18	Uk37	Stein, Weller, et al. (2014)
Lomonosov Ridge	IODP Exp 302, ACEX	Middle Eocene	46.1 (41.4)	87.9°N	10	Uk37	Stein, Weller, et al. (2014)
Lomonosov Ridge	IODP Exp 302, ACEX	Middle Eocene	46.1 (41.4)	87.9°N	8	TEX86	Sangiorgi et al. (2008)
Lomonosov Ridge	IODP Exp 302, ACEX	Middle Eocene	46 (41.1)	87.9°N	16	Uk37	Stein, Weller, et al. (2014)
Lomonosov Ridge	IODP Exp 302, ACEX	Middle Eocene	46 (41.1)	87.9°N	13	TEX86	Sangiorgi, van Soelen, et al. (2008)
Lomonosov Ridge	IODP Exp 302, ACEX	Middle Eocene	45.0 (38.1)	87.9°N	9	Uk37	Stein, Weller, et al. (2014)
Lomonosov Ridge	IODP Exp 302, ACEX	Middle Eocene	44.5 (36.8)	87.9°N	9	TEX86	Sangiorgi et al. (2008)
Lomonosov Ridge	IODP Exp 302, ACEX	Middle Eocene	44.4 (36.5)	87.9°N	15	Uk37	Stein, Weller, et al. (2014)
Lomonosov Ridge	IODP Exp 302, ACEX	Middle Eocene	44.4 (36.5)	87.9°N	5	TEX86	Sangiorgi, Brumsack, et al. (2008)
Lomonosov Ridge	IODP Exp 302, ACEX	Middle Miocene (Eoc.)	18.2 (36.1)	87.9°N	10	Uk37	Weller and Stein (2008)
Lomonosov Ridge	IODP Exp 302, ACEX	Middle Miocene (Eoc.)	18 (36)	87.9°N	14	Uk37	Weller and Stein (2008)
Lomonosov Ridge	IODP Exp 302, ACEX	Middle Miocene (Eoc.)	18 (36)	87.9°N	20	TEX86	Sangiorgi, Brumsack, et al. (2008)
Lomonosov Ridge	IODP Exp 302, ACEX	Late Miocene	11.5	87.9°N	10.5	Uk37	Stein et al. (2016)
Lomonosov Ridge	IODP Exp 302, ACEX	Late Miocene	9.1	87.9°N	15.5	Uk37	Stein et al. (2016)
Lomonosov Ridge	IODP Exp 302, ACEX	Late Miocene	7.5	87.9°N	8.9	Uk37	Stein et al. (2016)
Lomonosov Ridge	IODP Exp 302, ACEX	Late Miocene	6	87.9°N	5.4	Uk37	Stein et al. (2016)
Lomonosov Ridge	PS87/106	Late Miocene	6–9	81.2°N	4–7	Uk37	Stein et al. (2016)
Yermak Plateau	ODP Leg 151, Site 910	Early Pliocene	5	80°N	9	TEX86	Knies et al. (2014)
Yermak Plateau	ODP Leg 151, Site 910	Late Pliocene	2.5	80°N	3	TEX86	Knies et al. (2014)
Midlatitudes (45–75°)							
English Chalk Sea/SE England	English Chalk	Cenomanian/Turonian	93	45°N	26	$\delta^{18}O$	Jenkyns et al. (2004)
English Chalk Sea/SE England	English Chalk	Santonian	85	45°N	21	$\delta^{18}O$	Jenkyns et al. (2004)
English Chalk Sea/SE England	English Chalk	Campanian	82	45°N	18	$\delta^{18}O$	Jenkyns et al. (2004)
English Chalk Sea/SE England	English Chalk	Campanian	73	45°N	16	$\delta^{18}O$	Jenkyns et al. (2004)
English Chalk Sea/SE England	English Chalk	Maastrichtian	70	45°N	17	$\delta^{18}O$	Jenkyns et al. (2004)
Boreal Chalk Sea/Denmark	Stevens-1	Maastrichtian	67	45°N	17	$\delta^{18}O$	Thibault et al. (2016)
S-Pacific east of Australia	ODP Leg 189, Site 1172	PETM	56	65°S	26	TEX86	Bijl et al. (2009)
S-Pacific east of Australia	ODP Leg 189, Site 1172	Middle Eocene	50	65°S	35	TEX86	Bijl et al. (2009)
S-Pacific east of Australia	ODP Leg 189, Site 1172	Middle Eocene	46	65°S	26	TEX86	Bijl et al. (2009)
S-Pacific east of Australia	ODP Leg 189, Site 1172	Late Eocene	41	65°S	24	TEX86	Bijl et al. (2009)
S-Pacific east of Australia	ODP Leg 189, Site 1172	Late Eocene	37	65°S	21	TEX86	Bijl et al. (2009)
Greenland Sea/North Atlantic	ODP Leg 151, Site 913	Late Eocene	37	75°N	21	Uk37	Liu et al. (2009)
Greenland Sea/North Atlantic	ODP Leg 151, Site 913	Oligocene	33	75°N	11	Uk37	Liu et al. (2009)
Falkland Plateau/SW Atlantic	DSDP Leg 71, Site 511	Late Eocene	37	55°S	21	Uk37	Liu et al. (2009)
Falkland Plateau/SW Atlantic	DSDP Leg 71, Site 511	Oligocene	33	55°S	11	Uk37	Liu et al. (2009)

Paleoceanography and Paleoclimatology

10.1029/2018PA003433

Table 1
(continued)

Location/area	Expedition, core	Epoch	Age (Ma)	(Paleo-) lat.	SST (°C)	Proxy	Reference
Rockall Plateau/North Atlantic	ODP Leg 162, Site 982	Middle Miocene	16	55°N	28	Uk37	Herbert et al. (2016)
Rockall Plateau/North Atlantic	ODP Leg 162, Site 982	Late Miocene	12	55°N	26	Uk37	Herbert et al. (2016)
Rockall Plateau/North Atlantic	ODP Leg 162, Site 982	Late Miocene	6	55°N	18	Uk37	Herbert et al. (2016)
Rockall Plateau/North Atlantic	ODP Leg 162, Site 982	Early Pliocene	4.5	55°N	20	Uk37	Herbert et al. (2016)
Rockall Plateau/North Atlantic	ODP Leg 162, Site 982	Late Pliocene	2.5	55°N	14	Uk37	Herbert et al. (2016)
Iceland Plateau/North Atlantic	ODP Leg 151, Site 907	Late Miocene	12	70°N	20	Uk37	Stein et al. (2016)
Iceland Plateau/North Atlantic	ODP Leg 151, Site 907	Late Miocene	6	70°N	9	Uk37	Stein et al. (2016)
Iceland Plateau/North Atlantic	ODP Leg 151, Site 907	Early Pliocene	4.5	70°N	11	Uk37	Herbert et al. (2016)
Low latitudes (paleo < 30°)							
Pacific and Atlantic oceans	Composite record	Cenomanian/Turonian	93	0–30°N	36	$\delta^{18}O$, TEX86	O'Brien et al. (2017)
Pacific and Atlantic oceans	Composite record	Campanian	82	0–30°N	32	$\delta^{18}O$, TEX86	O'Brien et al. (2017)
Pacific and Atlantic oceans	Composite record	Maastrichtian	70	0–30°N	28	$\delta^{18}O$, TEX86	O'Brien et al. (2017)
Tanzania/East African margin	Tanzania	Early Eocene	55	20°S	31	TEX86	Pearson et al. (2007)
Tanzania/East African margin	Tanzania	Middle Eocene	50	20°S	34	TEX86	Pearson et al. (2007)
Tanzania/East African margin	Tanzania	Late Eocene	40	20°S	32	TEX86	Pearson et al. (2007)
Equatorial Western Atlantic	ODP Leg 154, Site 925	Late Eocene	40	5°N	28	Uk37, TEX86	Liu et al. (2009)
Equatorial Western Atlantic	ODP Leg 154, Site 925	Oligocene	33	5°N	28	Uk37, TEX86	Liu et al. (2009)
Equatorial East Pacific	ODP Leg 138, Site 850	Late Miocene	12	1°N	28	Uk37	Herbert et al. (2016)
Equatorial East Pacific	ODP Leg 138, Site 850	Late Miocene	6	1°N	27	Uk37	Herbert et al. (2016)
Equatorial East Pacific	ODP Leg 138, Site 850	Early Pliocene	4.5	1°N	26	Uk37	Herbert et al. (2016)
Equatorial East Pacific	ODP Leg 138, Site 850	Late Pliocene	2.5	1°N	24	Uk37	Herbert et al. (2016)

Note. Location/areas, expeditions/cores, epochs and age, paleolatitudes, mean SST values, used proxies, and references are listed. For the ACEX data, ages listed in brackets are based on Age Model 2 (Poirier & Hillaire-Marcel, 2011); the other ages are based on Backman et al. (2008). Sites included in the Late Cretaceous composite record from low latitudes are shown in Figure 16.

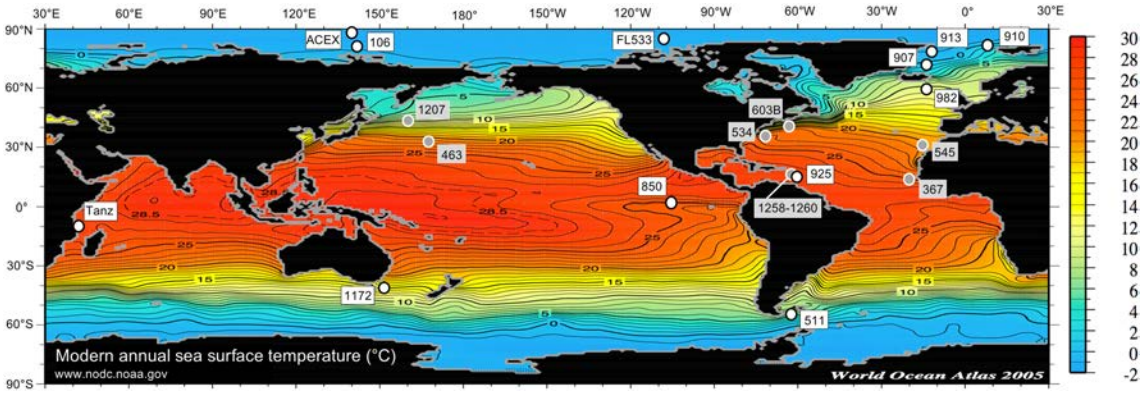

Figure 16. Map of global modern annual sea surface temperature (Source: World Ocean Atlas 2005; www.nodc.noaa.gov) with locations of sites used in this study. White circles represent sites where single SST records are shown in Figure 15. The gray circles represent low-latitude sites (low paleolatitudes <30°) where data have been used to compile the smoothed composite Late Cretaceous SST record (O'Brien et al., 2017) shown in Figure 15. See Table 1 for details.

Campanian/Maastrichtian, also reflected in the SST records from the boreal English Chalk (Jenkyns et al., 1994; Jenkyns et al., 2004) and the Boreal Chalk Sea (Stevns-1/Denmark; Thibault et al., 2016; Figure 15; for location, see Figure 9a). Using the English Chalk SST record that extends into the lowest Maastrichtian, Jenkyns et al. (2004) generated a tentative middle to Late Cretaceous paleotemperature curve for the Arctic Ocean, taking the Maastrichtian TEX_{86}-SST value from Core FL-533 as a calibration point (15 °C; Figure 9c) and assuming that the latitudinal gradient did not greatly change over the time period between about 70 and 100 Ma. Based on this (still tentative) approach, average Arctic Ocean SST probably reached values of 20 to 25 °C during much of the Cenomania-Turonian time interval, decreasing to about 13 °C in the uppermost Campanian (Figure 15; Jenkyns et al., 2004). Under these colder (summer) temperature conditions, winter SST values were probably below 0 °C, allowing some sea-ice formation as suggested from the occasional occurrence of IRD (Figure 9b). During the peak warm Cenomanian-Turonian, conversely, the Arctic Ocean was ice-free year-round as also supported by terrestrial records (O'Regan et al., 2011; see section 5.1). Comparing this high-latitude record with Late Cretaceous SST values from the low latitudes <30°, this suggests a Northern Hemisphere pole-equator temperature gradient of about 1–15 °C (Figure 15; Wilson & Opdyke, 1996; Jenkyns et al., 2004; O'Brien et al., 2017).

Unfortunately, for the upper Maastrichtian/Paleocene interval coinciding with reduced atmospheric CO_2 concentrations, no SST and sea-ice proxy data are available from the central Arctic Ocean. The occurrence of glendonites and erratics in otherwise fine-grained sediments of Paleocene/early Eocene age found on Svalbard requires near-freezing temperatures and the presence of at least seasonal sea ice (Figure 15; Spielhagen & Tripati, 2009). If seasonal sea ice occurred around Svalbard, then it should have occurred in the central Arctic Ocean during that time interval a fortiori.

Peak SST values of about 23–27 °C were reached during the PETM, ETM2, and EECO intervals, more or less contemporaneously with maximum atmospheric CO_2 concentrations (Figure 15; Sluijs et al., 2006, Sluijs et al., 2009; Weller & Stein, 2008; Brassell, 2014; Stein, Weller, et al., 2014). Under these extreme warm conditions, the Arctic Ocean was ice-free throughout the year. The pole-equator temperature gradient was very similar to that estimated for the Cenomanian/Turonian Thermal Maximum. For a long time, modelling studies failed to reproduce such extreme conditions, that is, the very high Arctic Ocean SST values and the more equable global climate with a reduced pole-equator temperature gradient (e.g., Shellito et al., 2003; Tindall et al., 2010). Huber and Caballero (2011) have demonstrated, however, that with a suitably large radiative forcing, the pattern of high-latitude amplification reconstructed by proxies can be largely, but not perfectly, reproduced.

When interpreting these SST data, one should have in mind that the early Eocene data including the PETM, ETM2, and Azolla events is based on TEX_{86} values (Brinkhuis et al., 2006; Sluijs et al., 2006; Sluijs et al., 2008; Sluijs et al., 2009), whereas the EECO values are based on U^{K}_{37} (Stein, Weller, et al., 2014). Unfortunately no U^{K}_{37}-SST values are available for most of the EECO due to the absence of alkenones in this interval (cf.

Weller & Stein, 2008). There are, however, some TEX_{86}-based SST values (Brinkhuis et al., 2006; Sluijs et al., 2008) that show surprisingly low values of 8–13 °C for the EECO; that is, they are about 10 °C lower than the U^{K}_{37}-SST values from close-by depth intervals (Figure 15; Table 1), a difference that is very similar to the Arctic seasonal temperature variability (Basinger et al., 1994; Greenwood & Wing, 1995; Suan et al., 2017; Wolfe, 1994). Thus, one possible explanation for this discrepancy could be that these TEX_{86}-SST values represent more the winter SST (for further details and discussion, see Weller & Stein, 2008), further supporting year-round ice-free conditions in the central Arctic Ocean under this extreme warmth.

With the post-EECO decrease in CO_2, the Arctic Ocean SST values decreased, following the global trend (Figure 15; Zachos et al., 2008). The decrease in Arctic Ocean SST values generally follows that found in subpolar records from the Northern and Southern hemispheres (for location of sites, see Figure 16); that is, Site 913 (Liu et al., 2009) and Site 1172 (Bijl et al., 2009), however, is much larger than that of the low latitudes (Site 925; Liu et al., 2009; Bijl et al., 2009). This results in a significantly increased pole-equator temperature gradient to >20 °C, that is, a value similar to that of today. If the Eocene cooling was predominantly controlled by a decrease in atmospheric greenhouse gas concentration that cooled both the high and the low latitudes (Huber & Sloan, 2001; Zachos et al., 2008), additional processes are required to explain the relative stability of tropical SSTs and the more significant cooling at higher latitudes (Bijl et al., 2009). That means, high-latitude climate feedbacks must have had a more important influence on climate change than previously thought. Differences in cloud/water vapor as well as ice-albedo effects have been mentioned as potential positive-feedback mechanism for middle Eocene cooling (Bijl et al., 2009). The general coincidence of onset and/or extension of sea ice with major SST cooling steps may support the importance of sea ice formation and related ice-albedo effects for the exceptional drop in Arctic Ocean SST. Based on the current (still incomplete) data set, sea ice started to occur when the (summer) SST values decreased below a threshold of about 17 °C, as indicated by the onset of IRD and sea-ice diatoms in the ACEX record (Figures 12 and 15). The datum of this prominent climatic change is at about 46.3 or 42 Ma, depending on the age model that is used.

Despite the ongoing debate about the exact age of the onset of Arctic sea ice, the new semiquantitative sea-ice and SST records are an important contribution to the ongoing and controversial debate about the reconstruction of the early (pre-Quaternary) Arctic Ocean sea-ice cover. Within this debate, the distinction between seasonal and perennial sea ice is critical, because year-round sea ice in the central Arctic implies very different climate feedback mechanisms (i.e., Earth's albedo and heat exchange conditions) than an environment with ice-free conditions during summer.

Between about 40 and 10 Ma, the most prominent steps of global climate change on the pathway from Greenhouse into Icehouse conditions are unfortunately not documented in the Arctic SST record so far, that is, the Eocene/Oligocene cooling event near 34 Ma characterized by a drastic drop in atmospheric CO_2 and the onset of massive glaciations on Antarctica (Escutia et al., 2011, 2014; Kennett & Shackleton, 1976) and the mid-Miocene cooling near 14 Ma with a further drop in atmospheric CO_2 and expansion of ice sheets on Antarctica (Shevenell et al., 2004; Tripati et al., 2009; Figure 15). A drastic cooling at the Eocene/Oligocene boundary in the high northern and southern latitudes is, however, supported from the SST records from Site 913 (75°N) and Site 511 (55°S), both showing a sharp contemporaneous drop in SST near 34 Ma (Figure 15; Liu et al., 2009). The mid-Miocene cooling event is reflected in the Northern High Latitudes by a significant increase in IRD flux in the Nordic seas, related to extended ice sheets on Svalbard and Greenland (Knies & Gaina, 2008; Tripati & Darby, 2019).

For the middle-late Miocene, quantitative information about the central Arctic Ocean is very limited as outlined in the previous section. Warm climatic conditions occurred in the Middle Miocene as reflected in the alkenone-based summer SSTs of 10–13 °C determined in a small number of ACEX sediment samples (Figure 15). For the late Miocene, proxy data as well as modeling results indicate ice-free conditions during the summer season (Stein et al., 2016). The latitudinal SST gradient seems to be about 15 °C when comparing the ACEX data with SST data from sites 907 (70°N), 982 (55°N), and 850 (1°N; Herbert et al., 2016; Stein et al., 2016), that is, lower than the modern one (Figure 15). With the middle-late Pliocene cooling, coinciding with a drop in atmospheric CO_2 (Pagani et al., 2010), SST values at the Arctic, subarctic, middle and low-latitude sites contemporaneously decreased. As the drop in temperatures is much more drastic in the higher

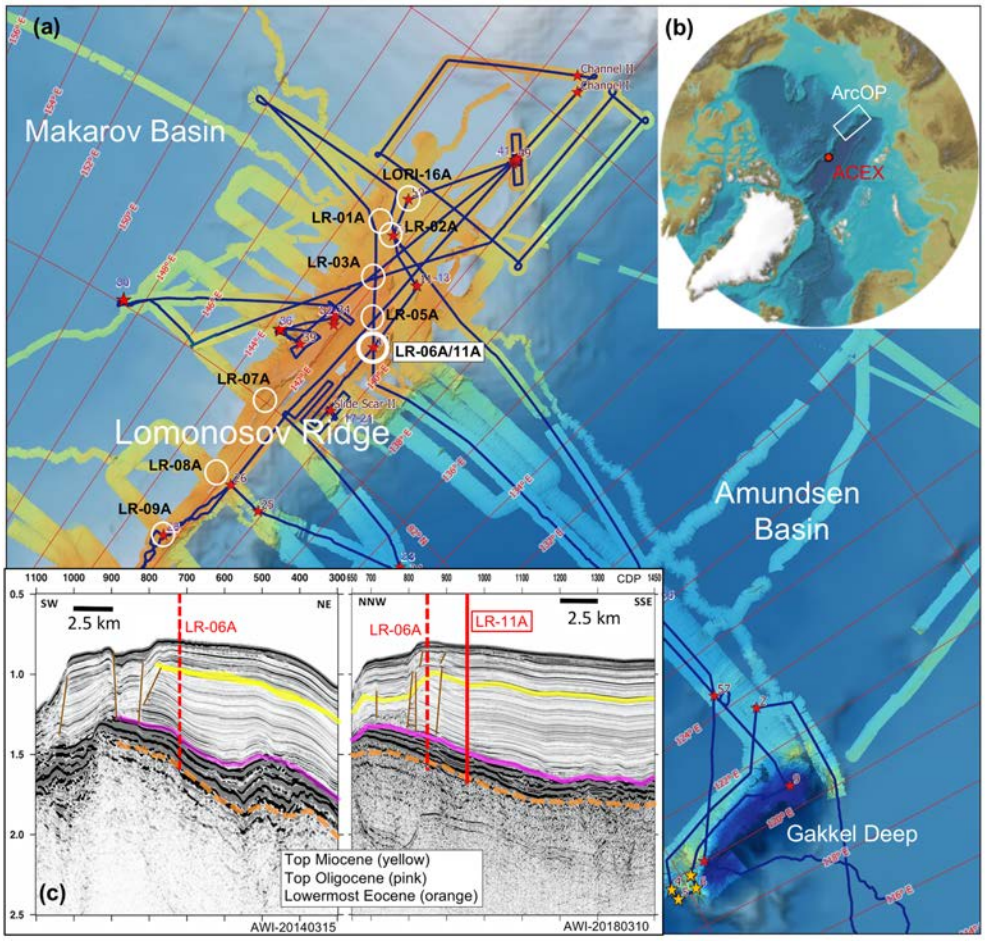

Figure 17. (a) Cruise track and stations of *Polarstern* Expedition PS115/2 in 2018 (Stein, 1019). Track lines of multibeam (Hydrosweep) bathymetric survey carried out during *Polarstern* Expedition PS87 (Stein, 2015) are also shown. Locations of the IODP drill sites proposed for IODP Expedition 377 (Arctic Ocean Paleoceanography/ArcOP; Stein et al., 2015; http://www.ecord.org/expedition377/) are indicated as large white circles (LR-1A to LR-9A, LR-11A, LORI-16A). The primary drill site location LR-11A is highlighted. (b) International Bathymetric Chart of the Arctic Ocean (IBCAO; Jakobsson et al., 2012) with location of the ACEX drill site and the area of PS87 site survey/work area of Expedition 377. (c) Seismic crossing profiles of line AWI-20140315 (shot during Expedition PS87; Jokat et al., 2015) and AWI-20180310 (shot during Expedition PS115/2; Weigelt et al., 2019) with interpretation of reflectors: top of Miocene ("yellow reflector"), top of Oligocene ("pink reflector") corresponding to top of the HARS ("high-amplitude reflector sequence"), and lower Eocene ("orange reflector"; cf. Stein et al., 2015), resulting in 230 m of Plio-Pleistocene, 460 m of Miocene, and >200 m of Oligocene-Eocene sedimentary sequences at Site LR-11A, respectively. Location and stratigraphic range of proposed primary drill site LR-11A and alternate site LR-06A are shown.

latitudes, the pole-equator temperature gradient increased to >20 °C (Figure 15). With the cooling trend, Arctic sea-ice cover became more severe.

For the Pliocene central Arctic Ocean, the available data point to strong temporal and spatial variabilities of the sea-ice cover rather than a stable perennial ice cover (Matthiessen, Knies, et al., 2009; Polyak et al., 2010). Contemporaneously with the late Pliocene global cooling (Figure 15), Northern Hemisphere ice sheets extended onto the shelves (Duk-Rodkin et al., 2004; Knies et al., 2009). Since that time probably also an increased input of meltwaters from ice sheets and low-salinity waters from the Pacific Ocean into the Arctic Ocean via Bering Strait may have caused a freshening of Arctic surface waters facilitating sea-ice formation (Haug et al., 2001; Matthiessen, Knies, et al., 2009; Polyak et al., 2010). Based on sedimentological and micropaleontological data, sea-ice conditions similar to those of today with a perennial sea-ice cover in the central Arctic Ocean probably became more dominant during the last about 1 Ma (Dipre et al., 2018). So far, however, additional multiproxy records distributed throughout the Arctic Ocean are needed

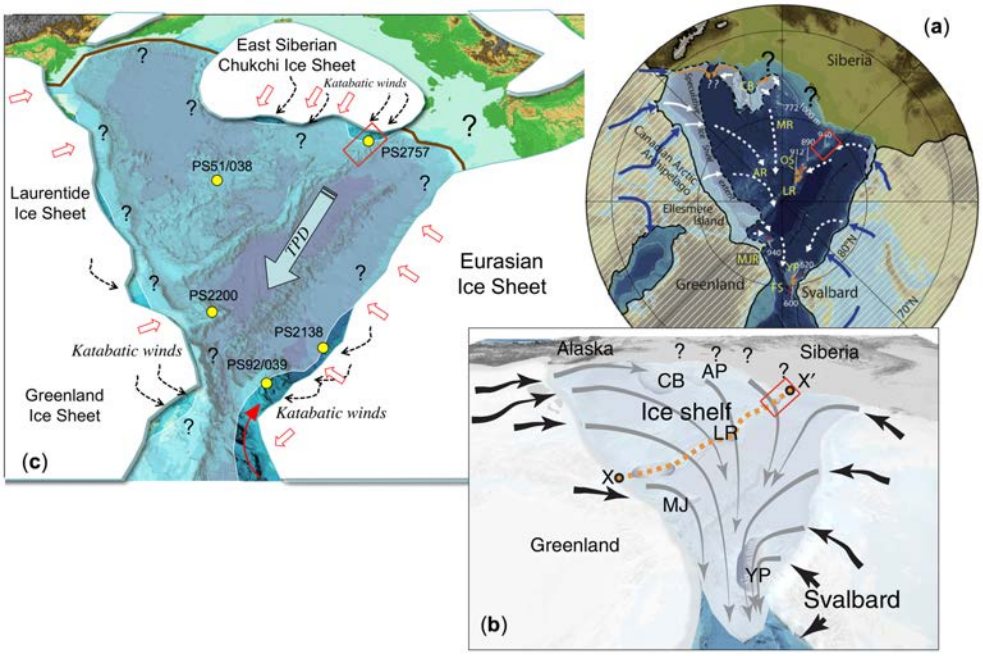

Figure 18. Schematic illustration of Arctic sea ice cover and circum-Arctic ice sheets during MIS6. (a) Tentative reconstruction of MIS 6 ice shelves and ice sheets. Orange arrows indicate ice flow inferred from geophysical mapping and white arrows hypothesized ice flow. The Eurasian Late Saalian Ice Sheet (MIS 6) is based on Svendsen et al. (2004); the North American Ice Sheet shown is the Late Wisconsinan based on Dyke et al. (2002) and England et al. (2009), assuming that the late Illinoian Ice Sheet (MIS 6) covered at least this area in the Arctic region (figure from Jakobsson et al., 2010, supplemented). (b) Cartoon of an ice shelf covering the entire central Arctic Ocean with flow lines generalized from mapped glacial landforms (Jakobsson et al., 2016). AP = Arlis Plateau; CB = Chukchi Borderland; LR = Lomonosov Ridge; MJ = Morris Jesup Rise; YP = Yermak Plateau; *x*–*x*′ highlights the crest of the Lomonosov Ridge. (c) Ice sheet configuration (Ehlers & Gibbard, 2007; Jakobsson et al., 2014), including the extended ice sheet on the East Siberian continental margin (Niessen et al., 2013), and sea-ice cover proposed by Stein et al. (2017). Strong katabatic winds related to the ice sheets (shown tentatively as stippled black arrows) were probably responsible for ice-free polynya-type conditions off the major ice sheets, causing phytoplankton and sea-ice algae productivity. Such conditions were recorded in biomarker records from cores PS2138 and PS2757 (see Stein et al., 2017 for further details). Large light blue arrow indicates the Transpolar Drift (TPD; figure from Stein et al., 2017, supplemented). In (a) to (c), the area of the proposed ArcOP Expedition is shown as a red rectangle.

for a more detailed reconstruction of the history of perennial versus seasonal sea ice and ice-free intervals during the past several million years (Matthiessen, Knies, et al., 2009; Polyak et al., 2010).

6. Outlook: The Challenge for Future Arctic Ocean IODP Drilling

The paleoceanographic and paleoclimate results obtained from ACEX studies were unprecedented and—in combination with additional punctual information from a few short sediment cores—give important insight into the long-term Arctic climate and sea-ice history on its pathway from Greenhouse to Icehouse conditions. Here especially the early onset of seasonal sea ice in the central Arctic Ocean during the middle Eocene and the presence of ice-free conditions during summers throughout the middle-late Miocene have to be highlighted. However, major questions related to the climate history of the Arctic Ocean during early Cenozoic times remain unanswered, partly due to the major mid-Cenozoic hiatus (or strongly reduced sedimentation rates) and partly to the poor recovery of the ACEX record (Backman et al., 2006; Backman et al., 2008; Poirier & Hillaire-Marcel, 2011). In order to decipher the pre-Quaternary climate (and sea-ice) history of this unique and sensitive, but still not well-known region on Earth, long continuous sedimentary records obtained by scientific drilling are needed. Such records are planned to be recovered within a new IODP drilling campaign on the southern Lomonosov Ridge, actually scheduled for late summer/early autumn 2021 (IODP Expedition 377 "Arctic Ocean Paleoceanography (ArcOP)"; http://www.ecord.org/expedition377/). Based on new seismic and coring data obtained during Polarstern Expedition PS87 in 2014 (Stein, 2015) and Polarstern Expedition PS115/2 in 2018 (Stein, 2019), several locations for potential drill sites have been proposed and further optimized (Figure 17; Stein et al., 2015; Stein, 2019). As primary drill site, Site LR-11A

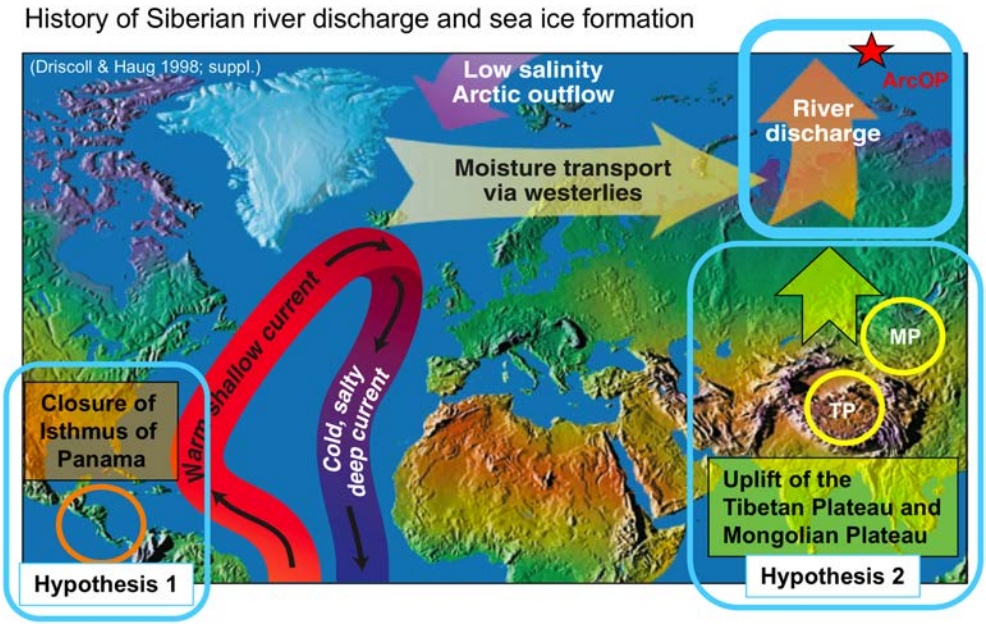

Figure 19. A simple schematic illustrating the ocean's thermohaline circulation in the North Atlantic and the proposed short circuit of the system through freshening of the Arctic Ocean (from Driscoll & Haug, 1998, supplemented). Hypothesis 1 (Driscoll & Haug, 1998) and Hypothesis 2 (Wang, 2004) as trigger mechanisms for increased Arctic river discharge are shown. TP = Tibetan Plateau, MP = Mongolian Plateau. For further details, see text.

has been selected where about 230 m of Plio-Pleistocene, 460 m of Miocene, and >200 m of Oligocene-Eocene may be recovered.

The primary objectives of ArcOP Expedition 377 (http://www.ecord.org/expedition377/) are mainly based on what we learned from the results of the ACEX Expedition (Backman et al., 2006; Backman & Moran, 2008, 2009; Stein, Weller, et al., 2014, Stein et al., 2015). Some of the key scientific themes and hypotheses to be tested using material and data of the ArcOP Expedition are described shortly in the following:

- History of Arctic Ice Sheets, Sea Ice, and Global Climate

An overall key theme is the detailed reconstruction of the history of the circum-Arctic ice sheets and the sea ice in relationship to the global climate record. Key questions still to be answered include the following: Did the Arctic Ocean climate follow the global trend shown in Figure 15? Are the Early Eocene Climate Optimum (poorly recovered in the ACEX record) and the middle Miocene warmings also reflected in Arctic Ocean records? Did extensive glaciations (such as the Oi-1 Glaciation) develop synchronously in both the Northern and Southern Hemispheres (Zachos et al., 2001; Zachos et al., 2008)? Did major East Siberian ice sheets occur during late Pliocene-Pleistocene as recently proposed by Niessen et al. (2013)? What are the related scale and timing of short- and long-term sea-level changes? What is the past variability of Cenozoic sea ice in terms of frequency, extent, and magnitude—a pressing scientific question—even after the accomplishment of the first ACEX campaign? Within this debate, the distinction between seasonal and perennial sea ice is critical, because year-round sea ice in the central Arctic implies very different climate feedback mechanisms, that is, Earth's albedo and heat exchange conditions, than an environment with ice-free conditions during summer.

As reconstructed from bathymetric, seismic/acoustic, and sediment core data as well as satellite and aerial photographs and geological field work on land, the Quaternary glacial history of the Arctic Ocean is characterized by the repeated build-up and decay of circum-Arctic ice sheets on the continental shelves, the development and disintegration of ice shelves, and related changes in ocean-circulation patterns and sea ice cover (Ehlers & Gibbard, 2007; Hughes et al., 1977; Jakobsson et al., 2014; Niessen et al., 2013; Svendsen et al., 2004). There is, however, still an ongoing and partly controversial debate about the timing

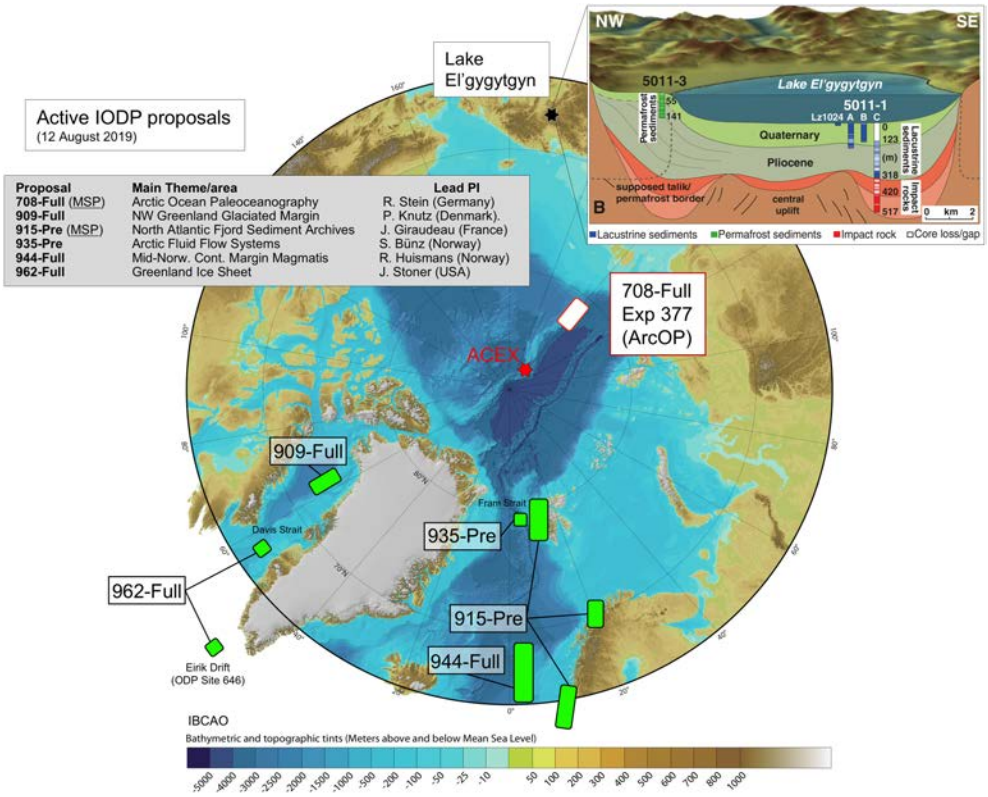

Figure 20. Active IODP proposals for Arctic Ocean drilling. Proposal 708-Full has been scheduled for 2021; all other proposals are still at the IODP Science Evaluation Panel (SEP) for review. (Source: http://www.iodp.org/proposals/active-proposals; Status 12 August 2019). In addition, the location of the International Continental Drilling Program (ICDP) drilling campaign carried out in the El'gygytgyn Lake in eastern Siberia (black star) and a schematic cross section of the El'gygytgyn basin stratigraphy with the location of ICDP sites 5011-1 (with holes 1A, 1B, and 1C) and 5011-3 are shown (Brigham-Grette et al., 2013; Melles et al., 2012).

and extent of maximum glaciations (Figure 18). A comprehensive circumpolar overview of glacial landforms, stratigraphies, and chronologies and their interpretation in terms of glacial history is given by Jakobsson et al. (2014), summarizing the current state of knowledge and identifying key questions arising from this synthesis. Based on new evidence of ice-shelf groundings on bathymetric highs in the central Arctic Ocean, Jakobsson et al. (2016) recently proposed an extended thick ice shelf covering the entire central Arctic Ocean (Figure 18b) and dated it to MIS 6 (~140 ka). Numerical simulations of a kilometer-thick Arctic ice shelf seem to be consistent with ice grounding observations (Gasson et al., 2018). Biomarker proxy records from sediment cores recovered at the Siberian and Barents Sea continental margin, however, indicate at least occasionally open-water conditions during MIS 6, that is, an ice edge situation, that allowed phytoplankton and ice algae production as well as increased flux of terrigenous matter (Figure 18c; Stein et al., 2017). Such polynya-like open-water conditions probably resulted from strong katabatic winds in front of the ice sheet (Figure 18c). One possible but still somewhat speculative explanation for these discrepancies could be a temporal succession of different scenarios, indicating a very dynamic system. During maximum glaciation, an extended thick ice shelf causing ice-shelf grounding (ice rise) with no ice algae production may have occurred, followed by an ice shelf decay and retreat causing polynya-like conditions with sea ice algae and phytoplankton production triggered by strong katabatic winds during the latest MIS 6 (Stein et al., 2017). A continuous Cenozoic Arctic Ocean sedimentary record representing Quaternary and Neogene/Paleogene cold and warm periods will allow us to test the different hypotheses related to changes in Arctic ice sheets and sea ice through time.

- History of Arctic River Discharge

The proximal location of the proposed ArcOP sites relative to the Siberian margin allows a detailed study of the history of Arctic river discharge and its paleoenvironmental significance. In this context, the Pliocene

closure of the Isthmus of Panama and/or the Neogene uplift of the Tibetan Plateau and the Mongolian Plateau might have been of particular interest. These plate tectonic processes might have triggered enhanced discharge rates of Siberian rivers and changed the freshwater balance of the Arctic's surface waters, considered to be an important factor for the formation of Arctic sea ice and onset of major glaciations (Figure 19; Driscoll & Haug, 1998; Haug et al., 2001; Wang, 2004). Furthermore, a record of the Siberian river discharge per se might give important insight into the evolution of continental climate in the hinterland through Miocene/Pliocene times.

- High-Resolution Characterization of the Pliocene Warm Period in the Arctic

During the Pliocene warm period, SST in several ocean basins were substantially warmer (Haywood et al., 2005; Lawrence et al., 2006; Marlow et al., 2000), and global mean surface temperature was estimated to be at least 3 °C higher than today (Haywood & Valdes, 2004). How did the Arctic Ocean evolve during the Pliocene warm period and subsequent cooling? How do the marine climate records correlate with terrestrial records obtained from the Siberian Lake El'gygytgyn (Figure 20; Melles et al., 2012; Brigham-Grette et al., 2013)?

- The "Hiatus Problem"

What is the cause of the major hiatus spanning the late Eocene to early Miocene time interval in the ACEX record (based on the original age model of Backman et al., 2008)? Does this hiatus in fact exist, or is it rather an interval of extremely reduced sedimentation rate as proposed by Poirier and Hillaire-Marcel (2011); Figure 10)? If there is a major hiatus, is it related to the subsidence history of Lomonosov Ridge (cf. O'Regan et al., 2008)? Was the hiatus a response to increased bottom water currents during the opening of surface and deep water connections via the Fram Strait (cf. Moore & the Expedition 302 Scientists, 2006)? Additional long sedimentary records from the Arctic Ocean with good microfossil recovery are needed to solve these obvious problems in chronology and related paleoenvironmental and tectonic reconstructions. An improvement of the chronology is also an important prerequisite for calculating rates of climate change, a fundamental aspect to better understand the processes controlling past and present climate change and to distinguish between natural and anthropogenic forcings.

The outcome of the second Arctic Ocean IODP drilling campaign will certainly help to improve our understanding of the complex ocean-atmosphere-ice system in the polar high northern latitudes and its role in the past, modern, and future global climate. In addition, this expedition will provide us the second long continuous sedimentary section representing the Cenozoic time interval to be used for detailed reconstructions of the long-term evolution of the Arctic paleoclimate from the early Cenozoic Greenhouse to the late Cenozoic Icehouse conditions. That means, this will certainly be another major step forward in Arctic Ocean paleoclimate research. Nevertheless, further scientific Arctic drilling expeditions have to follow during the coming years in order to fully understand the role of the Arctic Ocean in the Earth's system and its change through time (Coakley & Stein, 2010; Stein, 2011). Some active proposals are already in the IODP system, but they are not ready to be scheduled yet (Figure 20). More site survey data and review actions are still needed. Furthermore, some key areas for reconstruction of the early Arctic Ocean climate and also tectonic history are still missing, for example, the Alpha Ridge where Cretaceous sedimentary sections are almost outcropping at the seafloor (cf. section 5.1, Figure 9).

Acknowledgments
This publication is a contribution to the Research Programme PACES II, Topic 3 (The Earth system from a polar perspective: Data, modeling and synthesis) of the Alfred Wegener Institute Helmholtz Centre for Polar und Marine Research (AWI). The study used samples and data provided by AWI (grants AWI-PS87_01 and AWI-PS115/2_1) and the IODP Program. Many thanks to the reviewers, Helmut Weissert (ETH Zurich, Switzerland), and Matt O'Regan (Stockholm University, Sweden), for numerous constructive suggestions for improving the manuscript.

References

Aagaard, K., & Carmack, E. C. (1989). The role of sea ice and other fresh water in the Arctic circulation. *J. Geophys. Res.*, *94*(C10), 14,485–14,498. https://doi.org/10.1029/JC094iC10p14485

Aagaard, K., Swift, J. H., & Carmack, E. C. (1985). Thermohaline circulation in the Arctic Mediterranean seas. *Journal of Geophysical Research*, *90*(C3), 4833–4846. https://doi.org/10.1029/JC090iC03p04833

ACIA (2004). *Impacts of a warming Arctic: Arctic climate impact assessment* (139 pp.). Cambridge University Press, Cambridge. (http://www.acia.uaf.edu)

ACIA (2005). *Arctic climate impact assessment* (1042 p.). Cambridge: Cambridge University Press.

Alsenz, H., Regnery, J., Ashckenazi-Polivoda, S., Meilijson, A., Ron-Yankovich, L., Abramovich, S., et al. (2013). Sea surface temperature record of a Late Cretaceous tropical Southern Tethys upwelling system. *Palaeogeography, Palaeoclimatology, Palaeoecology*, *392*, 350–358. https://doi.org/10.1016/j.palaeo.2013.09.013

AMAP (2017). *Snow, water, ice and permafrost in the Arctic (SWIPA) 2017*. Oslo, Norway: Arctic Monitoring and Assessment Programme (AMAP). xiv + 269 pp

Anisimov, O. A., Shiklomanov, N. I., & Nelson, F. E. (1997). Effects of global warming on permafrost and active-layer thickness: Results from transient general circulation models. *Global and Planetary Change*, *15*(3-4), 61–77. https://doi.org/10.1016/S0921-8181(97)00009-X

Arthur, M. A., Dean, W. E., Stow, D. A. V. (1984). Models for the deposition of Mesozoic-Cenozoic fine-grained organic-carbon-rich sediments in the deep sea. In D. A. V. Stow & D. J. W. Piper (Eds.), *Fine-grained sediments: Deep-water processes and facies*. *Geol. Soc. London, Spec. Publ.* (15, pp. 527–560). London.

Arthur, M. A., Schlanger, S. O., & Jenkyns, H. C. (1987). The Cenomanian-Turonian Oceanic anoxic event, ii. Palaeoceanographic controls on organic-matter production and preservation. In J. Brooks & A. Fleet (Eds.), *Marine Petroleum Source Rocks*, *Geol. Soc. London, Spec. Publ.* (Vol. 26, pp. 401–420). London.

Backman, J., Jakobsson, M., Frank, M., Sangiorgi, F., Brinkhuis, H., Stickley, C., et al. (2008). Age model and core-seismic integration for the Cenozoic Arctic coring expedition sediments from the Lomonosov Ridge. *Paleoceanography*, *23*, PA1S03. https://doi.org/10.1029/2007PA001476

Backman, J., & Moran, K. (2008). Introduction to special section on Cenozoic Paleoceanography of the Central Arctic Ocean. *Paleoceanography*, *23*, PA1S01. https://doi.org/10.1029/2007PA001516

Backman, J., & Moran, K. (2009). Expanding the Cenozoic paleoceanographic record in the central Arctic Ocean: IODP Expedition 302 synthesis. *Central European Journal of Geoscience*, *1*, 157–175.

Backman, J., Moran, K., McInroy, D. B., et al. (2006). *Proceedings IODP*, (Vol. 302). College Station, Texas: Integrated Ocean Drilling Program Management International, Inc. https://doi.org/10.2204/iodp.proc.302.104.2006

Bakke, T., Hameedi, J., Kimstach, V., Macdonald, R., Melnikov, S., Robertson, A., et al. (1998). Chapter 10, Petroleum hydrocarbons. In A. Robertson (Ed.), *AMAP Assessment Report: Arctic Pollution Issues* (pp. 662–716). Oslo: AMAP.

Barry, R. G. (1996). The parameterization of surface albedo for sea ice and its snow cover. *Prog. Phys. Geogr.*, *20*(1), 63–79. https://doi.org/10.1177/030913339602000104

Basinger, J. F., Greenwood, D. R., & Sweda, T. (1994). Early Tertiary vegetation of Arctic Canada and its relevance to paleoclimatic interpretation. In M. C. Boulter, & H. C. Fischer (Eds.), *Cenozoic plants and climates of the high Arctic*, *NATO ASI Series 1* (Vol. 127, pp. 175–198). Heidelberg: Springer Verlag. https://doi.org/10.1007/978-3-642-79378-3_13

Beerling, D. J., & Royer, D. L. (2011). Convergent Cenozoic CO_2 history. *Nature Geoscience*, *4*(7), 418–420. https://doi.org/10.1038/ngeo1186

Belt, S. T. (2018). Source-specific biomarkers as proxies for Arctic and Antarctic sea ice. *Organic Geochemistry*, *125*, 277–298. https://doi.org/10.1016/j.orggeochem.2018.10.002

Belt, S. T., Cabedo-Sanz, P., Smik, L., Navarro-Rodriguez, A., Berben, S. M. P., Knies, J., & Husum, K. (2015). Identification of paleo Arctic winter sea ice limits and the marginal ice zone: Optimised biomarker-based reconstructions of late Quaternary Arctic sea ice. *Earth and Planetary Science Letters*, *431*, 127–139. https://doi.org/10.1016/j.epsl.2015.09.020

Belt, S. T., Massé, G., Rowland, S. J., Poulin, M., Michel, C., & LeBlanc, B. (2007). A novel chemical fossil of palaeo sea ice: IP_{25}. *Organic Geochemistry*, *38*(1), 16–27. https://doi.org/10.1016/j.orggeochem.2006.09.013

Belt, S. T., & Müller, J. (2013). The Arctic sea ice biomarker IP_{25}: A review of current understanding, recommendations for future research and applications in palaeo sea ice reconstructions. *Quaternary Science Reviews*, *79*, 9–25. https://doi.org/10.1016/j.quascirev.2012.12.001

Belt, S. T., Smik, L., Köseoğlu, D., Knies, J., & Husum, K. (2019). A novel biomarker-based proxy for the spring phytoplankton bloom in Arctic and sub-arctic settings—HBI T_{25}. *Earth and Planetary Science Letters*, *523*, 115703. https://doi.org/10.1016/j.epsl.2019.06.038

Bijl, P. K., Schouten, S., Sluijs, A., Reichart, G.-J., Zachos, J. C., & Brinkhuis, H. (2009). Early Palaeogene temperature evolution of the southwest Pacific ocean. *Nature*, *409*, 776–779.

Brassell, S. C. (2014). Climatic influences on the Paleogene evolution of alkenones. *Paleoceanography*, *29*, 255–272. https://doi.org/10.1002/2013PA002576

Brassell, S. C., Eglinton, G., Marlowe, I. T., Pflaumann, U., & Sarntheim, M. (1986). Molecular stratigraphy: A new tool for climate assessment. *Nature*, *320*(6058), 129–133. https://doi.org/10.1038/320129a0

Brice, K. L., Arthur, M. A., & Marincovich, L. Jr. (1996). Late Paleocene Arctic Ocean shallow-marine temperatures from mollusk stable isotopes. *Paleoceanography*, *11*, 241–249.

Brigham-Grette, J., Melles, M., Minyuk, P., Andreev, A., Tarasov, P., DeConto, R., et al. (2013). Pliocene warmth, extreme polar amplification, and stepped Pleistocene cooling recorded in NE Russia. *Science*, *340*(6139), 1421–1427. https://doi.org/10.1126/science.1233137

Bring, A., Fedorova, I., Dibike, Y., Hinzman, L., Mård, J., Mernild, S. H., et al. (2016). Arctic terrestrial hydrology: A synthesis of processes, regional effects and research challenges. *J. Geophys. Res. Biogeosci.*, *121*, 621–649. https://doi.org/10.1002/2015JG003131

Brinkhuis, H., Schouten, S., Collinson, M. E., Sluijs, A., Damsté, J. S. S., Dickens, G. R., et al., & the Expedition 302 Scientists (2006). Episodic fresh surface waters in the Eocene Arctic Ocean. *Nature*, *441*(7093), 606–609. https://doi.org/10.1038/nature04692

Bröder, L., Andersson, A., Tesi, T., Semiletov, I., & Gustafsson, Ö. (2019). Quantifying degradative loss of terrigenous organic carbon in surface sediments across the Laptev and East Siberian Sea. *Global Biogeochemical Cycles*, *33*(1), 85–99. https://doi.org/10.1029/2018GB005967

Bröder, L., Tesi, T., Andersson, A., Semiletov, I., & Gustafsson, Ö. (2018). Bounding cross-shelf transport time and degradation in Siberian-Arctic land-ocean carbon transfer. *Nature Communications*, *9*(1), 806. https://doi.org/10.1038/s41467-018-03192-1

Broecker, W. S. (1997). Thermohaline circulation, the Achilles Heel of our climate system: Will man-made CO_2 upset the current balance? *Science*, *278*(5343), 1582–1588. https://doi.org/10.1126/science.278.5343.1582

Brown, J., Ferrians, O. J. J., Heginbottom, J. A., & Melnikov, E. S. (1997). *International Permafrost Association circum-Arctic map of permafrost and ground ice conditions, Scale 1:10,000,000*. U.S. Geol. Surv.

Brown, T. A., Belt, S. T., Tatarek, A., & Mundy, C. J. (2014). Source identification of the Arctic sea ice proxy IP_{25}. *Nature Communications*, *5*(1), 4197. https://doi.org/10.1038/ncomms5197

Brumsack, H. J. (1980). Geochemistry of Cretaceous black shales from the Atlantic Ocean (DSDP Legs 11, 14, 36 and 41). *Chem. Geol.*, *31*, 1–25. https://doi.org/10.1016/0009-2541(80)90064-9

Bukry, D. (1984). Paleogene paleoceanography of the Arctic Ocean is constrained by the middle or late Eocene age of USGS Core FI-422: Evidence from silicoflagellates. *Geology*, *12*(4), 199–201. https://doi.org/10.1130/0091-7613(1984)12<199:PPOTAO>2.0.CO;2

Cavalieri, D. J., Gloersen, P., Parkinson, C. L., Comiso, J. C., & Zwally, H. J. (1997). Observed hemispheric asymmetry in global sea ice changes. *Science*, *278*(5340), 1104–1106. https://doi.org/10.1126/science.278.5340.1104

Cavalieri, D. J., & Parkinson, C. L. (2012). Arctic sea ice variability and trends, 1979–2010. *Cryosphere*, *6*(4), 881–889. https://doi.org/10.5194/tc-6-881-2012

Chakrapani, G. J. (2005). Factors controlling variations in river sediment loads. *Current Science*, *88*(4). 25 February 2005.
Clark, D. L. (1974). Late Mesozoic and early Cenozoic sediment cores from the Arctic Ocean. *Geology*, *2*(1), 41–44. https://doi.org/10.1130/0091-7613(1974)2<41:LMAECS>2.0.CO;2
Clark, D. L., Byers, C. W., & Pratt, L. M. (1986). Cretaceous black mud from the central Arctic Ocean. *Paleoceanography*, *1*(3), 265–271. https://doi.org/10.1029/PA001i003p00265
Clark, D. L., & Hanson, A. (1983). Central Arctic Ocean sediment texture: A key to ice transport mechanism, in: Molnia, B. F. (Ed.), *Glacial-marine sedimentation* (pp. 301-330). New York, Plenum Press. https://doi.org/10.1007/978-1-4613-3793-5_7.
Coachman, L. K., Aagaard, K., & Tripp, R. B. (1975). *Bering Strait: The regional physical oceanography*. Seattle: University of Washington Press.
Coakley, B., & Stein, R. (2010). Arctic Ocean scientific drilling: The next frontier. *Scientific Drilling*, *9*, 45–49. https://doi.org/10.5194/sd-9-45-2010
Colony, R., & Thorndike, A. S. (1985). Sea ice motion as a drunkard's walk. *Journal of Geophysical Research*, *90*(C1), 965–974. https://doi.org/10.1029/JC090iC01p00965
Conte, M. H., Eglinton, G., & Madureira, L. A. S. (1992). Long-chain alkenones and alkyl alkenoates as palaeotemperature indicators: Their production, flux and early sedimentary diagenesis in the eastern North Atlantic. *Organic Geochemistry*, *19*(1-3), 287–298. https://doi.org/10.1016/0146-6380(92)90044-X
Crane, K., Galasso, J., Brown, C., Cherkashov, G., Ivanov, G., Petrova, V., & Vanstayn, B. (2001). Northern ocean inventories of organo-chlorine and heavy metal contamination. *Marine Pollution Bulletin*, *43*(1-6), 28–60. https://doi.org/10.1016/S0025-326X(01)00084-4
Cronin, T. M., Polyak, L., Reed, D., Kandiano, E. S., Marzen, R. E., & Council, EA (2013). A 600-ka Arctic sea-ice record from Mendeleev Ridge based on ostracodes. *Quaternary Science Review*, *79*, 157–167. https://doi.org/10.1016/j.quascirev.2012.12.010
Cronin, T. M., Smith, S. A., Eynaud, F., O'Regan, M., & King, J. (2008). Quaternary paleoceanography of the central Arctic based on Integrated Ocean Drilling Program Arctic Coring Expedition 302 foraminiferal assemblages. *Paleoceanography*, *23*, PA1S18. https://doi.org/10.1029/2007PA001484
Crowley, T. J., & Berner, R. A. (2001). CO_2 and climate change. *Science*, *292*(5518), 870–872 (2001). https://doi.org/10.1126/science.1061664
Darby, D. A. (2003). Sources of sediment found in sea ice from the western Arctic Ocean, new insights into processes of entrainment and drift patterns. *Journal of Geophysical Research*, *108*(C8), 3257. https://doi.org/10.1029/2002JC001350
Darby, D. A. (2008). The Arctic perennial ice cover over the last 14 million years. *Paleoceanography*, *23*, PA1S07. https://doi.org/10.1029/2007PA001479
Darby, D. A. (2014). Ephemeral formation of perennial sea ice in the Arctic Ocean during the middle Eocene. *Nature Geoscience*, *7*(3), 210–213. https://doi.org/10.1038/NGEO2068
Davies, A., Kemp, A. E. S., & Pälike, H. (2011). Tropical ocean-atmosphere controls on inter-annual climate variability in the Cretaceous Arctic. *Geophysical Research Letters*, *38*, L03706. https://doi.org/10.1029/2010GL046151
Davies, A., Kemp, A. E. S., & Pike, J. (2009). Late Cretaceous seasonal ocean variability from the Arctic. *Nature*, *460*(7252), 254–258. https://doi.org/10.1038/nature08141
de Graciansky, P. C., Deroo, G., Herbin, J. P., Montadert, L., Müller, C., Schaaf, A., & Sigal, J. (1984). Ocean-wide stagnation episode in the Late Cretaceous. *Nature*, *308*(5957), 346–349. https://doi.org/10.1038/308346a0
De Lurio, J. L., & Frakes, L. A. (1999). Glendonites as a paleoenvironmental tool: Implications for Early Cretaceous high latitude climates in Australia. *Geochimica et Cosmochimica Acta*, *63*(7-8), 1039–1048. https://doi.org/10.1016/S0016-7037(99)00019-8
De Vernal, A., Gersonde, R., Goose, H., Seidenkrantz, M.-S., & Wolff, E. W. (2013). Sea ice in the paleoclimate system: The challenge of reconstructing sea ice from proxies–An introduction. *Quaternary Science Reviews*, *79*, 1–8. https://doi.org/10.1016/j.quascirev.2013.08.009
De Vernal, A., & Rochon, A. (2011). Dinocysts as tracers of sea-surface conditions and sea-ice cover in polar and subpolar environments. *IOP Conf. Series Earth Environm. Sci.*, *14*, 012007. https://doi.org/10.1088/1755-1315/14/1/012007
DeVernal, A., Rochon, A., Fréchette, B., Henry, M., Radi, T., & Solignac, S. (2013). Reconstructing past sea ice cover of the Northern Hemisphere from dinocyst assemblages: Status of the approach. *Quaternary Science Reviews*, *79*, 122–134. https://doi.org/10.1016/j.quascirev.2013.06.022
DeConto, R. M., & Pollard, D. (2003). Rapid Cenozoic glaciation of Antarctica induced by declining atmospheric CO_2. *Nature*, *421*(6920), 245–249. https://doi.org/10.1038/nature01290
DeConto, R. M., Pollard, D., Wilson, P. A., Pälike, H., Lear, C. H., & Pagani, M. (2008). Thresholds for Cenozoic bipolar glaciations. *Nature*, *455*(7213), 652–656. https://doi.org/10.1038/nature07337
Dell'Agnese, D. J., & Clark, D. L. (1994). Siliceous microfossils from the warm Late Cretaceous and early Cenozoic Arctic Ocean. *Journal of Paleontology*, *68*(1), 31–47. https://doi.org/10.1017/S0022336000025580
Demaison, G. J., & Moore, G. T. (1980). Anoxic environments and oil source bed genesis. *Organic Geochemistry*, *2*(1), 9–31. https://doi.org/10.1016/0146-6380(80)90017-0
Dethleff, D. (2005). Entrainment and export of Laptev Sea ice sediments, Siberian Arctic. *Journal of Geophysical Research*, *110*(C7), C07009. https://doi.org/10.1029/2004JC002740
Dethleff, D., Rachold, V., Tintelnot, T., & Antonow, M. (2000). Sea-ice transport of riverine particles from the Laptev Sea to Fram Strait based on clay mineral studies. *Internation Journal of Earth Sciences*, *89*(3), 496–502. https://doi.org/10.1007/s005310000109
Dickson, R. R., Osborn, T. J., Hurrell, J. W., Meincke, J., Blindheim, J., Adlandsvik, B., et al. (2000). The Arctic Ocean response to the North Atlantic Oscillation. *Journal of Climate*, *13*(15), 2671–2696. https://doi.org/10.1175/1520-0442(2000)013<2671:TAORTT>2.0.CO;2
Dipre, G. R., Polyak, L., Kuznetsov, A. B., Oti, E. A., Ortiz, J. D., Brachfeld, S. A., et al. (2018). Plio-Pleistocene sedimentary record from the Northwind Ridge: New insights into paleoclimatic evolution of the western Arctic Ocean for the last 5 Ma. *Arktos*, *4*(1), 24. https://doi.org/10.1007/s41063-018-0054-y
Ditchfield, P. W. (1997). High northern palaeolatitude Jurassic-Cretaceous palaeotemperature variation: New data from Kong Karls Land, Svalbard. *Palaeogeography, Palaeoclimatology, Palaeoecology*, *130*(1-4), 163–175. https://doi.org/10.1016/S0031-0182(96)00054-5
Dixon, J., Dietrich, J., Snowdon, L. R., Morrell, G., & McNeil, D. H. (1992). Geology and petroleum potential of Upper Cretaceous and Tertiary strata, Beaufort Mackenzie area, Northwest Canada. *Bulletin of American Association of Petroleum Geologists*, *76*, 927–947.
Dolezych, M., Reinhardt, L., Kus, J., & Annacker, V. (2018). Taxonomy of Cretaceous–Paleogene coniferous woods and their distribution in fossil Lagerstätten of the high latitudes. In K. Piepjohn, J. V. Strauss, L. Reinhardt, & W. C. McClelland (Eds.), *Circum-Arctic structural events: Tectonic evolution of the Arctic Margins and trans-Arctic links with adjacent orogens*, *Geol. Soc. Amer. Spec. Paper* (541). The Geological Society of America. https://doi.org/10.1130/2018.2541(02)

Driscoll, N. W., & Haug, G. H. (1998). A short circuit in thermohaline circulation: A cause for Northern Hemisphere glaciation? *Science*, *282*(5388), 436–438. https://doi.org/10.1126/science.282.5388.436

Duk-Rodkin, A., Barendregt, R. W., Froese, D. G., Weber, F., Enkin, R. J., Smith, I. R., et al. (2004). Timing and extent of Plio–Pleistocene glaciations in North–Western Canada and East–Central Alaska. In J. Ehlers & P. L. Gibbard (Eds.), *Quaternary glaciations—Extent and chronology, Part II, North America* (pp. 313–345). New York: Elsevier. https://doi.org/10.1016/S1571-0866(04)80206-9

Dyke, A. S., Andrews, J. T., Clark, P. U., England, J. H., Miller, G. H., Shaw, J., & Veillette, J. J. (2002). The Laurentide and Innuitian ice sheets during the last glacial maximum. *Quaternary Science Reviews*, *21*(1-3), 9–31. https://doi.org/10.1016/S0277-3791(01)00095-6

Eberle, J. J., Fricke, H. C., Humphrey, J. D., Hackett, L., Newbrey, M. G., & Hutchison, J. H. (2010). Seasonal variability in Arctic temperatures during early Eocene time. *Earth and Planetary Science Letters*, *296*(3-4), 481–486. https://doi.org/10.1016/j.epsl.2010.06.005

Ehlers, J., & Gibbard, P. L. (2007). The extent and chronology of Cenozoic global glaciation. *Quaternary International*, *164-165*, 6–20. https://doi.org/10.1016/j.quaint.2006.10.008

Eicken, H. (2004). The role of Arctic sea ice in transporting and cycling terrigenous organic matter. In R. Stein & R. W. Macdonald (Eds.), *The organic carbon cycle in the Arctic Ocean* (pp. 45–53). Heidelberg: Springer Verlag.

Eicken, H., Gradinger, R., Graves, A., Mahoney, A., & Rigor, I. (2005). Sediment transport by sea ice in the Chukchi and Beaufort Seas: Increasing importance due to changing ice conditions? *Deep Sea Research Part II: Tropical Studies in Oceanography*, *52*(24-26), 3281–3302. https://doi.org/10.1016/j.dsr2.2005.10.006

Eicken, H., Reimnitz, E., Alexandrov, V., Martin, T., Kassens, H., & Viehoff, T. (1997). Sea-ice processes in the Laptev Sea and their importance for sediment export. *Continental Shelf Research*, *17*(2), 205–233. https://doi.org/10.1016/S0278-4343(96)00024-6

Eldholm, O., Thiede, J., Taylor, E., et al. (Eds.) (1989). *Proc. ODP Sci. Results* (Vol. 104). College Station, Texas: Ocean Drilling Program.

Eldrett, J. S., Greenwood, D. R., Harding, I. C., & Huber, M. (2009). Increased seasonality through the Eocene to Oligocene transition in northern high latitudes. *Nature*, *459*(7249), 969–973. https://doi.org/10.1038/nature08069

Eldrett, J. S., Harding, I. C., Wilson, P. A., Butler, E., & Roberts, A. P. (2007). Continental ice in Greenland during the Eocene and Oligocene. *Nature*, *446*(7132), 176–179. https://doi.org/10.1038/nature05591

England, J. H., Furze, M. F. A., & Doupé, J. P. (2009). Revision of the NW Laurentide Ice Sheet: Implications for paleoclimate, the northeast extremity of Beringia, and Arctic Ocean sedimentation. *Quaternary Science Reviews*, *28*(17-18), 1573–1596. https://doi.org/10.1016/j.quascirev.2009.04.006

Environmental Working Group (EWG) (1998). Oceanography atlas for the summer period, in *Joint U.S.-Russian Atlas of the Arctic Ocean [CD-ROM]*, Univ. of Colorado, Boulder, Colorado.

Erba, E., Bartolini, A., & Larson, R. L. (2004). Valanginian Weissert oceanic anoxic event. *Geology*, *32*(2), 149–152. https://doi.org/10.1130/G20008.1

Erba, E., Bottini, C., Faucher, G., Gambacorta, G., & Visentin, S. (2019). The response of calcareous nannoplankton to Oceanic Anoxic Events: The Italian pelagic record. *Bollettino della Societa Paleontologica Italiana*, *58*, 51–71.

Erba, E., Duncan, R. A., Bottini, C., Tiraboschi, D., Weissert, H., Jenkyns, H. C., & Malinverno, A. (2015). Environmental consequences of Ontong Java Plateau and Kerguelen Plateau Volcanism. *GSA Special Paper*, *511*. https://doi.org/10.1130/2015.2511

Erbacher, J., Huber, B. T., Norris, R. D., & Markey, M. (2001). Increased thermohaline stratification as a possible cause for an ocean anoxic event in the Cretaceous period. *Nature*, *409*(6818), 325–327. https://doi.org/10.1038/35053041

Escutia, C., Brinkhuis, H., Klaus, A., & the IODP Expedition 318 Scientists (2011). IODP Expedition 318: From Greenhouse to Icehouse at the Wilkes Land Antarctic margin. *Scientific Drilling*, *12*, 15–23. https://doi.org/10.2204/iodp.sd.12.02.2011 12, September 2011

Escutia, C., Brinkhuis, H., and the IODP Expedition 318 Scientists, 2014. From Greenhouse to Icehouse at the Wilkes Land Antarctic margin: IODP Expedition 318 synthesis of results. In: Stein, R., Blackman, D. Inagaki, F., and Larsen, H.-C. (Eds.), *Earth and life processes discovered from subseafloor environment—A decade of science achieved by the Integrated Ocean Drilling Program (IODP)*, *Series Developments in Marine Geology*, Vol. 7, Elsevier Amsterdam/New York, p. 295-328.

Firth, J. V., & Clark, D. L. (1998). An early Maastrichtian organic-walled phytoplankton cyst assemblage from an organic-walled black mud in Core F1-533, Alpha Ridge: Evidence for upwelling conditions in the Cretaceous Arctic Ocean. *Marine Micropaleontology*, *34*(1-2), 1–27. https://doi.org/10.1016/S0377-8398(97)00046-7

Foster, G. L., Royer, D. L., & Lunt, D. J. (2017). Future climate forcing potentially without precedent in the last 420 million years. *Nature Communications*, *8*(1), 14,845. https://doi.org/10.1038/ncomms14845

Frakes, L. A. (1979). *Climates through geological time*. Amsterdam: Elsevier. 310 pp

Frakes, L. A., & Francis, J. E. (1988). A guide to Phanerozoic cold polar climates from high latitude ice-rafting in the Cretaceous. *Nature*, *333*(6173), 547–549. https://doi.org/10.1038/333547a0

Frey, K. E., McClelland, J. W., Holmes, R. M., & Smith, L. C. (2007). Impacts of climate warming and permafrost thaw on the riverine transport of nitrogen and phosphorus to the Kara Sea. *Journal of Geophysical Research*, *112*(G4), G04S58. https://doi.org/10.1029/2006JG000369

Friedrich, O., Norris, R. D., & Erbacher, J. (2012). Evolution of middle to Late Cretaceous oceans—A 55 m.y. record of Earth's temperature and carbon cycle. *Geology*, *40*(2), 107–110. https://doi.org/10.1130/G32701.1

Gambacorta, G., Bersezio, R., Weissert, H., & Erba, E. (2016). Onset and demise of Cretaceous Oceanic Anoxic Events: The coupling of surface and bottom oceanic processes in two pelagic basins of the western Tethys. *Paleoceanography and Paleoclimatology*, *31*, 732–757. https://doi.org/10.1002/2015PA002922

Gasson, E. G. W., DeConto, R. M., Pollard, D., & Clark, C. D. (2018). Numerical simulations of a kilometre-thick Arcticice shelf consistent with ice grounding observations. *Nature Communications*, *9*(1), 1510. https://doi.org/10.1038/s41467-018-03707-w

Gloersen, P., Campbell, W. J., Cavalieri, D. J., Comiso, J. C., Parkinson, C. L., & Zwally, H. J. (1992). Arctic and Antarctic sea ice, 1978–1987: Satellite passive-microwave observations and analysis. *NASA*, *SP-511*. 290 pp

Gordeev, V. V., Martin, J. M., Sidorov, I. S., & Sidorova, M. V. (1996). A reassessment of the Eurasian River Input of water, sediment, major elements, and nutrients to the Arctic Ocean. *American Journal of Science*, *296*(6), 664–691. https://doi.org/10.2475/ajs.296.6.664

Goulden, M. L., Wofsy, S. C., Harden, J. W., Trumbore, S. E., Crill, P. M., Gower, S. T., et al. (1998). Sensitivity of boreal forest carbon balance to soil thaw. *Science*, *279*(5348), 214–217. https://doi.org/10.1126/science.279.5348.214

Grantz, A., Hart, P., & Childers, V. A. (2011). Geology and tectonic development of the Amerasia and Canada Basins, Arctic Ocean. In A. M. Spencer, A. F. Embry, D. L. Gautier, A. V. Stoupakova, & K. Sørensen (Eds.), *Arctic Petroleum Geology*, *Geological Society of London, London, Memoirs* (Vol. 35, pp. 771–799).

Greenwood, D. G., & Wing, S. L. (1995). Eocene continental climates and latitudial temperatures gradients. *Geology*, *23*(11), 1044–1048. https://doi.org/10.1130/0091-7613(1995)023<1044:ECCALT>2.3.CO;2

Greenwood, D. R., Basinger, J. F., & Smith, R. Y. (2010). How wet was the Arctic Eocene rain forest? Estimates of precipitation from Paleogene Arctic macrofl oras. *Geology*, *38*(1), 15–18. https://doi.org/10.1130/G30218.1

Hallam, A. (1985). A review of Mesozoic climates. *Journal of Geological Society of London*, *142*(3), 433–445. https://doi.org/10.1144/gsjgs.142.3.0433

Haq, B. U. (2014). Cretaceous eustasy revisited. *Global and Planetary Change*, *113*, 44–58. https://doi.org/10.1016/j.gloplacha.2013.12.007

Haq, B. U., Hardenbol, J., & Vail, P. R. (1988). Mesozoic and Cenozoic chronostratigraphy and cycles of sea-level change. In C. K. Wilgus, B. S. Hastings, C. G. S. C. Kendall, H. W. Posamentier, C. A. Ross, & C. Van Wagoner (Eds.), *Sea level changes: An integrated approach*, *Soc. Econ. Petrol. Mineral. Spec. Publ.*, (Vol. 42, pp. 71–108). https://doi.org/10.2110/pec.88.01.0071

Haug, G. H., Tiedemann, R., Zahn, R., & Ravelo, A. C. (2001). Role of Panama uplift on oceanic freshwater balance. *Geology*, *29*(3), 207–210. https://doi.org/10.1130/0091-7613(2001)029<0207:ROPUOO>2.0.CO;2

Hay, W. W., De Conto, R. M., Wold, C. N., Wilson, K. M., Vogt, S., Schultz, M., et al. (1999). Alternative global Cretaceous paleogeography. In E. Barrera, & C. C. Johnson (Eds.), *Evolution of the Cretaceous ocean-climate system*, Geological Society of America (Vol. *332*, pp. 1–47). Boulder. https://doi.org/10.1130/0-8137-2332-9.1

Haywood, A. M., Dekens, P., Ravelo, A. C., & Williams, M. (2005). Warmer tropics during the mid-Pliocene? Evidence from alkenone paleothermometry and a fully coupled ocean atmosphere GCM. *Geochemistry, Geophysics, Geosystems*, *6*, Q03010. https://doi.org/10.1029/2004GC000799

Haywood, A. M., & Valdes, P. J. (2004). Modelling Pliocene warmth: Contribution of atmosphere, oceans and cryosphere. *Earth and Planetay Science Letters*, *218*(3-4), 363–377. https://doi.org/10.1016/S0012-821X(03)00685-X

Herbert, T. D., Lawrence, K. T., Tzanova, A., Cleaveland Peterson, L., Caballero-Gill, R., & Kelly, C. S. (2016). Late Miocene global cooling and the rise of modern ecosystems. *Nature Geoscience*, *9*(11), 843–847. https://doi.org/10.1038/NGEO2813

Herman, A. B., & Spicer, R. A. (1996). Palaeobotanical evidence for a warm Cretaceous Arctic Ocean. *Nature*, *380*(6572), 330–333. https://doi.org/10.1038/380330a0

Hibler, W. D. (1989). Arctic Ice-Ocean Dynamics. In Y. Herman (Ed.), *The Arctic Seas: Climatology, oceanography, geology, and biology*, (pp. 47–92). New York: Van Nostrand Reinhold Company. https://doi.org/10.1007/978-1-4613-0677-1_2

Hillaire-Marcel, C., & de Vernal, A. (Eds) (2007). *Proxies in Late Cenozoic paleoceanography*, *Developments in Mar. Geol.*, (Vol. 1). Amsterdam, 843 pp: Elsevier. https://doi.org/10.1016/S1572-5480(07)01005-6

Ho, S. L., Mollenhauer, G., Fietz, S., Martinez-Garcia, A., Lamy, F., Rueda, G., et al. (2014). Appraisal of the TEX_{86} and TEX_{86}^{L} thermometries in the subpolar and polar regions. *Geochimica et Cosmochimica Acta*, *131*, 213–226. https://doi.org/10.1016/j.gca.2014.01.001

Hofmann, P., Ricken, W., Schwark, L., & Leythaeuser, D. (2000). Carbon-sulfur-iron relationships and d13C of organic matter for late Albian sedimentary rocks froem the North Atlantic Ocean: Paleoceanographic implications. *Palaeogeography, Palaeoclimatology, Palaeoecology*, *163*(3-4), 97–113. https://doi.org/10.1016/S0031-0182(00)00147-4

Holmes, R. M., McClelland, J. W., Peterson, B. J., Shiklomanov, A. I., Zhulidov, A. V., Gordeev, V. V., & Bobrovitskaya, N. (2002). A circumpolar perspective on fluvial sediment flux to the Arctic Ocean. *Global Biogeochemical Cycles*, *16*(4, Seiten), 1098. https://doi.org/10.1029/2002GB001920

Holmes, R.M., Shiklomanov, A.I., Suslova, A., Tretiakov, M., McClelland, J.W., Spencer, R.G.M., Tank, S.E., 2018. River discharge (https://www.arctic.noaa.gov/Report-Card/Report-Card-2018/ArtMID/7878/ArticleID/786/River-Discharge).

Hong, S. K., & Lee, Y. I. (2012). Evaluation of atmospheric carbon dioxide concentrations during the Cretaceous. *Earth and Planetary Science Letters*, *327-328*, 23–28. https://doi.org/10.1016/j.epsl.2012.01.014

Huber, B. T. (1998). Tropical paradise at the Cretaceous poles? *Science*, *282*(5397), 2199–2200. https://doi.org/10.1126/science.282.5397.2199

Huber, B. T., Hodell, D. A., & Hamilton, C. P. (1995). Mid- to Late Cretaceous climate of the southern high latitudes. Stable isotopic evidence for minimal equator-to-pole thermal gradients. *Bulletin of the Geological Society of America*, *107*(10), 1164–1191. https://doi.org/10.1130/0016-7606(1995)107<1164:MLCCOT>2.3.CO;2

Huber, M., & Caballero, R. (2011). The early Eocene equable climate problem revisited. *Climate of the Past*, *7*(2), 603–633. https://doi.org/10.5194/cp-7-603-2011

Huber, M., & Sloan, L. C. (2001). Heat transport, deep waters, and thermal gradients: Coupled simulation of an Eocene 'greenhouse' climate. *Geophysical Research Letters*, *28*(18), 3481–3484. https://doi.org/10.1029/2001GL012943

Hughes, T., Denton, G. H., & Grosswald, M. G. (1977). Was there a late-Würm Arctic ice sheet? *Nature*, *266*(5603), 596–602. https://doi.org/10.1038/266596a0

Hunt, G. L. Jr., Blanchard, A. L., Boveng, P., et al. (2012). The Barents and Chukchi Seas: Comparison of two Arctic shelf ecosystems. *Journal of Marine Systems*, *109-110*, 43–68.

Jackson, H. R., Mudie, P. J., & Blasco, S. M. (1985). Initial geological report on CESAR—The Canadian Expedition to study the Alpha Ridge, Arctic Ocean. *Geological Survey of Canada Paper*, *84-22*. 177 pp

Jakobsson, M. (2002). Hypsometry and volume of the Arctic Ocean and its constituent seas. *Geochemistry, Geophysics, Geosystems*, *3*(5), 1028. https://doi.org/10.1029/2001GC000302

Jakobsson, M., Andreassen, K., Bjarnadottir, L. R., Dive, D., Dowdeswell, J. A., England, J. H., et al. (2014). Arctic Ocean glacial history. *Quaternary Science Reviews*, *92*, 40–67. https://doi.org/10.1016/j.quascirev.2013.07.033

Jakobsson, M., Backman, J., Rudels, B., Nycander, J., Frank, M., Mayer, L., et al. (2007). The early Miocene onset of a ventilated circulation regime in the Arctic Ocean. *Nature*, *447*(7147), 986–990. https://doi.org/10.1038/nature05924

Jakobsson, M., Mayer, L., Coakley, B., Dowdeswell, J. A., Forbes, S., Fridman, B., et al. (2012). The International Bathymetric Chart of the Arctic Ocean (IBCAO) version 3.0. *Geophysical Research Letters*, *39*, L12609. https://doi.org/10.1029/2012GL052219

Jakobsson, M., Nilsson, J., Anderson, L., Backman, J., Björk, G., Cronin, T. M., et al. (2016). Evidence for an ice shelf covering the central Arctic Ocean during the penultimate glaciation. *Nature Communications*, *7*(1), 10365. https://doi.org/10.1038/ncomms10365

Jakobsson, M., Nilsson, J., O'Regan, M., Backman, J., Löwemark, L., Dowdeswell, J. A., et al. (2010). An Arctic Ocean ice shelf during MIS 6 constrained by new geophysical and geological data. *Quaternary Science Reviews*, *29*(25-26), 3505–3517. https://doi.org/10.1016/j.quascirev.2010.03.015

Jenkyns, H. C., Forster, A., Schouten, S., & Sinninghe Damsté, J. S. (2004). High temperatures in the late Cretaceous Arctic Ocean. *Nature*, *432*(7019), 888–892. https://doi.org/10.1038/nature03143

Jenkyns, H. C., Gale, A. S., & Corfield, R. M. (1994). Carbon- and oxygen-isotope stratigraphy of the English Chalk and Italian Scaglia and its paleoclimatic significance. *Geological Magazine*, *131*(1), 1–34. https://doi.org/10.1017/S0016756800010451

Johannessen, O. M., Bengtsson, L., Miles, M. W., Kuzmina, S. I., Semenov, V. A., Alekseev, G. V., et al. (2004). Arctic climate change, observed and modelled temperature and sea-ice variability. *Tellus*, *56A*(4), 328–341.
Johannessen, O. M., Shalina, E. V., & Miles, M. W. (1999). Satellite evidence for an Arctic Sea ice cover in transformation. *Science*, *286*(5446), 1937–1939. https://doi.org/10.1126/science.286.5446.1937
Jokat, W., Geissler, W., Coakley, B., Eagles, G., Eisermann, H., Gebhardt, C., et al. (2015). Seismic investigations across the Lomonosov Ridge. In R. Stein (Ed.), *The Expedition PS87 of the research vessel Polarstern to the Arctic Ocean in 2014*, Reports on Polar and Marine Research (Vol. *688*, pp. 49–56). Bremerhaven: Alfred Wegener Institute.
Jorgenson, M. T., Racine, C. H., Walters, J. C., & Osterkamp, T. E. (2001). Permafrost degradation and ecological changes associated with a warming climate in central Alaska. *Climatic Change*, *48*(4), 551–579. https://doi.org/10.1023/A:1005667424292
Kanao, M., Suvorov, V. D., Toda, S., & Tsuboi, S. (2015). Seismicity, structure and tectonics in the Arctic region. *Geoscience Frontiers*, *6*(5), 665–677. https://doi.org/10.1016/j.gsf.2014.11.002
Kemper, E. (1987). Das Klima der Kreidezeit. *Geologisches Jahrbuch A*, *96*, 5–185.
Kennett, J. P., & Shackleton, N. J. (1976). Oxygen isotopic evidence for the development of the psychrosphere 38 Myr ago. *Nature*, *260*(5551), 513–515. https://doi.org/10.1038/260513a0
Kent, D. V., & Muttoni, G. (2013). Modulation of Late Cretaceous and Cenozoic climate by variable drawdown of atmospheric pCO_2 from weathering of basaltic provinces on continents drifting through the equatorial humid belt. *Climate of the Past*, *9*(2), 525–546. https://doi.org/10.5194/cp-9-525-2013
Kim, J. H., Schouten, S., Hopmans, E. C., Donner, B., & Sinninghe Damsté, J. S. (2008). Global sediment core-top calibration of the TEX86 paleothermometer in the ocean. *Geochimica et Cosmochimica Acta*, *72*(4), 1154–1173. https://doi.org/10.1016/j.gca.2007.12.010
Knies, J., Cabedo-Sanz, P., Belt, S. T., Baranwal, S., Fietz, S., & Rosell-Melé, A. (2014). The emergence of modern sea ice cover in the Arctic Ocean. *Nature Communications*, *5*(1), 5608. https://doi.org/10.1038/ncomms6608
Knies, J., & Gaina, C. (2008). Middle Miocene ice sheet expansion in the Arctic—Views from the Barents Sea. *Geochemistry, Geophysics, Geosystems*, *9*, Q02015. https://doi.org/10.1029/2007GC001824
Knies, J., Matthiessen, J., Vogt, C., Laberg, J. S., Hjelstuen, B. O., Smelror, M., et al. (2009). The Plio–Pleistocene glaciation of the Barents Sea–Svalbard region: A new model based on revised chronostratigraphy. *Quaternary Science Reviews*, *28*(9-10), 812–829. https://doi.org/10.1016/j.quascirev.2008.12.002
Knies, J., Müller, C., Nowaczyk, N., Vogt, C., & Stein, R. (2000). A multiproxy approach to reconstruct the environmental changes along the Eurasian continental margin over the last 150 kyr. *Marine Geology*, *163*(1-4), 317–344. https://doi.org/10.1016/S0025-3227(99)00106-1
Knorr, G., Butzin, M., Micheels, A., & Lohmann, G. (2011). A warm Miocene climate at low atmospheric CO_2 levels. *Geophysical Research Letters*, *38*, L20701. https://doi.org/10.1029/2011GL048873
Knorr, G., & Lohmann, G. (2014). Climate warming during Antarctic ice sheet expansion at the Middle Miocene transition. *Nature Geoscience*, *7*(5), 376–381. https://doi.org/10.1038/ngeo2119
Koç, N., Jansen, E., & Haflidason, H. (1993). Paleoceanographic reconstructions of surface ocean conditions in the Greenland, Iceland and Norwegian seas through the last 14 ka based on diatoms. *Quaternary Science Reviews*, *12*(2), 115–140. https://doi.org/10.1016/0277-3791(93)90012-B
Koppers, A. A. P., Escutia, C., Inagaki, F., Pälike, H., Saffer, D. M., & Thomas, D. (2019). *Scientific ocean drilling: Looking to the future*, *Oceanography, Spec. Issue* (Vol. 32, 248 pp.). Rockville: Oceanography Society.
Krause, G. (1969). Ein Beitrag zum Problem der Erneuerung des Tiefenwassers im Arkona-Becken. *Kieler Meeresforschung*, *25*, 268–271.
Kristoffersen, Y., 1990. Eurasian basin, in: Grantz, A., Johnson, L., Sweeny, J.F. (Eds.), *The Arctic Ocean region, Geology of North America* Vol. L., Geol. Soc. Am., Boulder, Colorado, 365-378.
Kristoffersen, Y. & Tholfsen, A., 2016. Ice drift station FRAM-2014/2015 weekly reports. *NERSC Technical Reports* No. 365, Nansen Environmental and Remote Sensing Center, Bergen, Norway, 333 pp.
Kristoffersen, Y., Tholfsen, A., Hall, J., & Stein, R. (2016). Scientists spend Arctic winter adrift on sea ice. *Eos*, *97*. https://doi.org/10.1029/2016EO060711
Krylov, A. A., Andreeva, I. A., Vogt, C., Backman, J., Krupskaya, V. V., Grikurov, G. E., et al. (2008). A shift in heavy and clay mineral provenance indicates a middle Miocene onset of a perennial sea-ice cover in the Arctic Ocean. *Paleoceanography*, *23*, PA1S06. https://doi.org/10.1029/2007PA001497
Kwok, R., & Cunningham, G. F. (2015). Variability of Arctic sea ice thickness and volume from CryoSat-2. *Philosophical Transactions of the Royal Society A: Mathematical, Physical and Engineering Sciences*, *373*(2045), 20140157. https://doi.org/10.1098/rsta.2014.0157
Langrock, U., & Stein, R. (2004). Origin of marine petroleum source rocks from the Late Jurassic/Early Cretaceous Norwegian Greenland Seaway—Evidence for stagnation and upwelling. *Marine and Petroleum Geology*, *21*(2), 157–176. https://doi.org/10.1016/j.marpetgeo.2003.11.011
Langrock, U., Stein, R., Lipinski, M., & Brumsack, H. J. (2003a). Late Jurassic to Early Cretaceous black shale formation and paleoenvironment in high northern latitudes—Examples from the Norwegian-Greenland-Seaway. *Paleoceanography*, *18*(3), n/a. https://doi.org/10.1029/2002PA000867
Langrock, U., Stein, R., Lipinski, M., & Brumsack, H. J. (2003b). Paleoenvironment and sea-level change in the Early Cretaceous Barents Sea—Implications from near-shore marine sapropels. *Geo-Marine Letters*, *23*(1), 34–42. https://doi.org/10.1007/s00367-003-0122-5
Larsen, H. C., Saunders, A. D., Clift, P. D., Beget, J., Wei, W., Spezzaferri, S., & ODP Leg 152 Scientific Party (1994). Seven million years of glaciation in Greenland. *Science*, *264*(5161), 952–955. https://doi.org/10.1126/science.264.5161.952
Lawrence, K. T., Liu, Z., & Herbert, T. D. (2006). Evolution of the eastern tropical Pacific through Plio-Pleistocene glaciation. *Science*, *312*(5770), 79–83. https://doi.org/10.1126/science.1120395
Lear, C. H., Elderfield, H., & Wilson, P. A. (2000). Cenozoic deep-sea temperatures and global ice volumes from Mg/Ca in benthic foraminiferal calcite. *Science*, *287*(5451), 269–272. https://doi.org/10.1126/science.287.5451.269
Leith, T. L., Weiss, H. M., Mørk, A., Arhus, N., Elvebakk, G., Embry, A. F., et al. (1992). Mesozoic hydrocarbon source-rocks of the Arctic region. In T. O. Vorren, et al. (Eds.), *Arctic geology and petroleum potential*, NPF Spec. Publ. (Vol. *2*, pp. 1–25). Tromsö: Norwegian Petroleum Society.
Lenniger, M., Nøhr-Hansen, H., Hills, L. V., & Bjerrum, C. J. (2014). Arctic black shale formation during Cretaceous Oceanic Anoxic Event 2. *Geology*, *42*(9), 799–802. https://doi.org/10.1130/G35732.1

Limoges, A., Ribeiro, S., Weckström, K., Heikkilä, M., Zamelczyk, K., Andersen, T. J., et al. (2018). Linking the modern distribution of biogenic proxies in High Arctic Greenland shelf sediments to sea ice, primary production, and Arctic-Atlantic inflow. *Journal of Geophysical Research: Biogeosciences*, *123*(3), 760–786. https://doi.org/10.1002/2017JG003840

Lipinski, M., Warning, B., & Brumsack, H.-J. (2003). Trace metal signatures of Jurassic/Cretaceous black shales from the Norwegian Shelf and the Barents Sea. *Palaeogeography, Palaeoclimatology, Palaeoecology*, *190*, 459–475. https://doi.org/10.1016/S0031-0182(02)00619-3

Littler, K., Roinson, S. A., Bown, P. R., Nederbragt, A. J., & Pancost, R. D. (2011). High sea-surface temperatures during the Early Cretaceous Epoch. *Nature Geoscience*, *4*(3), 169–172. https://doi.org/10.1038/ngeo1081

Liu, Z., Pagani, M., Zinniker, D., DeConto, R., Huber, M., Brinkhuis, H., et al. (2009). Global cooling during the Eocene-Oligocene climate transition. *Science*, *323*(5918), 1187–1190. https://doi.org/10.1126/science.1166368

Lückge, A., Boussafir, M., Lallier-Vergès, E., & Littke, R. (1996). Comparative study of organic matter preservation in immature sediments along the continental margins of Peru and Oman, part I: Results of petrographical and bulk geochemical data. *Organic Geochemistry*, *24*(4), 437–451. https://doi.org/10.1016/0146-6380(96)00045-9

Macdonald, R. (1996). Awakenings in the Arctic. *Nature*, *380*(6572), 286–287. https://doi.org/10.1038/380286a0

Markwick, P. J. (1998). Fossil crocodilians as indicators of Late Cretaceous and Cenozoic climates: Implications for using palaeontological data in reconstructing palaeoclimate. *Palaeogeography, Palaeoclimatology, Palaeoecology*, *137*(3-4), 205–271. https://doi.org/10.1016/S0031-0182(97)00108-9

Marlow, J. R., Lange, C. B., Wefer, G., & Rosell-Melé, A. (2000). Upwelling intensification as part of the Pliocene-Pleistocene climate transition. *Science*, *290*(5500), 2288–2291. https://doi.org/10.1126/science.290.5500.2288

Marlowe, I. T., Brassell, S. C., Eglinton, G., & Green, J. C. (1984). Long chain unsaturated ketones and esters in living algae and marine sediments. *Organic Geochemistry*, *6*, 135–141. https://doi.org/10.1016/0146-6380(84)90034-2

Marlowe, I. T., Brassell, S. C., Eglinton, G., & Green, J. C. (1990). Long-chain alkenones and alkyl alkenoates and the fossil coccolith record of marine sediments. *Chemical Geology*, *88*(3-4), 349–375. https://doi.org/10.1016/0009-2541(90)90098-R

Martin, J. M., Guan, D. M., Elbaz-Poulichet, F., Thomas, A. J., & Gordeev, V. V. (1993). Preliminary assessment of the distributions of some trace elements (As, Cd, Cu, Fe, Ni, Pb and Zn) in a pristine aquatic environment: The Lena River estuary (Russia). *Marine Chemistry*, *43*(1-4), 185–199. https://doi.org/10.1016/0304-4203(93)90224-C

Matthews, R. K., & Frohlich, C. (2002). Maximum flooding surfaces and sequence boundaries: Comparisons between observations and orbital forcing in the Cretaceous and Jurassic (65-190 Ma). *GeoArabia*, *7*, 503–538.

Matthiessen, J., Brinkhuis, H., Poulsen, N., & Smelror, M. (2009). *Decahedrella martinheadii* Manum 1997—A stratigraphically and paleoenvironmentally useful Miocene acritarch of the high northern latitudes. *Micropaleontology*, *55*, 171–186.

Matthiessen, J., Knies, J., Nowaczyk, N. R., & Stein, R. (2001). Late Quaternary dinoflagellate cyst stratigraphy at the Eurasian continental margin, Arctic Ocean: Indications for Atlantic water inflow in the past 150,000 years. *Global and Planetary Change*, *31*(1-4), 65–86. https://doi.org/10.1016/S0921-8181(01)00113-8

Matthiessen, J., Knies, J., Vogt, C., & Stein, R. (2009). Pliocene paleoceanography of the Arctic Ocean and subarctic seas. *Philosophical Transactions of the Royal Society*, *367*(1886), 21–48. https://doi.org/10.1098/rsta.2008.0203

McClelland, J. W., Holmes, R. M., Dunton, K. H., & Macdonald, R. W. (2012). The Arctic Ocean estuary. *Estuaries and Coasts*, *35*(2), 353–368. https://doi.org/10.1007/s12237-010-9357-3

Méhay, S., Keller, C. E., Bernasconi, S. M., Weissert, H., Erba, E., Bottini, C., & Hochuli, P. A. (2009). A volcanic CO_2 pulse triggered the Cretaceous Oceanic Anoxic Event 1a and a biocalcification crisis. *Geology*, *37*(9), 819–822. https://doi.org/10.1130/G30100A.1

Melles, M., Brigham-Grette, J., Minyuk, P. S., Nowaczyk, N. R., Wennrich, V., DeConto, R. M., et al. (2012). 2.8 million years of Arctic climate change from Lake El'gygytgyn, NE Russia. *Science*, *337*(6092), 315–320. https://doi.org/10.1126/science.1222135

Michaelson, G. J., Ping, C. L., & Kimble, J. M. (1996). Carbon storage and distribution in tundra soils of Arctic Alaska, U.S.A. *Arctic and Alpine Research*, *28*(4), 414–424. https://doi.org/10.2307/1551852

Miller, K. G., Fairbanks, R. G., & Mountain, G. S. (1987). Tertiary oxygen isotope synthesis, sea level history, and continental margin erosion. *Paleoceanography*, *2*(1), 1–19. https://doi.org/10.1029/PA002i001p00001

Miller, K. G., Wright, J. D., & Browning, J. V. (2005). Visions of ice sheets in a greenhouse world. *Marine Geology*, *217*(3-4), 215–231. https://doi.org/10.1016/j.margeo.2005.02.007

Milliman, J. D., & Meade, R. H. (1983). World-wide delivery of river sediment to the oceans. *Journal of Geology*, *91*(1), 1–21. https://doi.org/10.1086/628741

Moore, T. C., & the Expedition 302 Scientists (2006). Sedimentation and subsidence history of the Lomonosov Ridge, in Arctic Coring Expedition (ACEX), Proc. Integr. Ocean Drill. Program, 302. https://doi.org/10.2204/iodp.proc.302.105.2006

Moran, K., Backman, J., Brinkhuis, H., Clemens, S. C., Cronin, T., Dickens, G. R., et al. (2006). The Cenozoic palaeoenvironment of the Arctic Ocean. *Nature*, *441*(7093), 601–605. https://doi.org/10.1038/nature04800

Morison, J., Aagaard, K., & Steele, M. (2000). Recent environmental changes in the Arctic: A review. *Arctic*, *53*, 359–371.

Moritz, R. E., Bitz, C. M., & Steig, E. J. (2002). Dynamics of recent climate change in the Arctic. *Science*, *297*(5586), 1497–1502. https://doi.org/10.1126/science.1076522

Müller, J., Massé, G., Stein, R., & Belt, S. T. (2009). Variability of sea-ice conditions in the Fram Strait over the past 30,000 years. *Nature Geoscience*, *2*(11), 772–776. https://doi.org/10.1038/ngeo665

Müller, J., Wagner, A., Fahl, K., Stein, R., Prange, M., & Lohmann, G. (2011). Towards quantitative sea-ice reconstructions in the northern North Atlantic: A combined biomarker and numerical modeling approach. *Earth and Planetary Science Letters*, *306*(3-4), 137–148. https://doi.org/10.1016/j.epsl.2011.04.011

Müller, P. J., Kirst, G., Ruhland, G., von Storch, I., & Rosell-Melé, A. (1998). Calibration of the alkenone paleotemperature index U^{k}_{37}-based on core-tops from the eastern South Atlantic and the global ocean (60°N–60°S). *Geochimica et Cosmochimica Acta*, *62*(10), 1757–1772. https://doi.org/10.1016/S0016-7037(98)00097-0

Müller, R. D., Sdrolias, M., Gaina, C., & Roest, W. R. (2008). Age, spreading rates and spreading symmetry of the world's ocean crust. *Geochemistry, Geophysics, Geosystems*, *9*, Q04006. https://doi.org/10.1029/2007GC001743

Mutterlose, J., Brumsack, H., Flögel, S., Hay, W., Klein, C., Langrock, U., et al. (2003). The Greenland-Norwegian Seaway: A key for understanding Late Jurassic to Early Cretaceous paleoenvironments. *Paleoceanography*, *18*(1), 1010. https://doi.org/10.1029/2001PA000625

Mutterlose, J., & Kessels, K. (2000). Early Cretaceous calcareous nannofossils from high latitudes: Implications for palaeobiogeography and palaeoclimate. *Palaeogeography, Palaeoclimatology, Palaeoecology*, *160*(3-4), 347–372. https://doi.org/10.1016/S0031-0182(00)00082-1

Mutterlose, J., Malkoc, M., Schouten, S., Sinninghe Damsté, J. S., & Forster, A. (2010). TEX_{86} and stable $\delta^{18}O$ paleothermometry of Early Cretaceous sediments: Implications for belemnite ecology and paleotemperature proxy application. *Earth and Planetary Science Letters*, *298*(3-4), 286–298. https://doi.org/10.1016/j.epsl.2010.07.043

Nelson, F. E., Shiklomanov, N. I., & Mueller, G. R. (1999). Variability of active-layer thickness at multiple spatial scales, northcentral Alaska, U.S.A. *Arctic, Antarctic, and Alpine Research*, *31*, 158–165.

Nghiem, S. V., Rigor, I. G., Perovich, D. K., Clemente-Colón, P., Weatherly, J. W., & Neumann, G. (2007). Rapid reduction of Arctic perennial sea ice. *Geophysical Research Letters*, *34*, L19504. https://doi.org/10.1029/2007GL031138

Niederdrenk, A. L., & Notz, D. (2018). Arctic sea ice in a 1.5°C warmer world. *Geophysical Research Letters*, *45*(4), 1963–1971. https://doi.org/10.1002/2017GL076159

Nies, H., Harms, I. H., Karcher, M. J., Dethleff, D., Bahe, C., Kuhlmann, G., et al. (1998). Anthropogenic radioactivity in the Nordic Seas and the Arctic Ocean—Results of a joint project. *Deutsche Hydrographische Zeitschrift (Germ. J. Hydrogr.)*, *50*(4), 313–343. https://doi.org/10.1007/BF02764228

Niessen, F., Hong, J. K., Hegewald, A., Matthiessen, J., Stein, R., Kim, H., et al. (2013). Repeated Pleistocene glaciation of the East Siberian continental margin. *Nature Geoscience*, *6*(10), 842–846. https://doi.org/10.1038/NGEO1904

Nørgaard-Pedersen, N., Spielhagen, R. F., Erlenkeuser, H., Grootes, P. M., Heinemeier, J., & Knies, J. (2003). The Arctic Ocean during the Last Glacial Maximum: Atlantic and polar domains of surface water mass distribution and ice cover. *Paleoceanography*, *18*(3), 1063. https://doi.org/10.1029/2002PA000781

Nørgaard-Pedersen, N., Spielhagen, R. F., Thiede, J., & Kassens, H. (1998). Central Arctic surface ocean environment during the past 80.000 years. *Paleoceanography*, *13*(2), 193–204. https://doi.org/10.1029/97PA03409

Norris, R. D., Bice, K. L., Magno, E. A., & Wilson, P. A. (2002). Jiggling the tropical thermostat in the Cretaceous hothouse. *Geology*, *30*(4), 299–302. https://doi.org/10.1130/0091-7613(2002)030<0299:JTTTIT>2.0.CO;2

Notz, D., & Stroeve, J. (2016). Observed Arctic sea-ice loss directly follows anthropogenic CO_2 emission. *Science*, *354*(6313), 747–750. https://doi.org/10.1126/science.aag2345

Notz, D., & Stroeve, J. (2018). The trajectory towards a seasonally-ice-free Arctic Ocean. *Current Climate Change Reports*, *4*(4), 407–416. https://doi.org/10.1007/s40641-018-0113-2

Nürnberg, D., Wollenburg, I., Dethleff, D., Eicken, H., Kassens, H., Letzig, T., et al. (1994). Sediments in Arctic sea ice: Implications for entrainment, transport and release. *Mar. Geol.*, *119*, 185–214.

O'Regan, M. (2011). Late Cenozoic paleoceanography of the central Arctic Ocean. *IOP Conference Series: Earth and Environmental Science* (Vol. 14), 012002. IOP Publishing Ltd. https://doi.org/10.1088/1755-1315/14/1/012002

O'Brien, C. L., Robinson, S. A., Pancost, R. D., Sinninghe Damsté, J. S., Schouten, S., Lunt, D. J., et al. (2017). Cretaceous sea-surface temperature evolution: Constraints from TEX86 and planktonic foraminiferal oxygen isotopes. *Earth-Science Reviews*, *172*, 224–247. https://doi.org/10.1016/j.earscirev.2017.07.012

O'Connor, L. K., Robinson, S. A., Naafs, B. D. A., Jenkyns, H. C., Henson, S., Clarke, M., & Pancost, R. D. (2019). Late Cretaceous temperature evolution of the southern high latitudes: A TEX86 perspective. *Paleoceanography and Paleoclimatology*, *34*, 436–454. https://doi.org/10.1029/2018PA003546

Ohkouchi, N., Kuroda, J., & Taira, A. (2015). The origin of Cretaceous black shales: A change in the surface ocean ecosystem and its triggers. *Proceedings of the Japan Academy, Series B, Physical and Biological Sciences*, *91*(7), 273–291. https://doi.org/10.2183/pjab.91.273

O'Regan, M., King, J., Backman, J., Jakobsson, M., Pälike, H., Moran, K., et al. (2008). Constraints on the Pleistocene chronology of sediments from the Lomonosov Ridge. *Paleoceanography*, *23*, PA1S19. https://doi.org/10.1029/2007PA001551

O'Regan, M., Williams, C. J., Frey, K. E., & Jakobsson, M. (2011). A synthesis of the long-term paleoclimatic evolution of the Arctic. *Oceanography*, *24*(3), 66–80. https://doi.org/10.5670/oceanog.2011.57

Pagani, M., Liu, Z., LaRiviere, J., & Ravelo, A. C. (2010). High Earth-system climate sensitivity determined from Pliocene carbon dioxide concentrations. *Nature Geoscience*, *3*(1), 27–30. https://doi.org/10.1038/ngeo724

Pagani, M., Zachos, J. C., Freeman, K. H., Tipple, B., & Bohaty, S. (2005). Marked decline in atmospheric carbon dioxide concentrations during the Paleogene. *Science*, *309*(5734), 600–603. https://doi.org/10.1126/science.1110063

Park, K., Kang, S. M., & Kim, D. (2018). Contrasting local and remote impacts of surface heating on polar warming and amplification. *American Meteorological Society*, *31*, 3155–3166.

Parrish, J. T., & Spicer, R. A. (1988). Late Cretaceous terrestrial vegetation: A near-polar temperature curve. *Geology*, *16*(1), 22–25. https://doi.org/10.1130/0091-7613(1988)016<0022:LCTVAN>2.3.CO;2

Pearson, P. N., & Palmer, M. R. (2000). Atmospheric carbon dioxide concentrations over the past 60 million years. *Nature*, *406*(6797), 695–699. https://doi.org/10.1038/35021000

Pearson, P. N., van Dongen, B. E., Nicholas, C. J., Pancost, R. D., Schouten, S., Singano, J. M., & Wade, B. S. (2007). Stable warm tropical climate through the Eocene Epoch. *Geology*, *35*(3), 211–214. https://doi.org/10.1130/G23175A.1

Peterson, B. J., Holmes, R. M., McClelland, J. W., Vorosmarty, C. J., Lammers, R. B., Shiklomanov, A. I., et al. (2002). Increasing river discharge to the Arctic Ocean. *Science*, *298*(5601), 2171–2173. https://doi.org/10.1126/science.1077445

Petrov, O., Morozov, A., Shokalsky, S., Kashubin, S., Artemieva, I. M., Sobolev, N., et al. (2016). Crustal structure and tectonic model of the Arctic region. *Earth Science Reviews*, *154*, 29–71. https://doi.org/10.1016/j.earscirev.2015.11.013

Pfirman, S., Gascard, J.-C., Wollengurg, I., Mudie, P., & Abelmann, A. (1989). Particle-laden Eurasian Arctic sea ice: Observations from July and August 1987. *Polar Research*, *7*(1), 59–66. https://doi.org/10.1111/j.1751-8369.1989.tb00604.x

Pfirman, S. L., Colony, R., Nürnberg, D., Eicken, H., & Rigor, I. (1997). Reconstructing the origin and trajectory of drifting Arctic sea ice. *Journal of Geophysical Research*, *102*(C6), 12575–12586. https://doi.org/10.1029/96JC03980

Poirier, A., & Hillaire-Marcel, C. (2011). Improved Os-isotope stratigraphy of the Arctic Ocean. *Geophysical Research Letters*, *38*, n/a. https://doi.org/10.1029/2011GL047953

Polyak, L., Alley, R. B., Andrews, J. T., Brigham-Grette, J., Cronin, T. M., Darby, D. A., et al. (2010). History of sea ice in the Arctic. *Quaternary Science Reviews*, *29*(15-16), 1757–1778. https://doi.org/10.1016/j.quascirev.2010.02.010

Pound, M. J., Haywood, A. M., Salzmann, U., Riding, J. B., Lunt, D. J., & Hunter, S. J. (2011). A Tortonian (Late Miocene, 11.61–7.25 Ma) global vegetation reconstruction. *Palaeogeography, Palaeoclimatology, Palaeoecology*, *300*(1-4), 29–45. https://doi.org/10.1016/j.palaeo.2010.11.029

Prahl, F. G., & Wakeham, S. G. (1987). Calibration of unsaturation pattern in long-chain ketone compositions for paleotemperature assessment. *Nature*, *330*(6146), 367–369. https://doi.org/10.1038/330367a0

Price, G. D., Ruffell, A. H., Jones, C. E., Kalin, R. M., & Mutterlose, J. (2000). Isotopic evidence for temperature variation during the Early Cretaceous (late Ryazanian-mid Hauterivian). *Journal of the Geological Society of London*, *155*, 335–343.
Rachold, V., Bolshiyanov, D. Y., Grigoriev, M. N., Hubberten, H. W., Junker, R., Kunitsky, V. V., et al. (2007). Nearshore Arctic subsea permafrost in transition. *EOS*, *88*(13), 149–150. https://doi.org/10.1029/2007EO130001
Rachold, V., Eicken, H., Gordeev, V. V., Grigoriev, M. N., Hubberten, H.-W., Lisitzin, A. P., et al. (2004). Modern terrigenous organic carbon input to the Arctic Ocean. In R. Stein, & R. W. Macdonald (Eds.), *The organic carbon cycle in the Arctic Ocean*, (pp. 33–56). Heidelberg: Springer Verlag. https://doi.org/10.1007/978-3-642-18912-8_2
Rais, P., Louis-Schmid, B., Bernasconi, S. M., & Weissert, H. (2007). Palaeoceanographic and palaeoclimatic reorganization around the Middle–Late Jurassic transition. *Palaeogeography, Palaeoclimatology, Palaeoecology*, *251*(3-4), 527–546. https://doi.org/10.1016/j.palaeo.2007.05.008
Raymo, M. E., Jansen, E., Blum, P., & Herbert, T. D. (1999). *Proc. ODP, Sci. Results*, (Vol. 162). College Station, TX: Ocean Drilling Program.
Raymo, M. E., Rind, D., & Ruddiman, W. F. (1990). Climatic effects of reduced Arctic sea ice limits in the GISS II general circulation model. *Paleoceanography*, *5*(3), 367–382. https://doi.org/10.1029/PA005i003p00367
Rekant, P., Cherkashev, G., Vanstein, B., & Krinitsky, P. (2005). Submarine permafrost in the nearshore zone of the southwestern Kara Sea. *Geo-Marine Letters*, *25*, 167–182.
Ribeiro, S., Sejr, M. K., Limoges, A., Heikkilä, M., Andersen, T. J., Tallbberg, P., et al. (2017). Sea ice and primary production proxies in surface sediments from a High Arctic Greenland fjord: Spatial distribution and implications for palaeoenvironmental studies. *Ambio*, *46*, S106–S118.
Robinson, S. A., Dickson, A. J., Pain, A., Jenkyns, H. C., O'Brien, C. L., Farnsworth, A., & Lunt, D. J. (2019). Southern Hemisphere sea surface temperatures during the Cenomanian–Turonian: Implications for the termination of Anoxic Event 2. *Geology*, *47*(2), 131–134. https://doi.org/10.1130/G45842.1
Romanovskii, N. N., Hubberten, H. W., Gavrilov, A. V., Eliseeva, A. A., & Tipenko, G. S. (2005). Offshore permafrost and gas hydrate stability zone on the shelf of the East Siberian Seas. *Geo-Marine Letters*, *25*(2-3), 167–182. https://doi.org/10.1007/s00367-004-0198-6
Romanovskii, N. N., Hubberten, H.-W., Gavrilov, A. V., Tumskoy, V. E., & Kholodov, A. L. (2004). Permafrost of the east Siberian Arctic shelf and coastal lowlands. *Quaternary Science Reviews*, *23*(11-13), 1359–1369. https://doi.org/10.1016/j.quascirev.2003.12.014
Romanovsky, V. E., Smith, S. L., & Christiansen, H. H. (2010). Permafrost thermal state in the polar Northern Hemisphere during the International Polar Year 2007–2009: A synthesis. *Permafrost and Periglacial Processes*, *21*(2), 106–116. https://doi.org/10.1002/ppp.689
Royer, D. L. (2010). Fossil soils constrain ancient climate sensitivity. *Proceedings of the National Academy of Sciences*, *107*(2), 517–518. https://doi.org/10.1073/pnas.0913188107
Ruddiman, W. F. (2010). A paleoclimatic enigma? *Science*, *328*(5980), 838–839. https://doi.org/10.1126/science.1188292
Rudels, B., Jones, E. P., Anderson, L. G., & Kattner, G. (1994). On the intermediate depth waters of the Arctic Ocean. *AGU Geophysical Monographs*, *85*, 33–46.
Sakshaug, E. (2004). Primary and secondary production in the Arctic Seas. In R. Stein, & R. W. Macdonald (Eds.), *The organic carbon cycle in the Arctic Ocean*, (pp. 57–82). Heidelberg: Springer Verlag. https://doi.org/10.1007/978-3-642-18912-8_3
Salpin, M., Schnyder, J., Baudin, F., Suan, G., Suc, J.-P., Popescu, S.-M., et al. (2018). Evidence for subtropical warmth in the Canadian Arctic (Beaufort-Mackenzie, Northwest Territories, Canada) during the early Eocene. In K. Piepjohn, J. V. Strauss, L. Reinhardt, & W. C. McClelland (Eds.), *Circum-Arctic structural events: Tectonic evolution of the Arctic margins and trans-Arctic links with adjacent orogens*, Geol. Soc. Amer. Spec. Paper (Vol. *541*, 28 pp.). Boulder: Geological Society of America. https://doi.org/10.1130/2018.2541(27
Sangiorgi, F., Brumsack, H.-J., Willard, D. A., Schouten, S., Stickley, C., O'Regan, M., et al. (2008). A 26 million year gap in the central Arctic record at the greenhouse-icehouse transition: Looking for clues. *Paleoceanography*, *23*, PA1S04. https://doi.org/10.1029/2007PA001477
Sangiorgi, F., van Soelen, E. E., Spofforth, D. A. J., Pälike, H., Stickley, C., St. John, K., et al. (2008). Cyclicity in the middle Eocene central Arctic Ocean sediment record: Orbital forcing and environmental response. *Paleoceanography*, *23*, PA1S08. https://doi.org/10.1029/2007PA001487
Sarnthein, M., Pflaumann, U., & Weinelt, M. (2003). Past extent of sea ice in the northern North Atlantic inferred from foraminiferal paleotemperature estimates. *Paleoceanography*, *18*(2), 1047. https://doi.org/10.1029/2002PA000771
Schauer, U., Loeng, H., Rudels, B., Ozhigin, V. K., & Dieck, W. (2002). Atlantic water flow through the Barents and Kara Seas. *Deep-Sea Research*, *49*(12), 2281–2298. https://doi.org/10.1016/S0967-0637(02)00125-5
Schlanger, S. O., & Jenkyns, H. C. (1976). Cretaceous oceanic anoxic events—Causes and consequences. *Geologie en Mijnbouw*, *55*, 179–184.
Schlüter, M., Sauter, E. J., Schäfer, A., & Ritzrau, W. (2000). Spatial budget of organic carbon flux to the seafloor of the northern North Atlantic (60°N–80°N). *Global Biogeochemical Cycles*, *14*(1), 329–340. https://doi.org/10.1029/1999GB900043
Schmelzer, N., & Holfort, J. (2015). Das Eis in der Nord- und Ostsee. In J. L. Lozán, H. Grassl, D. Kasang, D. Notz, & H. Escher-Vetter (Eds.), *Warnsignal Klima: Das Eis der Erde* (pp. 210–217). Hamburg. www.klima-warnsignale.uni-hamburg.de, https://doi.org/10.2312/warnsignal.klima.eis-der-erde.32
Schouten, J., Hopmans, E. C., & Sinninghe Damsté, J. S. (2004). The effect of maturity and depositional redox conditions on archaeal tetraether lipid palaeothermometry. *Organic Geochemistry*, *35*(5), 567–571. https://doi.org/10.1016/j.orggeochem.2004.01.012
Schouten, S., Hopmans, E. C., Schefuß, E., & Sinninghe Damsté, J. S. (2002). Distributional variations in marine crenarchaeotal membrane lipids: A new tool for reconstructing ancient sea water temperatures? *Earth and Planetary Science Letters*, *204*(1-2), 265–274. https://doi.org/10.1016/S0012-821X(02)00979-2
Schreck, M., Matthiessen, J., & Head, M. J. (2012). A magnetostratigraphic calibration of Middle Miocene through Pliocene dinoflagellate cyst and acritarch events in the Iceland Sea (Ocean Drilling Program Hole 907A). *Review of Palaeobotany and Palynology*, *187*, 66–94. https://doi.org/10.1016/j.revpalbo.2012.08.006
Schuur, E., Bockheim, J., Canadell, J., Euskirchen, E., Field, C., Goryachkin, S., et al. (2008). Vulnerability of permafrost carbon to climate change: Implications for the global carbon cycle. *Bioscience*, *58*(8), 701–714. https://doi.org/10.1641/B580807
Scotese, C. R. (2001). *Atlas of Earth history, PALEOMAP Project*. Arlington: Department of Geology, University of Texas at Arlington. ISBN: 0-9700020-0-9.
Screen, J. A., & Deser, C. (2019). Pacific Ocean variability influences the time of emergence of a seasonally ice-free Arctic Ocean. *Geophysical Research Letters*, *46*(4), 2222–2231. https://doi.org/10.1029/2018GL081393

Seidenkrantz, M. S. (2013). Benthic foraminifera as palaeo sea-ice indicators in the subarctic realm—Examples from the Labrador Sea-Baffin Bay region. *Quaternary Science Reviews*, *79*, 135–144. https://doi.org/10.1016/j.quascirev.2013.03.014

Semiletov, I. P., Savelieva, N. I., Weller, G. E., Pipko, I. I., Pugach, S. P., Gukov, A. Y., & Vasilevskaya, L. N. (2000). The dispersion of Siberian river flows into coastal waters: Meteorological, hydrological and hydrochemical aspects. In E. L. Lewis (Ed.), *The Freshwater Budget of the Arctic Ocean*, (pp. 323–366). Dordrecht: Kluwer Academic Publishers. https://doi.org/10.1007/978-94-011-4132-1_15

Serreze, M. C., & Barry, R. G. (2011). Processes and impacts of Arctic amplification: A research synthesis. *Global and Planetary Change*, *77*(1-2), 85–96. https://doi.org/10.1016/j.gloplacha.2011.03.004

Serreze, M. C., Holland, M. M., & Stroeve, J. (2007). Perspectives on the Arctic's shrinking sea-ice cover. *Science*, *315*(5818), 1533–1536. https://doi.org/10.1126/science.1139426

Serreze, M. C., Walsh, J. E., Chapin, F. S., Osterkamp, T., Dyurgerov, M., Romanovsky, V., et al. (2000). Observational evidence of recent change in the northern high-latitude environment. *Climatic Change*, *46*(1/2), 159–207. https://doi.org/10.1023/A:1005504031923

Shackleton, N. J., & Kennett, J. P. (1975). Paleotemperature history of the Cenozoic and the initiation of Antarctic glaciation: Oxygen and carbon isotope analysis in DSDP Sites 277, 279, and 281. *Initial Reports - Deep Sea Drilling Project*, *29*, 743–755.

Shellito, C. J., Sloan, L. C., & Huber, M. (2003). Climate model sensitivity to atmospheric CO_2 levels in the early-middle Paleogene. *Palaeogeography, Palaeoclimatology, Palaeoecology*, *193*(1), 113–123. https://doi.org/10.1016/S0031-0182(02)00718-6

Shephard, G. E., Müller, R. D., & Seton, M. (2013). The tectonic evolution of the Arctic since Pangea breakup: Integrating constraints from surface geology and geophysics with mantle structure. *Earth Science Reviews*, *124*, 148–183. https://doi.org/10.1016/j.earscirev.2013.05.012

Shevenell, A. E., Kennett, J. P., & Lea, D. W. (2004). Middle Miocene Southern Ocean cooling and Antarctic cryosphere expansion. *Science*, *305*(5691), 1766–1770. https://doi.org/10.1126/science.1100061

Sigmond, M., Fyfe, J. C., & Swart, N. C. (2018). Ice-free Arctic projections under the Paris Agreement. *Nature Climate Change*, *8*(5), 404–408 . https://doi.org/10.1038/s41558-018-0124-y

Singh, R. K., Maheshwari, M., Oza, S. R., & Kumar, R. (2013). Long-term variability in Arctic sea surface temperatures. *Polar Science*, *7*(3-4), 233–240. https://doi.org/10.1016/j.polar.2013.10.003

Sinninghe Damsté, J. S., van Bentum, E. C., Reichart, G.-J., Pross, J., & Schouten, S. (2010). A CO_2 decrease-driven cooling and increased latitudinal temperature gradient during the mid-Cretaceous Oceanic Anoxic Event 2. *Earth and Planetary Science Letters*, *293*(1–2), 97–103. https://doi.org/10.1016/j.epsl.2010.02.027

Sluijs, A., Röhl, U., Schouten, S., Brumsack, H.-J., Sangiorgi, F., Sinninghe Damsté, J. S., & Brinkhuis, H. (2008). Arctic late Paleocene–early Eocene paleoenvironments with special emphasis on the Paleocene-Eocene Thermal Maximum (Lomonosov Ridge, Integrated Ocean Drilling Program Expedition 302). *Paleoceanography*, *23*, PA1S11. https://doi.org/10.1029/2007PA001495

Sluijs, A., Schouten, S., Donders, T. H., Schoon, P. L., Röhl, U., Reichart, G.-J., et al. (2009). Warm and wet conditions in the Arctic region during Eocene Thermal Maximum 2. *Nature Geoscience*, *2*(11), 777–780. https://doi.org/10.1038/ngeo668

Sluijs, A., Schouten, S., Pagani, M., Woltering, M., Brinkhuis, H., Damsté, J. S. S., et al., & the Expedition 302 Scientists (2006). Subtropical Arctic Ocean temperatures during the Palaeocene/Eocene thermal maximum. *Nature*, *441*(7093), 610–613. https://doi.org/10.1038/nature04668

Smik, L., Cabedo-Sanz, P., & Belt, S. T. (2016). Semi-quantitative estimates of paleo Arctic sea ice concentration based on source-specific highly branched isoprenoid alkenes: A further development of the PIP25 index. *Organic Geochemistry*, *92*, 63–69. https://doi.org/10.1016/j.orggeochem.2015.12.007

Spencer, A. M., Embry, A. F., Gautier, D. L., Stoupakova, A. V., & Sørensen, K. (Eds) (2011). Arctic petroleum geology. *Geological Society, London, Memoirs*, *35*, 818 pp(1), 1–15. https://doi.org/10.1144/M35.1

Spicer, R. A., & Herman, A. B. (2010). The Late Cretaceous environment of the Arctic: A quantitative reassessment based on plant fossils. *Palaeogeography, Palaeoclimatology, Palaeoecology*, *295*(3-4), 423–442. https://doi.org/10.1016/j.palaeo.2010.02.025

Spielhagen, R., Baumann, K.-H., Erlenkeuser, H., Nowaczyk, N. R., Nørgaard-Pedersen, N., Vogt, C., & Weiel, D. (2004). Arctic Ocean deep-sea record of Northern Eurasian ice sheet history. *Quaternary Science Reviews*, *23*(11-13), 1455–1483. https://doi.org/10.1016/j.quascirev.2003.12.015

Spielhagen, R. F., & Bauch, H. A. (2015). The role of Arctic Ocean freshwater during the past 200 ky. *Arktos*, *1*(1), 18. https://doi.org/10.1007/s41063-015-0013-9

Spielhagen, R. F., & Tripati, A. (2009). Evidence from Svalbard for near-freezing temperatures and climate oscillations in the Arctic during the Paleocene and Eocene. *Palaeogeography, Palaeoclimatology, Palaeoecology*, *278*(1-4), 48–56. https://doi.org/10.1016/j.palaeo.2009.04.012

Spreen, G., Kaleschke, L., & Heygster, G. (2008). Sea ice remote sensing using AMSR-E 89 GHz channels. *Journal of Geophysical Research*, *113*, C02S03.

Srivastava, S. P., Arthur, M. A., Clement, B., et al. (1989). *Proc. ODP, Sci. Results*, (Vol. 105). College Station, TX: Ocean Drilling Program.

St. John, K. (2008). Cenozoic ice-rafting history of the Central Arctic Ocean: Terrigenous sands on the Lomonosov Ridge. *Paleoceanography*, *23*, PA1S05. https://doi.org/10.1029/2007PA001483

Stein, R. (2007). Upper Cretaceous/lower Tertiary black shales near the North Pole: Organic-carbon origin and source-rock potential. *Marine and Petroleum Geology*, *24*(2), 67–73. https://doi.org/10.1016/j.marpetgeo.2006.10.002

Stein, R. (2008). *Arctic Ocean sediments: Processes, proxies, and palaeoenvironment*, *Developments in Marine Geology*, (Vol. 2). Amsterdam: Elsevier. 587 pp

Stein, R. (2011). The great challenges in Arctic Ocean paleoceanography. *IOP Conference Series: Earth and Environmental Science* (Vol. 14). IOP Publishing Ltd. https://doi.org/10.1088/1755-1315/14/1/012001

Stein, R. (Ed) (2015). *The Expedition PS87 of the research vessel Polarstern to the Arctic Ocean in 2014, Reports on Polar and Marine Research 688*. Bremerhaven: Alfred Wegener Institute for Polar and Marine Research 688, 273 pp. http://epic.awi.de/37728/1/BzPM_0688_2015.pdf

Stein, R. (2017). From Greenhouse to Icehouse: The late Mesozoic-Cenozoic Arctic Ocean sea-ice and climate history. *Polarforschung*, *87*, 61–78.

Stein, R. (2019). *The Expedition PS115/2 of the research vessel POLARSTERN to the Arctic Ocean in 2018. Reports on Polar and Marine Research*. Bremerhaven: Alfred Wegener Institute for Polar and Marine Research 728, 249 p. https://doi.org/10.2312/BzPM_0728_2019, https://epic.awi.de/id/eprint/49226/

Stein, R., Blackman, D., Inagaki, F., & Larsen, H.-C. (Eds) (2014). Earth and life processes discovered from subseafloor environment—A decade of science achieved by the Integrated Ocean Drilling Program (IODP). In *Series Developments in Marine Geology*, (Vol. 7). Amsterdam/New York: Elsevier. 800 pp

Stein, R., Boucsein, B., Fahl, K., Garcia de Oteyza, T., Knies, J., & Niessen, F. (2001). Accumulation of particulate organic carbon at the Eurasian continental margin during late Quaternary times: Controlling mechanisms and paleoenvironmental significance. *Global and Planetary Change*, *31*(1-4), 87–102.

Stein, R., Boucsein, B., & Meyer, H. (2006). Anoxia and high primary production in the Paleogene central Arctic Ocean: First detailed records from Lomonosov Ridge. *Geophysical Research Letters*, *33*, L18606. https://doi.org/10.1029/2006GL026776

Stein, R., Fahl, K., Gierz, P., Niessen, F., & Lohmann, G. (2017). Arctic Ocean sea ice cover during the penultimate glacial and the last interglacial. *Nature Communications*, *8*, 373. https://doi.org/10.1038/s41467-017-00552-1

Stein, R., Fahl, K., & Müller, J. (2012). Proxy reconstruction of Arctic Ocean sea-ice history: "From IRD to IP_{25}". *Polarforschung*, *82*, 37–71. hdl:10013/epic.40432.d001

Stein, R., Fahl, K., Schreck, M., Knorr, G., Niessen, F., Forwick, M., et al. (2016). Evidence for ice-free summers in the late Miocene central Arctic Ocean. *Nature Communications*, *7*, 11148. https://doi.org/10.1038/ncomms11148

Stein, R., Jokat, W., Niessen, F., & Weigelt, E. (2015). Exploring the long-term Cenozoic Arctic Ocean Climate History—A challenge within the International Ocean Discovery Program (IODP). *Arktos*, *1*(1), 3. https://doi.org/10.1007/s41063-015-012-x

Stein, R., & Macdonald, R. W. (Eds) (2004). *The organic carbon cycle in the Arctic Ocean*. Heidelberg, 363 pp: Springer Verlag. https://doi.org/10.1007/978-3-642-18912-8

Stein, R., Rullkötter, J., & Welte, D. H. (1986). Accumulation of organic-carbon-rich sediments in the Late Jurassic and Cretaceous Atlantic Ocean—A synthesis. *Chemical Geology*, *56*, 1–32.

Stein, R., Weller, P., Backman, J., Brinkhuis, H., Moran, K., & Pälike, H. (2014). Cenozoic Arctic Ocean climate history: Some highlights from the IODP Arctic Coring Expedition (ACEX). In R. Stein, D. Blackman, F. Inagaki, & H.-C. Larsen (Eds.), *Earth and life processes discovered from subseafloor environment—A decade of science achieved by the Integrated Ocean Drilling Program (IODP)*, *Series Developments in Marine Geology*, (Vol. 7, pp. 259–293). Amsterdam/New York: Elsevier.

Steinsund, P. I., & Hald, M. (1994). Recent calcium carbonate dissolution in the Barents Sea: Paleoceanographic applications. *Marine Geology*, *117*(1-4), 303–316. https://doi.org/10.1016/0025-3227(94)90022-1

Stickley, C. E., St. John, K., Koc, N., Jordan, R. W., Passchier, S., Pearce, R. B., & Kearns, L. E. (2009). Evidence for middle Eocene Arctic sea ice from diatoms and ice-rafted debris. *Nature*, *460*(7253), 376–379. https://doi.org/10.1038/nature08163

Stocker, T., Dahe, Q., Plattner, G.-K., Tignor, M.M.B., Allen, S.K., Boschung, J., et al., 2013. Climate change 2013, The physical science basis. *Intergovernmental Panel on Climate Change (IPCC)*, Cambridge University Press, New York, 1535 pp.; https://doi.org/10.1017/CBO9781107415324.

Stroeve, J., & Notz, D. (2018). Changing state of Arctic sea ice across all seasons. *Environmental Research Letters*, *13*(10), 103001. https://doi.org/10.1088/1748-9326/aade56

Stroeve, J. C., Holland, M. M., Meier, W., Scambos, T., & Serreze, M. (2007). Arctic sea ice decline: Faster than forecast. *Geophysical Research Letters*, *34*, L09501. https://doi.org/10.1029/2007GL029703

Stroeve, J. C., Serreze, M. C., Holland, M. M., Kay, J. E., Malanik, J., & Barrett, A. P. (2012). The Arctic's rapidly shrinking sea ice cover: A research synthesis. *Climatic Change*, *110*(3-4), 1005–1027. https://doi.org/10.1007/s10584-011-0101-1

Suan, G., Popescu, S.-M., Suc, J.-P., Schnyder, J., Fauquette, S., Baudin, F., et al. (2017). Subtropical climate conditions and mangrove growth in Arctic Siberia during the early Eocene. *Geology*, *45*(6), 539–542. https://doi.org/10.1130/G38547.1

Svendsen, J. I., Alexanderson, H., Astakhov, V. I., Demidov, I., Dowdeswell, J. A., Henriksen, M., et al. (2004). Late Quaternary ice sheet history of northern Eurasia. *Quaternary Science Reviews*, *23*(11-13), 1229–1271. https://doi.org/10.1016/j.quascirev.2003.12.008

Talwani, M., Udintsev, G., et al. (Eds) (1976). *Initial Reports DSDP*, (Vol. 38). Washington: US Goct. Printing Office.

Tarduno, J. A., Brinkman, D. B., Renne, P. R., Cottrell, R. D., Scsher, H., & Castillo, P. (1998). Evidence for extreme climatic warmth from Late Cretaceous Arctic vertebrates. *Science*, *282*(5397), 2241–2243. https://doi.org/10.1126/science.282.5397.2241

Tarnocai, C., Canadell, J. G., Schuur, E. A. G., Kuhry, P., Mazhitova, G., & Zimov, S. (2009). Soil organic carbon pools in the northern circumpolar permafrost region. *Global Biogeochemical Cycles*, *23*, GB2023. https://doi.org/10.1029/2008GB003327

Taylor, G. H., Teichmüller, M., Davis, A., Dissel, C. F. K., Littke, R., Robert, P., 1998, *Organic petrology*, Stuttgart, Schweitzerbart, pp. 0-704.

Tesi, T., Muschitiello, F., Smittenberg, R. H., Jakobsson, M., Vonk, J. E., Hill, P., et al. (2016). Massive remobilization of permafrost carbon during post-glacial warming. *Nature Communications*, *7*(1), 13653. https://doi.org/10.1038/ncomms13653

Thibault, N., Harlou, R., Schovbso, N. H., Stemmerik, L., & Surlyk, F. (2016). Late Cretaceous (late Campanian–Maastrichtian) sea-surface temperature record of the Boreal Chalk Sea. *Climate of the Past*, *12*(2), 429–438. https://doi.org/10.5194/cp-12-429-2016

Thiede, J., Clark, D. L., & Hermann, Y. (1990). *Late Mesozoic and Cenozoic paleoceanography of the northern polar oceans, in: The geology of North America*, (pp. 427–458). The Arctic Ocean Region: Vol. L.

Thiede, J., Myhre, A. M., Firth, J. V., Johnson, G. L., & Ruddiman, W. F. (Eds) (1996). *Proc. ODP, Sci. Results*, (Vol. 151). Texas (Ocean Drilling Program): College Station.

Thiede, J., Winkler, A., Wolf-Welling, T., Eldholm, O., Myhre, A., Baumann, K.-H., et al. (1998). Late Cenozoic history of the Polar North Atlantic: Results from Ocean Drilling. In A. Elverhøi, et al. (Eds.), *Glacial and Oceanic History of the Polar North Atlantic Margins*, Quat. Sci. Rev. (Vol. *17*, pp. 185–208). Amsterdam, London: Pergamon.

Thomas, D. N., & Diekmann, G. S. (2010). *Sea Ice*. Oxford: Blackwell Publishing.

Thorndike, A. S., & Colony, R. (1982). Sea ice motion in response to geostrophic winds. *Journal of Geophysical Research*, *87*, 5845–5852.

Tindall, J., Flecker, R., Valdes, P., Schmidt, D. N., Markwick, P., & Harris, J. (2010). Modelling the oxygen isotope distribution of ancient seawater using a coupled ocean-atmosphere GCM: Implications for reconstructing early Eocene climate. *Earth and Planetary Science Letters*, *292*(3-4), 265–273. https://doi.org/10.1016/j.epsl.2009.12.049

Tremblay, L.-B., Schmidt, G. A., Pfirman, S., Newton, R., & Derepentigny, P. (2015). Is ice-rafted sediment in a North Pole marine record evidence of perennial sea-ice cover? *Philosophical Transactions of the Royal Society*, *A373*, 20140168.

Tripati, A., & Darby, D. (2019). Evidence for ephemeral middle Eocene to early Oligocene Greenland glacial ice and pan-Arctic sea ice. *Nature Communications*, *9*(1), 1038. https://doi.org/10.1038/s41467-018-03180-5

Tripati, A. K., Eagle, R. A., Morton, A., Dowdeswell, J. A., Atkinson, K. L., Bahé, Y., et al. (2008). Evidence for glaciation in the Northern Hemisphere back to 44 Ma from ice-rafted debris in the Greenland Sea. *Earth and Planetary Science Letters*, *265*(1-2), 112–122. https://doi.org/10.1016/j.epsl.2007.09.045

Tripati, A. K., Roberts, C. D., & Eagle, R. A. (2009). Coupling of CO_2 and ice sheet stability over major climate transitions of the last 20 million years. *Science*, *326*(5958), 1394–1397. https://doi.org/10.1126/science.1178296

Utescher, T., Bondarenko, O. V., & Mosbrugger, V. (2015). The Cenozoic cooling—Continental signals from the Atlantic and Pacific side of Eurasia. *Earth and Planetary Science Letters*, *415*, 121–133. https://doi.org/10.1016/j.epsl.2015.01.019

Volkman, J. K., Eglinton, G., Corner, E. D. S., & Forsberg, T. E. V. (1980). Long-chain alkenes and alkenones in the marine coccolithophorid *Emiliania huxleyi*. *Phytochemistry*, *19*(12), 2619–2622. https://doi.org/10.1016/S0031-9422(00)83930-8

Vonk, J. E., Sanchéz-García, L., van Dongen, B. E., Alling, V., Kosmach, D., Charkin, A., et al. (2012). Activation of old carbon by erosion of coastal and subsea permafrost in Arctic Siberia. *Nature*, *489*(7414), 137–140. https://doi.org/10.1038/nature11392

Vonk, J. E., Tank, S. E., Bowden, W. B., Laurion, I., Vincent, W. F., Alekseychik, P., et al. (2015). Reviews and syntheses: Effects of permafrost thaw on Arctic aquatic ecosystems. *Biogeosciences*, *12*(23), 7129–7167. https://doi.org/10.5194/bg-12-7129-2015

Wahsner, M., Müller, C., Stein, R., Ivanov, G., Levitan, M., Shelekova, E., & Tarasov, G. (1999). Clay mineral distributions in surface sediments from the Central Arctic Ocean and the Eurasian continental margin as indicator for source areas and transport pathways: A synthesis. *Boreas*, *28*(1), 215–233. https://doi.org/10.1111/j.1502-3885.1999.tb00216.x

Walker, J. C. G., Hays, P. B., & Kastings, J. F. (1981). A negative feedback mechanism for the long-lasting stabilization of the Earth's surface temperature. *Journal of Geophysical Research*, *86*, 9776–9782. https://doi.org/10.1029/JC086iC10p09776

Wang, M., & Overland, J. E. (2012). A sea ice free summer Arctic within 30 years: An update from CMIP5 models. *Geophysical Research Letters*, *39*, L18501. https://doi.org/10.1029/2012GL052868

Wang, P. (2004). Cenozoic deformation and the history of sea-land interactions in Asia. *American Geophysical Union* 10.1029/Series#LettersChapter#, 1–22.

Washburn, A. L. (1980). *Geocryology: A survey of periglacial processes and environments*. New York: Halsted Press.

Wassmann, P. (2011). Arctic marine ecosystems in an era of rapid climate change. *Progress in Oceanography*, *90*(1-4), 1–17. https://doi.org/10.1016/j.pocean.2011.02.002

Weigelt, E., Berglar, K., Ebert, T., Eggers, T., Gaedicke, C., Freiman, S., et al. (2019). Geophysics—Tectonic evolution of the Arctic Ocean: Seismic reflection. In R. Stein (Ed.), *The Expedition PS115/2 of the research vessel POLARSTERN to the Arctic Ocean in 2018*, Reports on Polar and Marine Research (Vol. *728*, pp. 45–52). Bremerhaven: Alfred Wegener Institute.

Weijers, J. W. H., Schouten, S., Spaargaren, O. C., & Sinninghe Damsté, J. S. (2006). Occurrence and distribution of tetraether membrane lipids in soils: Implications for the use of the TEX86 proxy and the BIT index. *Organic Geochemistry*, *37*(12), 1680–1693. https://doi.org/10.1016/j.orggeochem.2006.07.018

Weissert, H., & Erba, E. (2004). Volcanism, CO_2 and palaeoclimate: A Late Jurassic–Early Cretaceous carbon and oxygen isotope record. *Journal of the Geological Society, London*, *161*(4), 695–702. https://doi.org/10.1144/0016-764903-087

Weissert, H., & Lini, A. (1991). Ice age interludes during the time of Cretaceous greenhouse climate? In D. W. Mueller, J. A. Mckenzie, & H. Weissert (Eds.), *Controversies in modern geology*, (pp. 173–191). London: Academic Press.

Weller, P., & Stein, R. (2008). Paleogene biomarker records from the central Arctic Ocean (IODP Expedition 302): Organic-carbon sources, anoxia, and sea-surface temperature. *Paleoceanography*, *23*, PA1S17. https://doi.org/10.1029/2007PA001472

West, C. K., Greenwood, D. R., & Basinger, J. F. (2015). Was the Arctic Eocene 'rainforest' monsoonal? Estimates of seasonal precipitation from early Eocene megafloras from Ellesmere Island, Nunavut. *Earth and Planetary Science Letters*, *427*, 18–30. https://doi.org/10.1016/j.epsl.2015.06.036

Westerhold, T., & Röhl, U. (2009). High resolution cyclostratigraphy of the early Eocene—New insights into the origin of the Cenozoic cooling trend. *Climate of the Past*, *5*(3), 309–327. https://doi.org/10.5194/cp-5-309-2009

Wilkin, R. T., Arthur, M. A., & Dean, W. E. (1997). History of water-column anoxia in the Black Sea indicated by pyrite framboid size distributions. *Earth and Planetary Science Letters*, *148*(3-4), 517–525. https://doi.org/10.1016/S0012-821X(97)00053-8

Wilson, P. A., & Opdyke, B. N. (1996). Equatorial sea-surface temperatures for the Maastrichtian revealed through remarkable preservation of metastable carbonate. *Geology*, *24*(6), 555–558. https://doi.org/10.1130/0091-7613(1996)024<0555:ESSTFT>2.3.CO;2

Winterfeld, M., Laepple, T., & Mollenhauer, G. (2015). Characterization of particulate organic matter in the Lena River delta and adjacent nearshore zone, NE Siberia—Part I: Radiocarbon inventories. *Biogeosciences*, *12*(12), 3769–3788. https://doi.org/10.5194/bg-12-3769-2015

Winterfeld, M., Mollenhauer, G., Dummann, W., Köhler, P., Lembke-Jene, L., Meyer, V. D., et al. (2018). Deglacial mobilization of pre-aged terrestrial carbon from degrading permafrost. *Nature Communications*, *9*(1), 3666. https://doi.org/10.1038/s41467-018-06080-w

Wolfe, J. A. (1994). Tertiary climatic changes at middle latitudes of western North America. *Palaeogeography, Palaeoclimatology, Palaeoecology*, *108*(3-4), 195–205. https://doi.org/10.1016/0031-0182(94)90233-X

Woodgate, R. A., Aagaard, K., & Weingartner, T. J. (2005). A year in the physical oceanography of the Chukchi Sea: Moored measurements from autumn 1990–1991. *Deep Sea Research II*, *52*(24-26), 3116–3149. https://doi.org/10.1016/j.dsr2.2005.10.016

Wuchter, C., Schouten, S., Coolen, M. J. L., & Sinninghe Damste, J. S. (2004). Temperature dependent variation in the distribution of tetraether membrane lipids of marine Crenarchaeota: Implications for TEX86 paleothermometry. *Paleoceanography*, *19*, PA4028. https://doi.org/10.1029/2004PA001041

Wüst, G., & Brögmus, W. (1955). Ozeanographische Ergebnisse einer Untersuchungsfahrt mit Forschungskutter "Südfall"durch die Ostsee Juni/Juli 1954 (anlässlich der totalen Sonnenfinsternis auf Öland). *Kieler Meeresforschungen*, *11*, 3–21.

Zachos, J., Pagani, M., Sloan, L., Thomas, E., & Billups, K. (2001). Trends, rhythms, and aberrations in global climate 65 Ma to present. *Science*, *292*, 868–693.

Zachos, J. C., Dickens, G. R., & Zeebe, R. E. (2008). An early Cenozoic perspective on greenhouse warming and carbon-cycle dynamics. *Nature*, *451*, 281–283.

Zhang, Y. G., Pagani, M., & Liu, Z. (2014). A 12-million-year temperature history of the tropical Pacific Ocean. *Science*, *344*(6179), 84–87. https://doi.org/10.1126/science.1246172

Zhang, Y. G., Pagani, M., Liu, Z., Bohaty, S. M., & DeConto, R. (2013). A 40-million-year history of atmospheric CO_2. *Philosophical Transactions of the Royal Society A: Mathematical, Physical and Engineering Sciences*, *371*(2001), 20130096. https://doi.org/10.1098/rsta.2013.0096

Zimov, N. S., Zimov, S. A., Zimova, A. E., Zimova, G. M., Chuprynin, V. I., & Chapin, F. S. III (2009). Carbon storage in permafrost and soils of the mammoth tundra-steppe biome: Role in the global carbon budget. *Geophysical Research Letters*, *36*, L02502. https://doi.org/10.1029/2008GL036332